UNIVERSITE CATHOLIQUE DE LOUVAIN
INSTITUT DE RECHERCHE EXPERIMENTALE ET CLINIQUE
PÔLE DE NÉPHROLOGIE

MECHANISMS & REGULATION OF WATER TRANSPORT ACROSS THE PERITONEAL MEMBRANE

par

JOHANN MORELLE

PROMOTEUR: PROF. OLIVIER DEVUYST
CO-PROMOTEUR: PROF. ERIC GOFFIN

THESE PRESENTEE EN VUE DE L'OBTENTION DU GRADE DE
DOCTEUR EN SCIENCES MEDICALES

2016

REMERCIEMENTS

Ma reconnaissance va d'abord aux Professeurs de la Faculté de Médecine qui ont dirigé ma formation médicale et scientifique. Qu'à travers le Professeur Vincent Blondel, Recteur de l'Université catholique de Louvain, et le Professeur Dominique Vanpee, Doyen de la Faculté de Médecine, ils reçoivent l'expression de ma gratitude.

Parmi eux, le Professeur Olivier Devuyst m'a accueilli dans son laboratoire et prodigué les conseils, la formation et l'environnement scientifique stimulant mon intérêt pour la recherche fondamentale et translationnelle en néphrologie - en particulier dans le domaine de la dialyse péritonéale. Les Professeurs Michel Jadoul et Eric Goffin m'ont accueilli dans le service de néphrologie des Cliniques universitaires Saint-Luc, offert l'opportunité de me former dans le secteur de la dialyse extra-hospitalière, et permis de consacrer le temps nécessaire à ces travaux de recherche. Je leur en serai toujours redevable.

Les travaux présentés dans cette thèse sont le fruit d'un travail d'équipe. J'exprime ici mes plus vifs remerciements à l'ensemble des membres du laboratoire de néphrologie – techniciens, secrétaire, doctorants et post-doctorants - avec qui j'ai eu le plaisir et la chance de travailler au cours de ces six années. Je remercie tout particulièrement Yvette Cnops, Huguette Debaix, Nicole Van Oost, Hendrica Belge, Claudia Raggi, Céline Maréchal, Sylvie Janas, Sarah Terryn, Vanessa Guy-Viterbo, Samira Azarzar, Sébastien Druart, Sébastien Rosar, Amadou Sow, Nicolas Hautem, et Eric Ollinger pour leur accueil, leur soutien et leur aide inestimable.

Ce travail n'aurait pas été possible sans la contribution des membres du service de néphrologie des Cliniques universitaires Saint-Luc, en ce compris : les infirmiers et infirmières de l'équipe de dialyse extra-hospitalière, les secrétaires, et l'ensemble des collègues médecins et infirmiers. Merci à tous, ainsi qu'aux patients qui ont accepté de participer à ces études, pour leur intérêt, leur aide et leur implication active dans ces travaux de recherche.

Je remercie aussi les Professeurs Sonia Brichard, Jean-Luc Balligand, Philippe Gailly, François Huaux et Michel Jadoul, ainsi que le Professeur Thierry Lobbedez, de l'Université de Caen, d'avoir accepté de siéger dans le

Jury de cette thèse de doctorat et de l'avoir encadrée de manière efficace et constructive.

Ces travaux ont également été permis grâce à de nombreuses collaborations avec les équipes des Professeurs et Docteurs Ralph Crott (Institut de Recherche Santé et Société, Université catholique de Louvain), Didier Vertommen (de Duve Institute of Cellular Pathology, Université catholique de Louvain), Charles-André Fustin (Institut de la Matière Condensée et des Nanosciences, Université catholique de Louvain), Caroline Bouzin (Institut de Recherche Expérimentale et Clinique, Université catholique de Louvain), Andrea Yool (University of Adelaide, Australia), Friedo Dekker et Marion Verduijn (Leiden University Medical Center, The Netherlands), Simon Davies (Keele University, United Kingdom), Raymond Krediet (Academic Medical Center, The Netherlands), Rafael Selgas (University of Madrid, Spain), Pieter Evenepoel et Bert Bammens (KUL, Leuven), Pierre Ripoche (CEA/Saclay, France), Philippe Bovy (Clinique Saint-Joseph, Liège), Bengt Rippe et Carl Oberg (University of Lund, Sweden), et Bengt Lindholm (Karolinska Institute, Sweden).

Ces travaux ont reçu le soutien financier du Fonds National pour la Recherche Scientifique, de la Fondation Saint-Luc, de la Fondation Horlait-Dapsens, de la Société Francophone de Dialyse, et d'un Extramural Grant de Baxter Healthcare.

Ma famille, en particulier mes parents, mon épouse et mes enfants, méritent tout le crédit des efforts consentis pour me permettre l'accomplissement de ce travail.

Bruxelles, décembre 2016

PERSONAL CONTRIBUTIONS

Original articles

Yool AJ, Morelle J, Cnops Y, Verbavatz JM, Campbell EM, Beckett EA, Booker GW, Flynn G, Devuyst O. AqF026 is a pharmacologic agonist of the water channel aquaporin-1. *J Am Soc Nephrol.* 2013;24:1045-52.

Morelle J, Sow A, Vertommen D, Jamar F, Rippe B, Devuyst O. Quantification of osmotic water transport in vivo using fluorescent albumin. *Am J Physiol Renal Physiol*. 2014;307:F981-9.

Morelle J, Goffin E. Peritoneal dialysis for stroke: amazing, but promising! *Perit Dial Int.* 2014;34:7-8.

Morelle J, Sow A, Hautem N, Bouzin C, Crott R, Devuyst O, Goffin E. Interstitial Fibrosis Restricts Osmotic Water Transport in Encapsulating Peritoneal Sclerosis. *J Am Soc Nephrol*. 2015;26:2521-33.

Morelle J, Goffin E, Devuyst O. Molecular Physiology of Water Balance. *N Engl J Med*. 2015;373:196.

Morelle J, Devuyst O. Water and solute transport across the peritoneal membrane. *Curr Opin Nephrol Hypertens.* 2015;24:434-43.

Morelle J, Sow A, Hautem N, Devuyst O, Goffin E. Ultrafiltration Failure and Impaired Sodium Sieving During Long-Term Peritoneal Dialysis: More Than Aquaporin Dysfunction? *Perit Dial Int*. 2016;36:227-231.

Hautem N*, Morelle J*, Sow A, Corbet C, Feron O, Goffin E, Huaux F, Devuyst O. The NLRP3 Inflammasome Plays a Critical Role in Peritoneal Dialysis-Related Peritonitis, submitted to *J Am Soc Nephrol*.

Morelle J, Sow A, Fustin CA, Fillée C, Garcia-Lopez E, Lindholm B, Goffin E, Vandemaele F, Öberg C, Rippe B, Devuyst O. Fundamental Mechanisms of Crystalloid *versus* Colloid Osmosis across the Peritoneal Membrane. *Manuscript in preparation.*

Morelle J*, Marechal C*, Crott R, Verduijn M, Dekker F, Bovy P, Evenepoel P, Bammens B, Selgas R, Bajo A, Yu Z, Davies S, Coester A, Sow A, Hautem N, Krediet R, Ripoche P, Goffin E, Devuyst O. A Common Variant in *AQP1* Promoter Influences Water Transport and Outcome in Peritoneal Dialysis. *Manuscript in preparation.*

Abstracts

Morelle J, Terryn S, Cnops Y, Goffin E, Devuyst O. Aquaporin-1 Mice Provide Novel Insights into the Physiology of Crystalloid and Colloid Osmosis across the Peritoneal Membrane. Kidney week, American Society of Nephrology 2012, *J Am Soc Nephrol* 2012;23:546A.

Morelle J, Terryn S, Cnops Y, Rippe A, Rippe B, Devuyst O. Fluorescent Albumin to Assess Water Transport in a Mouse Model of Peritoneal Dialysis. Kidney week, American Society of Nephrology 2012, *J Am Soc Nephrol* 2012;23:546A.

Morelle J, Yool A, Devuyst O. Aquaporin-1 agonist AqF026 modulates water transport during PD. EuroPD 2013, Maastricht, The Netherlands.

Devuyst O, Morelle J, Yool A. AqF026 is a pharmacologic agonist of the water channel aquaporin-1. Kidney week, American Society of Nephrology 2013, *J Am Soc Nephrol* 2013;24:236A.

Sow A, Morelle J, Hautem N, Cnops Y, Druart S, Devuyst O. Molecular mechanisms of acid-base transport during peritoneal dialysis. International Societyl of Peritoneal Dialysis 2014, Madrid, Spain.

Hautem N, Morelle J, Sow A, Azarzar S, Druart S, Huaux F, Devuyst O. The NALP3 inflammasome complex is involved in the inflammatory response during acute peritoneal dialysis. International Societyl of Peritoneal Dialysis 2014, Madrid, Spain.

Morelle J, Sow A, Hautem N, Bouzin C, Crott R, Devuyst O, Goffin E. Interstitial Fibrosis Restricts Osmotic Water Transport in Encapsulating Peritoneal Sclerosis. 52th ERA-EDTA Congress, London, UK, 2015.

Morelle J, Sow A, Cnops Y, Druart S, Fustin CA, Goffin E, Devuyst O. Osmotic Water Transport Induced by Icodextrin Occurs Independently of Water Channels and Resembles Colloid Osmosis. 52th ERA-EDTA Congress, London, UK, 2015.

TABLE OF CONTENTS

INTRODUCTION

1. The burden of chronic kidney disease

Chronic kidney disease (CKD) is defined as abnormalities of kidney structure or function (mainly a reduced glomerular filtration rate [GFR], increased urinary albumin excretion, or both), present for at least 3 months (Table 1) (KDIGO Group, 2012). CKD is increasingly recognized as a major public health issue because of its high prevalence (8-16% worldwide) and related complications (reviewed in Jha et al, 2013). These include increased all-cause and cardiovascular mortality, acute kidney injury, cognitive decline, anemia, mineral and bone disorders, and kidney-disease progression. Prognosis and classification of CKD is based on the level of GFR, and the degree of urinary albumin excretion (Fig. 1).

Table 1. Chronic kidney disease: definition

- Duration >3 months
- Glomerular filtration rate (GFR) <60 mL/min per 1.73 m²
- Kidney damage as defined by structural abnormalities or functional abnormalities other than decreased GFR
  - *Pathological abnormalities*
  - *History of kidney transplantation*
  - *Albuminuria*
  - *Abnormalities in urinary sediment*
  - *Imaging abnormalities*
  - *Renal tubular syndromes*

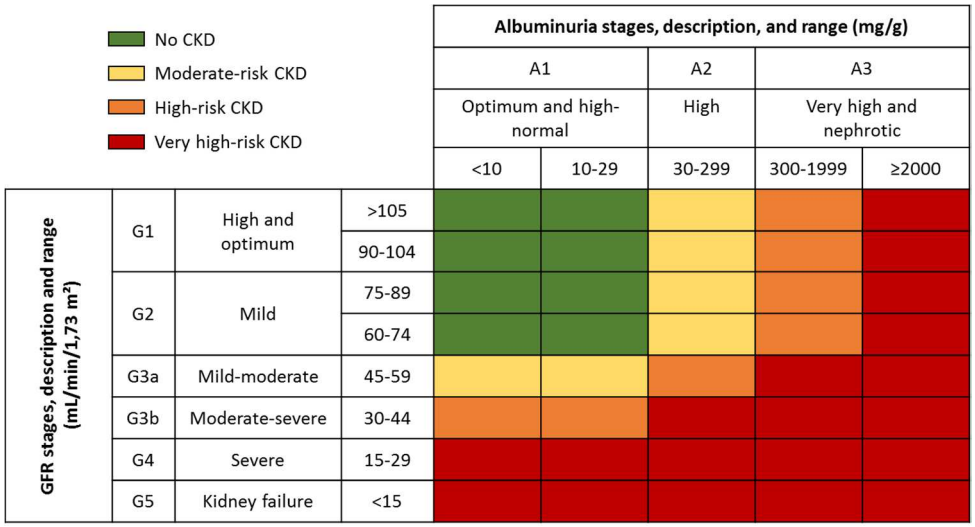

Figure 1. Prognosis and classification of CKD by GFR and albuminuria. Colors show how adjusted relative risk is ranked for five outcomes, including all-cause mortality, cardiovascular mortality, kidney failure treated by dialysis and transplantation, acute kidney injury, and progression of kidney disease. Mean rank numbers: 1–8=green, 9–14=pink, 15–21=orange, and 22–28=red. Adapted from Kidney International and Kidney Disease Improving Global Outcomes (Levey et al, 2010).

Chronic kidney failure is defined as a GFR persistently below 15 mL/min per 1.73 m² and represents end-stage renal disease (ESRD) (reviewed in Ortiz et al, 2013). Renal replacement therapy (RRT), achieved by hemodialysis, hemodiafiltration, peritoneal dialysis (PD), or kidney transplantation, is life-saving for patients with ESRD. However, mortality rates in patients on RRT remains high, and in developing countries RRT is initiated in less than 25% of patients with chronic kidney failure. Each year about 440,000 patients worldwide start RRT, but 3,200,000 have no access to RRT and die prematurely (Ortiz et al, 2013). The Global Burden of Disease 2010 study identified chronic kidney failure as one of the three causes of death with the greatest increase from 1990 to 2010. Improving access to dialysis and efficiency of RRT represents major challenges for coming years and decades.

2. Peritoneal dialysis for the treatment of end-stage renal disease

Like other dialysis techniques, the primary goal of PD is to remove the excess of water and uremic solutes accumulating in the organism of patients with ESRD. The basic principle of PD relies on iterative infusion of a dialysis solution into the peritoneal cavity, followed by a variable dwell time and subsequent drainage. During the dwell, solutes and fluids are exchanged between the capillary blood and the intraperitoneal fluid through a biologic membrane, the peritoneum.

As compared with hemodialysis, PD – the most widely used home-based dialysis technique – offers better patient-reported outcomes, increased flexibility and autonomy to patients, and is associated with lower societal costs (reviewed in Mehrotra et al, 2016). The reimbursement incentives for PD have therefore recently been enhanced in several countries (including from Europe and the United States), with a PD population that is rapidly growing in many parts of the world, including developing countries (Jain et al, 2012; Mehrotra et al, 2016). In the United States for instance, the introduction of a bundled payment system in 2011 led to an unprecedented expansion in the use of PD, with a 22% and 24% increase in incidence and prevalence rates, respectively, between 2010 and 2012 (Hansson et al, 2016). In the same time, the incidence rate of hemodialysis – less cost-effective than PD – decreased by 2% (Hansson et al, 2016).

Significant improvement in the efficiency of PD has been achieved over the last thirty years, thanks to technical innovations including the development of indwelling catheters to provide access to the peritoneal cavity; standardization of the composition of dextrose-based dialysate solutions; changes in connectology to reduce the risk of infections; introduction of volumetric cyclers; and generation of alternatives to conventional glucose-based PD solutions. As a result, PD is now used for the long-term treatment of ESRD, with survival rates that are equivalent to those of hemodialysis, both in the short and longer term (Mehrotra et al, 2011).

3. Peritoneal membrane: structure, function and models

The specificity of PD relies on the use of the peritoneum as a dialysis membrane, to draw waste products and the excess water from the blood of ESRD patients. The peritoneum is a thin, translucent membrane covering the inner surface of the abdominal wall and the majority of the visceral organs. The peritoneum can be viewed as a semi-permeable, heteroporous membrane containing three major components: a monolayer of mesothelial cells; an interstitial tissue consisting of bundles of collagen in a mucopolysaccharide hydrogel; and a dense network of capillaries (Krediet, 2009) (Fig. 2A). The endothelium lining peritoneal capillaries and venules offers the major rate-limiting hindrance for the transport of water and solutes during PD, restricting solute exchange to <0.1% of its total surface area (reviewed in Devuyst et al, 2014).

Computer simulations suggested the capillary endothelium to be functionally described by a three-pore model (Rippe et al, 1991) (Fig. 2B). This model postulates that the major transport barrier of the peritoneum is the capillary endothelium, which contains three distinct types of pores. The 'small pores' (*radius*, 40 to 50 Å) correspond to the clefts, or gaps, located between endothelial cells. They account for ~95% of the hydraulic conductance (LpS), and represent the vast majority of the total pore surface area available for the diffusion of small solutes. The 'large pores' (*radius*, 250 Å), thought to correspond to the venular interendothelial gaps, account for 5% of LpS, and are involved in the transport of macromolecules. The water-specific 'ultrasmall pores' (*radius*, <3 Å) are located in the endothelial cells and account only for 1-2% of LpS. However, because they reject solutes but facilitate the transport of water, ultrasmall pores are extremely important during crystalloid osmosis. Indeed, they have been predicted to mediate up to half of water removal (or ultrafiltration, UF) during a dwell with hypertonic glucose (Rippe et al, 1991).

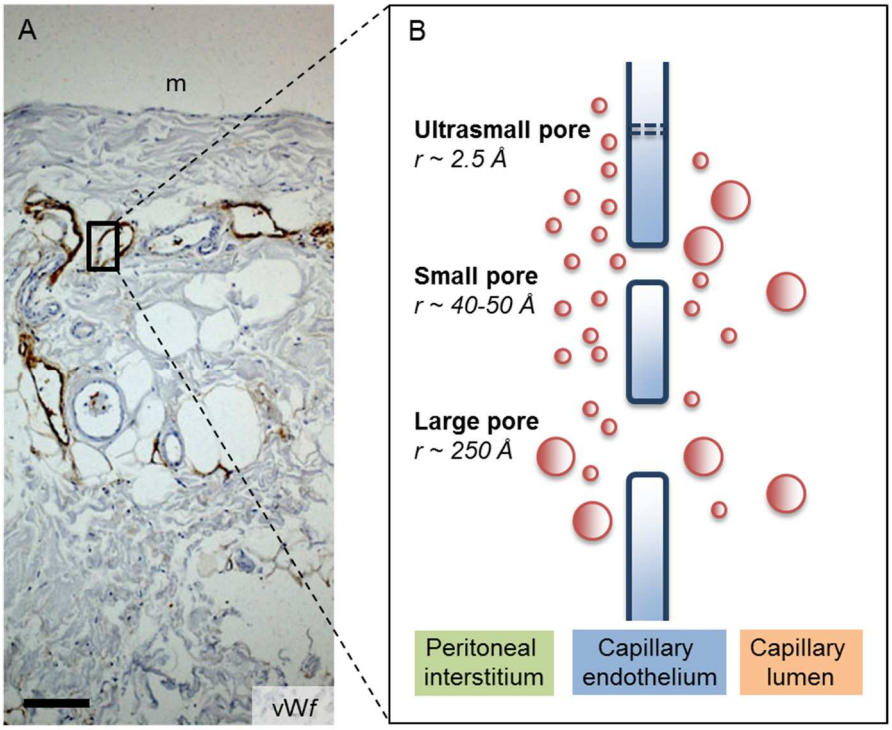

Figure 2. Structure of the peritoneal membrane and the three-pore model. (A) Cross-section of the human parietal peritoneum stained for the von Willebrand factor (vWf). m, mesothelium; bar, 100 µm. (B) The continuous endothelium lining the peritoneal capillaries can be functionally described by a three-pore model. Å, angström (10^{-10} m); r, functional *radius*. Adapted from Devuyst et al, 2014.

Although the three-pore model is practical for clinical purposes and accurately estimates solute and water transport in normal clinical settings, it does not take into account the interstitial tissue surrounding capillaries, lymphatics, and the distributed nature of the capillaries in the peritoneal tissue – so that profound capillaries (deeper than 500 µm to 1 mm to the peritoneal surface) are only exposed to a fraction of the actual osmotic pressure in the dialysate and are probably contributing less to UF. The 'distributed model' has been introduced to circumvene these limitations, by integrating the microvasculature with the surrounding cells and interstitium within the peritoneal membrane using two-dimensional simulations (Flessner et al, 1984; Flessner, 1991). Similarly, an extended version of the three-pore model

- the so-called 'serial membrane-fibre matrix model' - postulates that the fibrotic interstitium represents a second barrier outside the capillaries, restricting osmotic water transport without affecting small solute transport (Rippe et al, 2007).

4. Mechanisms of solute and water transport across the peritoneal membrane

Diffusion and convection are the mechanisms involved in the transport of solutes during PD (reviewed in Krediet, 2009). Removal of solutes such as urea, creatinine, phosphate and other metabolic end products from the body relies on the presence of a concentration gradient, and is driven by the process of diffusion. According to Fick's principles, peritoneal solute transport rate (PSTR) is primarily determined by the number of perfused peritoneal capillaries in contact with the dialysis solution (the 'effective peritoneal surface area'), the diffusive permeability of the membrane to that solute (ratio between its free diffusion coefficient and the diffusion distance) and the concentration gradient between blood and dialysate:

$$J_s = \frac{D_f}{\Delta x} \times A\Delta C$$

in which J_s is the rate of solute transfer, D_f is the free diffusion coefficient, Δx is the diffusion distance, A is the surface area, and ΔC is the concentration gradient. $D_f A/\Delta x$ is called the permeability surface area product or the mass transfer area coefficient.

Convective transport or solute drag occurs in conjunction with the transport of water, and thus during UF. It is determined by the water flux (J_v), the mean solute concentration (C) in the membrane, and the solute reflection coefficient (σ):

$$J_s = J_v C(1 - \sigma)$$

Staverman's reflection coefficient σ is the fraction of the maximal osmotic pressure a solute can exert across a semi-permeable membrane. It equals 1.0 for an ideal semi-permeable membrane (permeable to water but not to solutes)

and 0 when the membrane offers no resistance to the transport of a solute (Krediet, 2009).

Fluid transport during PD consists of water transport from the peritoneal capillaries into the peritoneal cavity by transcapillary UF and by fluid loss out of the peritoneal cavity (reviewed in Krediet, 2009). The latter consists of transcapillary back-filtration and fluid uptake into the lymphatic system and the peritoneal interstitium. Water removal from the body at the end of a dwell period, defined as net UF, is therefore the difference between the cumulative transcapillary UF and fluid uptake. The transport of water across the capillary wall occurs through the small pore system and ultrasmall pores. Small pores-mediated transport is driven by hydrostatic and colloid osmotic forces, while transport through the ultrasmall pores depends upon the osmotic gradient across the capillary wall.

According to Starling's law, the transcapillary UF rate in PD is determined by the UF coefficient of the peritoneal membrane and the driving forces between the peritoneal capillaries and the abdominal cavity. These forces are exerted by hydrostatic, crystalloid osmotic, and colloid osmotic pressure gradients. The dependency of the transcapillary UF rate (TCUFR) can be described by the following equation:

$$TCUFR = UFC \times (\Delta P - \Delta \Pi + \sigma \Delta O)$$

in which UFC is the peritoneal UF coefficient, ΔP is the hydrostatic pressure gradient, $\Delta \Pi$ is the colloid osmotic pressure gradient, σ the reflection coefficient and ΔO the crystalloid osmolality gradient. The UF coefficient of the peritoneum is the product of the hydraulic permeability and surface area. Little is known about determinants of the hydraulic permeability, which is most likely dependent on the combination of intracapillary pressure, and the number and size of the pores. The state of the interstitial tissue, possibly containing sites of fibrosis, may also be one of the determinants.

5. Osmotic agents for PD

The efficiency of PD to restore water homeostasis in patients with ESRD relies on the presence of an osmotic agent which creates an osmotic gradient driving water flow into the dialysis cavity.

Glucose has served as the prototypical osmotic agent in PD for more than four decades because it is cheap and effective. Dextrose is available in 3 different concentrations in conventional PD solutions: 1.36%, 2.27% and 3.86%. Unfortunately, the non-physiological composition of conventional glucose-based solutions (including the high concentrations of glucose and glucose degradation products, low pH, lactate buffer) is harmful for the peritoneal membrane and also has systemic effects in the patient. The negative local effects include impairment of mesothelial cell viability, adverse effects on leukocyte recruitment, accelerated angiogenesis and vascular proliferation, and low-grade inflammation, fibrosis and thickening of the peritoneal membrane (for review, see Garcia-Lopez et al, 2012). The high concentration of glucose and glucose degradation products also promote the formation of advanced glycation end products, which are deposited within the peritoneal membrane. In addition, the absorption of 100-200 g of glucose per day from the solutions worsens metabolic and nutritional problems - such as impaired glucose tolerance, hyperinsulinemia, hyperlipidemia, and, in some patients, abdominal obesity.

Icodextrin has been developed as an alternative osmotic agent to glucose (for review, see Garcia-Lopez et al, 2012). Icodextrin is an iso-osmolar mixture of glucose polymers with different molecular weights that are more slowly absorbed than glucose from the peritoneal cavity, mainly *via* the lymphatics. Ultrafiltration continues for several more hours with icodextrin as slow absorption of the oncotic agent prevents the fluid reabsorption that occurs with glucose-based solutions once the glucose has dissipated - making icodextrin particularly suited for long (8-12 h) dwells. Concerns about increased levels of circulating icodextrin metabolites, in particular maltose, currently limit the approved use of this solution to one single daily exchange. Icodextrin is widely used worldwide mainly because of its demonstrated superiority in terms of fluid and sodium removal during the long dwells,

particularly in patients with inadequate peritoneal UF, as well as improvements in glycemic control and glucose-induced lipid abnormalities. Aminoacids are another available alternative osmotic agent. They have been designed to enhance nutrition in malnourished, hypo-albuminemic PD patients as it acts both as a dialysis solution and as a protein source. The use of aminoacids-based dialysis solutions is also restricted to one daily exchange to reduce the risk of symptomatic uremia and acidosis.

However, despite their usefulness in daily clinical practice, and contrarily to glucose, the fundamental mechanisms of water transport during osmosis induced by large icodextrin molecules or aminoacids have not been investigated to date. A better understanding of these mechanisms would provide an opportunity to rationally prescribe and use these solutions in PD patients, and also contribute to the development of novel, more effective osmotic agents.

6. Aquaporins and osmotic water transport

Achieving euvolemia is key to successful PD, and relies on adherence to sodium- and water-restricted diet, implementation of strategies to preserve residual kidney function, and generation of an effective osmotic water transport across the peritoneal membrane.

From a physiological point of view, the phenomenon of osmosis occurs through a barrier restricting the transport of solute compared to that of water. For the peritoneal membrane, the existence of solute-impermeable, ultrasmall pores in the capillary endothelium has been postulated to explain the effectiveness of glucose as an osmotic agent despite its small size (3.7 Å). Computer simulations based on the three-pore model predicted that ultrasmall pores have a major clinical importance for PD, by mediating up to half of the UF during a dwell with hypertonic glucose and contributing to the sieving of the dialysate sodium, i.e. the rapid fall in dialysate sodium concentration during a dwell with hypertonic glucose dialysate, resulting from free-water transport (Rippe et al, 1991; Rippe et al, 2004).

In the early 1990's, aquaporin-1 (AQP1) was identified as the archetypal member of a family of membrane water channels, conserved in all living organisms including plants (Preston et al, 1992; Moon et al, 1993; Agre, 2004). Aquaporins (AQPs) are organized as homotetramers in plasma membranes, with each monomer containing six membrane-spanning α-helices surrounding a single central pore (Fig. 3A-B). The selectivity of the pore for water (against protons) is ensured by several elements, including a narrow constriction of 2.8 Å (Murata et al, 2000), a conserved arginine residue lining the pore and providing a fixed positive charge, a transient reorientation of the water dipole resulting from the simultaneous formation of hydrogen bonding with the side chains of two conserved asparagine residues (NPA motifs), and two partial positive charges at the centre of the channel resulting from two non-membrane-spanning α helices (Agre, 2004) (Fig. 3C).

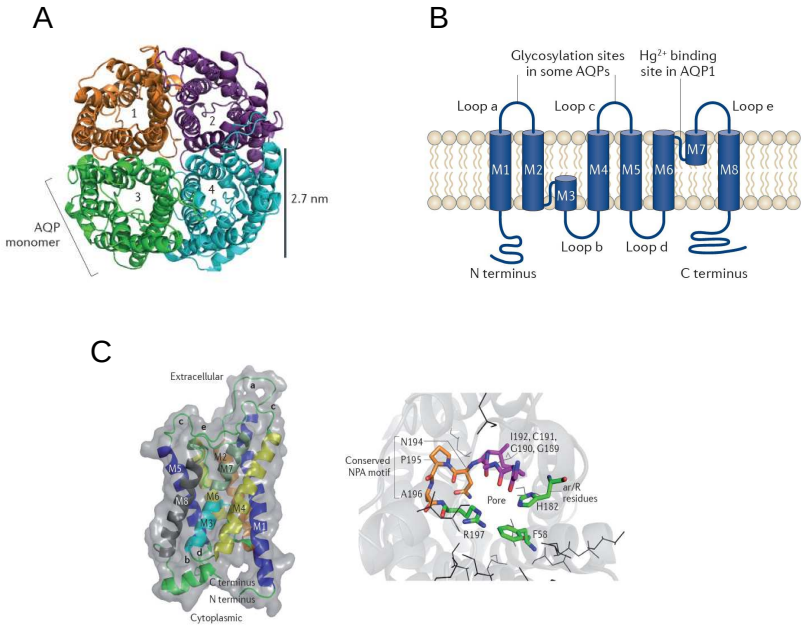

Figure 3. Structure of AQP water channels. Water channels present as homo-tetramers in membranes (A), with a water pore at the center of each unit. Every monomeric unit consists of 6 transmembrane alpha-helices, and 5 connecting loops (B). Conserved NPA motifs contribute to the typical hour-glass 3D conformation with a narrow diameter of 2.8 angströms, and the presence of aromatic residues to proton repulsion, thereby ensuring water specificity (C). Adapted from Verkman, 2014.

AQP1 was initially discovered in red blood cells and in renal proximal tubule cells (Preston et al, 1992; Agre, 2004; Nielsen et al, 1993), and is also constitutively expressed in endothelial cells lining peritoneal capillaries (Nielsen et al, 1993; Devuyst et al, 1998; Combet et al, 1999) (Fig. 4A-B). The targeted deletion of *Aqp1* in mice provided critical insights into the role of AQP1 in water homeostasis. *Aqp1*-knockout mice show a severe defect in their urinary concentrating ability during water deprivation test (due to a defect in creating a hypertonic medullary interstitium by countercurrent multiplication) (Ma et al, 1998), and a reduced osmotic water transport across the peritoneal membrane (Yang et al, 1999). Several lines of evidence demonstrated that AQP1 also constitutes the molecular counterpart of the ultrasmall pore in the peritoneal membrane (reviewed in Devuyst et al, 2014). Functional studies conducted in rats and rabbits have shown that classical AQP antagonists such as mercurial agents inhibit water transport across the peritoneum (Carlsson et al, 1996; Zweers et al, 2001). The development of mouse models of PD and their application to *Aqp1* mice contributed to delineate the critical role of AQP1 water channels during PD (Yang et al, 1999; Ni et al, 2005; Ni et al, 2006). In these models, the deletion of *Aqp1* resulted in a ~70% decrease in the initial, solute-free UF rate, a ~50% decrease in cumulative UF, and a complete abolition of the sodium sieving, as compared with their wild-type littermates (Ni et al, 2006) (Fig. 4C-D). Taken together, these studies in *Aqp1* mice validated two major predictions of the three-pore model: (*i*) ultrasmall pores mediate 50% of UF during PD with a hypertonic glucose dialysate; and (*ii*) free-water transport accounts for the observed sodium sieving (Rippe et al, 1991; Devuyst et al, 2014). To date, AQP1 is the only identified molecular counterpart that is directly involved in transport processes sustaining PD.

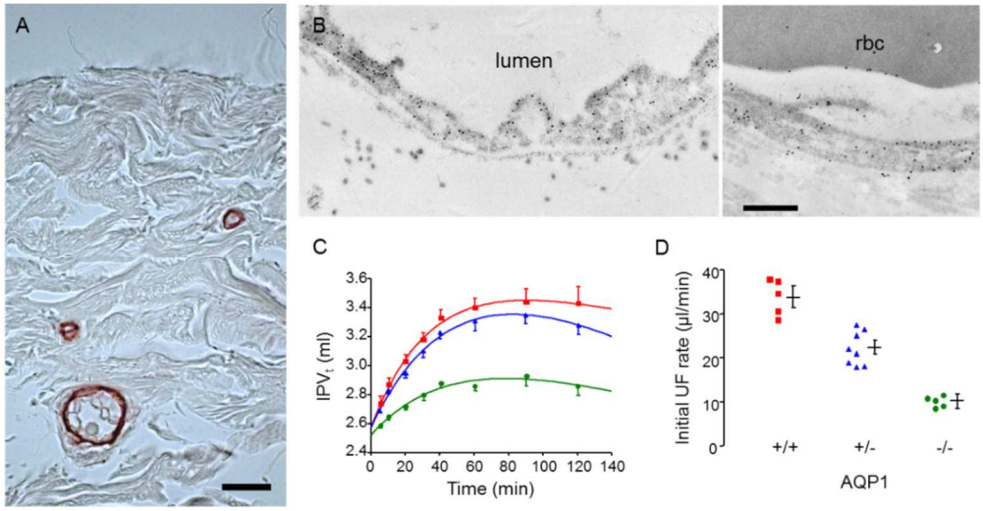

Figure 4. Distribution and role of AQP1 in the peritoneal membrane. (A) Cross-section of the human parietal peritoneum stained for AQP1. AQP1 is detected in the endothelium lining peritoneal capillaries, venules, and small veins. m, mesothelium; bar, 20 µm. (B) Immunogold labeling on mouse visceral peritoneum revealed a very strong signal for AQP1 in plasma membranes and plasma membrane infoldings of capillary endothelial cells. rbc, red blood cells; bar, 500 nm. (C and D) Effect of *Aqp1* deletion on the transport of water across the peritoneal membrane. The intraperitoneal volume versus time curves (IPVt) (C) and the initial UF rates (D) are determined in *Aqp1*$^{+/+}$ mice (red symbols), *Aqp1*$^{+/-}$ mice (blue symbols), and *Aqp1*$^{-/-}$ mice (green symbols) during a 2-hour exchange with hypertonic dialysate. Adapted from Ni et al, 2006 and Devuyst et al, 2014.

The critical role of AQP1 in osmotic water transport during PD suggested water channels could represent potential targets to increase UF and restore fluid balance in PD patients (Ni et al, 2006). The proof-of-principle for that concept was provided by a study in a rat model of PD (Stoenoiu et al, 2003). In this model, high-dose dexamethasone increased AQP1 expression in peritoneal capillaries - through a glucocorticoid element response in the promoter of the *Aqp1* gene, and enhanced free-water transport and total UF. Importantly, changes in water transport occurred without any modification in solute transport nor change in the osmotic gradient. The effect of corticosteroids on AQP1 expression and water transport was recently confirmed in PD patients, by comparing data from functional testing before and after living-donor kidney transplantation. As compared with results from the pre-transplantation period, peritoneal exchange tests performed in 3

patients treated with high doses of corticosteroids after kidney transplantation evidenced a 2-fold increase in sodium sieving, paralleled by an increase in the ultrasmall pore-mediated water transport, while solute transport and small pore-mediated water transport remained unchanged (de Arteaga et al, 2011).

In addition to molecules upregulating the expression of water channels, the search for pharmacologic agonists of AQPs emerged as an exciting field of investigation. Initial observations revealed that plants counteract fluctuations in water supply during drought stress or flooding through the gating of their AQPs (Fig. 5A) (Tournaire-Roux et al, 2003). X-ray crystallography demonstrated that the rapid gating of plant AQP results from conformational changes of the intra-cytoplasmic loop D, which acts as a cap occluding or opening the internal pore of water channels, in response to dephosphorylation of conserved serine residues (drought stress), or to protonation of a conserved histidine (flooding) (Fig. 5B) (Törnroth-Horsefield et al, 2006).

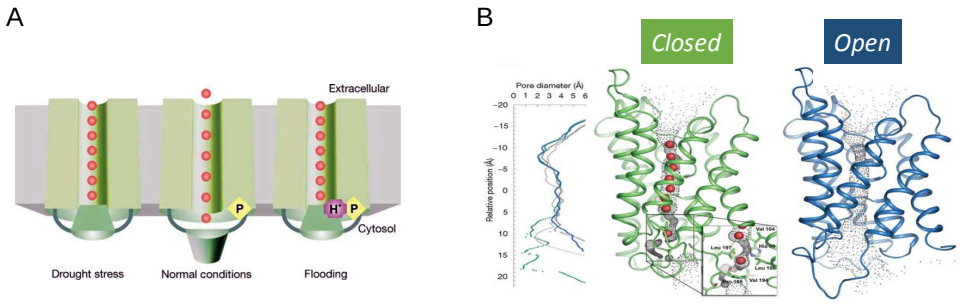

Figure 5. Regulation of plant AQPs by gating/docking process. (A) In normal conditions, plant AQPs are open, to allow exchange of water with the environment. On the contrary, drought stress and flooding induce the closure of water channels – either through dephosphorylation or protonation, to avoid desiccation or intracellular water accumulation, respectively. (B) X-ray crystallography studies showed that the gating/docking process of plant aquaporins is mediated by the intracytosolic loop D, which acts as a cap to close (green) or open (blue) the internal pore of water channels, thereby modulating aquaporin-mediated water flow. Adapted from Tournaire-Roux et al, 2003 and Törnroth-Horsefield et al, 2006.

This gating mechanism appeared conserved throughout all plant plasma membrane AQPs, and recent evidence has suggested it also occurs in mammals. The bumetanide derivative AqB013 (Aq, aquaporin ligand; B, bumetanide scaffold) blocks rat AQP1 and the closely related AQP4 *in vitro*,

by a mechanism thought to involve physical occlusion of the intracytoplasmic water channel pore (Migliati et al, 2009).

No direct pharmacologic agonist of AQPs has previously been described. An agonist of AQP1 would be expected to enhance water transport and UF, thereby increasing the efficiency of dialysis. Furthermore, because PD allows the specific assessment of AQP1-mediated water transport, as opposed to effects on small solute transport and osmotic gradient, it is an advantageous model for assessing potential modulators of AQP1 *in vivo*.

7. Long-term changes in the peritoneal membrane

Functional alterations of the peritoneal membrane constitute an obstacle to long-term PD, because they are associated with technical failure and increased morbidity and mortality (Davies et al, 2001; Devuyst et al, 2010; Devuyst et al 2009). Prolonged exposure of the peritoneal membrane to dialysis leads to vascular proliferation, vasculopathy, and peritoneal fibrosis. These structural alterations are associated with transport defects, including faster solute transport rate (resulting from an enlarged vascular surface area), early dissipation of the osmotic gradient and ensuing loss of UF capacity (Fig. 6) (Davies et al, 1998; Davies et al, 2001; Williams et al, 2002; Williams et al, 2003; Honda et al, 2008; Devuyst et al, 2010).

Causative factors are likely multifactorial and include the PD catheter, dialysate composition (glucose exposure, low pH, glucose degradation products), inflammation, systemic factors, peritonitis episodes and potentially a genetic predisposition. The molecular mechanisms of peritoneal remodeling remain largely debated, but likely involve an excessive release of growth factors such as vascular endothelial growth factor and tumor-growth factor-β1. In turn, these factors lead to vascular proliferation, activation and accumulation of resident myofibroblasts, and excessive deposition of extracellular matrix in the peritoneal interstitium.

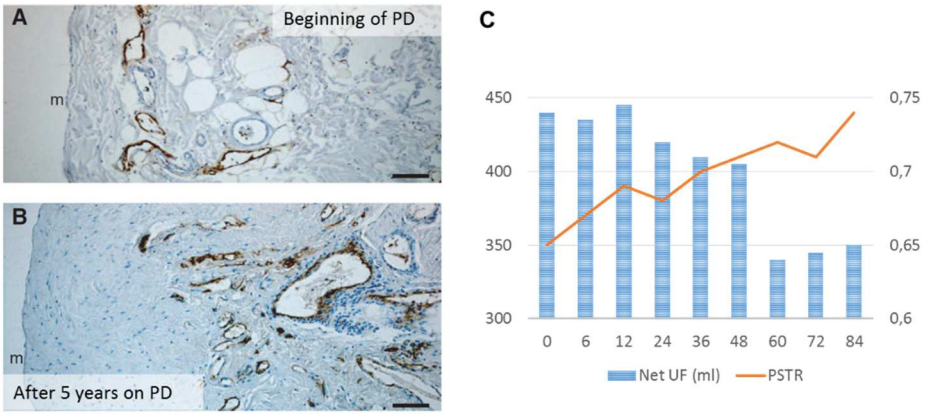

Figure 6. Changes in peritoneal structure and function in patients on long-term PD. (A) Structure at the beginning of therapy. (B) Structural alterations - loss of mesothelial integrity, submesothelial fibrosis, vasculopathy, and vascular proliferation - after 5 years on PD. Brown staining indicates immunoreactivity for factor VIII, indicating the presence of blood vessels. m, mesothelium. Bar = 100 µm. (C) Changes in net ultrafiltration (UF, blue bars) and peritoneal solute transport rate (PSTR, orange line) during prolonged exposure to PD. Adapted from Davies et al, 2004 and Devuyst et al, 2010.

Encapsulating peritoneal sclerosis (EPS) is the most severe complication of PD (for review, see Korte et al, 2011), and consists in an exaggerated fibrogenic response of the peritoneal membrane, leading to encapsulation of the bowels and intestinal obstruction (Fig. 7). Although EPS affects a minority (0.9%-3.5%) of patients on long-term PD, it has a mortality rate reaching 50%, resulting from intestinal occlusion, malnutrition, and sepsis (Korte et al, 2010). EPS is probably a multifactorial disease, in which PD duration represents an important risk factor (Brown et al, 2009; Johnson et al, 2010; Korte et al, 2011). Other conditions that have been inconsistently associated with EPS include cumulative glucose exposure, younger age, peritonitis episodes, β-blockers, and kidney transplantation (Brown et al, 2009; Johnson et al, 2010; Korte et al, 2011). Surprisingly, symptoms of EPS occur after PD withdrawal in most cases (Brown et al, 2009; Johnson et al, 2010; Korte et al, 2011).

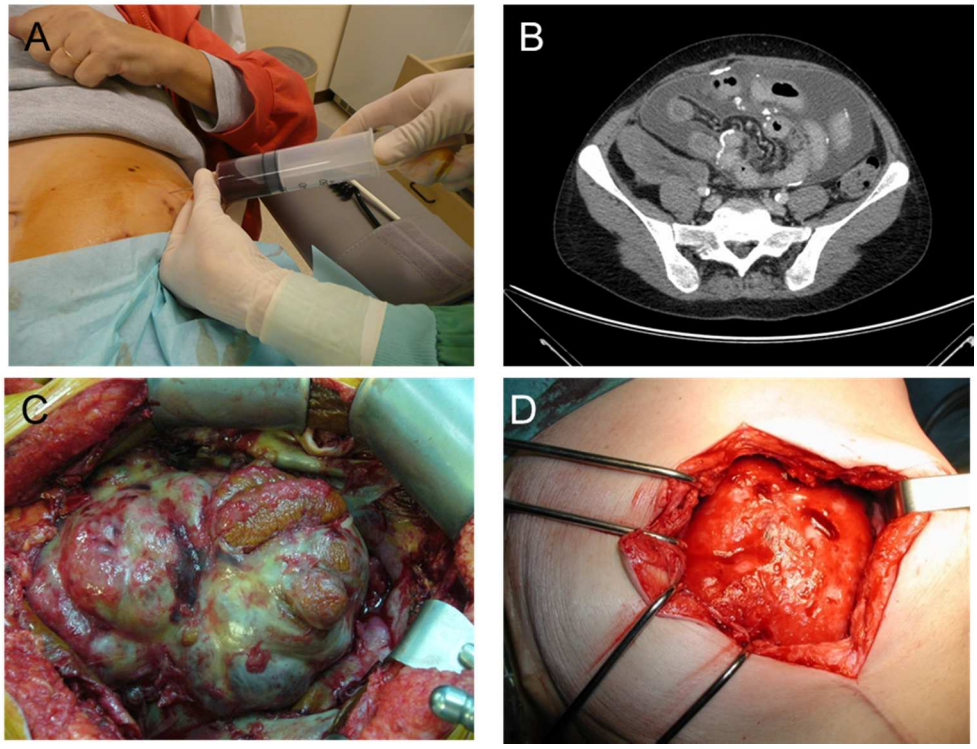

Figure 7. Encapsulating peritoneal sclerosis. (A) Bloody dialysate at early stages of the disease. (B) Typical features of EPS on computed tomography, with thickening and calcifications of the peritoneal layers. (C-D) Macroscopic appearance of EPS, with a fibrotic cocoon that encapsulates the bowel and contributes to intestinal obstruction. Courtesy of Prof. Eric Goffin, Christian Verger, and Titus Augustine.

There are currently no definitive criteria that enable the detection of early stages of EPS. Arguably, a better understanding of the early phase of the disease may help identifying patients at risk and developing prevention strategies. Preliminary studies suggested that a progressive loss of UF capacity often precedes EPS development (Lambie et al, 2010; Sampinon et al, 2011). However, these studies were limited by small numbers, the absence of appropriate matching with long-term PD controls, and/or a lack of evaluation of free-water transport. In addition, the mechanisms of impaired water transport in patients with EPS have not been investigated and remain unelucidated.

8. Peritoneal function testing and determinants of peritoneal transport

Transport properties of the peritoneal membrane may be assessed and quantified in clinical practice through peritoneal equilibration tests (PET). The original PET is performed during a standardized 4-hour dwell using a 2.27% glucose-based dialysis solution (Twardowski et al, 1987). Peritoneal solute transport rate (PSTR) is estimated from the rate of equilibration of small solutes (creatinine, urea) between the blood and the dialysis solution. Dialysate-over-plasma ratio (D/P) of creatinine at the end of procedure therefore indicates how fast small solutes are eliminated across the membrane. The substitution of the 2.27% by a 3.86% glucose-based solution for the PET allows (*i*) a more accurate evaluation of net UF, (*ii*) the diagnosis of UF failure (net UF < 400ml at the end of the 4h dwell with 3.86% glucose, as defined by the International Society for Peritoneal Dialysis [Mujais et al, 2000]), and (*iii*) the assessment of sodium sieving, a reliable - albeit indirect - indicator of AQP-mediated free-water transport (La Milia et al, 2006; Clerbaux et al, 2006; Ni et al, 2006).

The theoretical explanation of PSTR postulates that its main determinant is the density of perfused capillaries in contact with dialysate, an assumption that is supported by both clinical observations and studies (reviewed in Davies, 2014). For example, peritonitis causes a rapid increase in PSTR because of the effects of severe local inflammation mediated by local nitric oxide production, as does the addition to dialysate of vasodilators. Both are associated with reversible changes in capillary perfusion, whereas there is direct evidence in patients that the long-term increase in PSTR associated with membrane injury occurs in parallel with an increase in vascular density.

Based on PSTR, patients can be categorized as slow, average or fast transporters. It is estimated that approximately 15% of patients have a fast transport status at the start of PD. Patients with high PSTR also rapidly absorb dialysate glucose, leading to an early dissipation of the crystalloid osmotic gradient between the dialysate and the blood, and low UF volumes. In addition to the potential suboptimal UF volumes, cohort studies have demonstrated that high PSTR is an independent risk factor of death and technique survival among patients undergoing continuous ambulatory PD

(Churchill et al, 1998; Brown et al, 2003; Brimble et al, 2006; Lin et al, 2010). These data were summarized in a 2006 meta-analysis of 20 observational studies, in which there was an increase in the relative risk of death of 1.15 (95% confidence interval, 1.07-1.23) for every 0.1 increase in the D/P creatinine at 4 hours (Brimble et al, 2006). As compared with patients with low PSTR, an increased mortality risk of 22%, 46%, and 77% was noted for patients with a low-average, high-average and high PSTR, respectively. The reason for the decreased survival of fast transporters is unclear, but might involve poor UF and fluid overload, increased protein losses, and chronic inflammation (Brimble et al, 2006). The high frequency of hypertension and left ventricular hypertrophy among patients with high baseline PSTR, and the reversibility of these findings when the PD prescription is rationalized and individualized (Tonbul et al, 2003), supported the hypothesis that increased risk associated with baseline transport status is related to fluid overload. This assumption has been validated in large cohort studies, in which the use of short dwell times (using a cycler, in patients on automated PD) and the prescription icodextrin for the long dwells abrogated the risk conferred by baseline PSTR (Brown et al, 2003; Davies, 2006; Rumpsfeld et al, 2006; Johnson et al, 2010). Altogether, these data support the recommendation of evaluating peritoneal function to identify patients at increased risk of death or technical failure, and to individualize PD prescription to mitigate the risk conferred by a high PSTR.

Data from large cohorts of patients with peritoneal function testing at the initiation of PD indicate an important - more than two-fold - interindividual variability in the initial PSTR (Churchill et al, 1998; Davies, 1998; Brown et al, 2003; Brimble et al, 2006; Mehrotra et al, 2015). Age, gender, body-mass index and body surface area, serum albumin level, ethnic origin, comorbiditiy index, and diabetes have been identified as independent predictors of baseline PSTR (Chruchill et al, 1998; Davies, 2004; Gillerot et al, 2005; Rumpsfeld et al, 2006; Clerbaux et al, 2006). Concentrations of interleukin (IL)-6 in the dialysate - taken as a surrogate for intraperitoneal inflammation - have also been associated with PSTR. Interleukin-6, a cytokine mediating the acute-phase inflammatory reaction able to increase vascular permeability *in vitro*, is produced by mesothelial and resident cells in the peritoneal membrane

(reviewed in Davies, 2014). The Global Fluid Study, a multinational, multicentre, prospective cohort, including almost 1000 PD patients, recently confirmed this association, by showing that dialysate IL-6 level is the most important and independent determinant of PSTR in both incident and prevalent PD patients (Lambie et al, 2013).

However, the effect of clinical and biological variables on initial PSTR is fairly modest (approximately 20-30%), suggesting that genetics may play a role in variability of PSTR (reviewed in Siddique et al, 2015). Candidate-gene association studies, including proof-of-concept studies from our group (Gillerot et al, 2005), suggested that at least some of the variability in peritoneal membrane function is heritable. These studies indeed identified a common polymorphism in *IL6* gene as an independent predictor of baseline PSTR (Gillerot et al, 2005; Hwang et al, 2009). The biological effect of the -174G/C *IL6* polymorphism was substantiated by significant changes in IL-6 expression in the peritoneal membrane, peritoneal effluent and plasma, further supporting the role of peritoneal inflammation as a major determinant of PSTR (Gillerot et al, 2005).

Similarly, peritoneal water transport at initiation of PD is only partially explained by clinical and biological variables (age, gender, PSTR, residual kidney function, sodium sieving) (La Milia et al, 2006). However, the potential role of variants, including in *AQP1* gene, on water transport in patients treated with PD is unknown. Given the importance of water balance for the efficiency of the technique, the identification of genetic determinants of fluid removal during PD may have critical implications for outcome in this population. In addition, it may help identifying patients at risk and individualizing PD prescription – opening avenues for the development of precision medicine in PD.

9. Animal models of PD

Animal models are important for understanding the physiology of the peritoneal membrane, to test new therapeutic interventions and - *in fine* - to improve the outcome of patients treated with PD.

Mechanistic investigations of peritoneal permeability in rat and rabbit models of PD were mostly based on intervention studies using pharmacologic agents, blocking antibodies, or transient expression systems including adenoviral vectors. These models are often limited by a lack of specificity, side effects, as well as a transient efficacy and safety concerns. Until recently, the body size of a *species* was considered as the major limiting factor to perform *in vivo* studies of PD. The availability of microsample analysis and molecular biology techniques alleviated this restriction, allowing the investigation of permeability parameters and multiple molecules at the mRNA and protein levels from minute volumes and tissue samples. These new possibilities led our group to propose that genetically modified mice could provide an attractive alternative to the above models to investigate the molecular counterparts of PD (Ni et al, 2005).

Since the 1980s, the mouse has emerged as a major model organism for investigations of many aspects of human diseases, as well as basic human biology at the cellular, tissular, and whole organism levels. Its striking similarity to humans in terms of anatomy, physiology and genetics (with >95% of the mouse genome being similar to our own) provides a direct relevance for the study of human physiology and pathology. As an experimental model for mammalian biology, the mouse offers critical advantages, including low cost, fast turnover, easy breeding, accelerated lifespan (one mouse years equals about 30 human years) and multiple possibilities of genetic manipulations. In our laboratory, knockout mice have been used to demonstrate the relative role of nitric oxide synthase isoforms in the permeability modifications and structural changes associated with acute peritonitis (Ni et al, 2003). Based on the molecular and functional similarities between the mouse and human peritoneal membrane, a novel mouse model was then developed to specifically investigate peritoneal transport (Ni et al,

2005). Application of this model to transgenic *Aqp1* mice contributed to validate predictions from the three-pore model, by demonstrating the critical role of endothelial AQP water channels during PD with glucose-based dialysis solutions (Ni et al, 2006).

The availibility of transgenic mice lacking such water channels has stressed the need for novel strategies to accurately assess osmotic water transport *in vivo*. During last decades, radioiodinated serum albumin has been the most widely used tracer for intraperitoneal volume measurement in rodent models of PD (Rippe et al, 2007; Rippe, 2006). However, its use is limited by the emission of ionizing radiation, imposing stringent safety regulations for storage, use, and waste handling. Fluorescent probes have been developed to overcome the limitations of radioactive agents and are increasingly used to assess various processes *in vivo*, including plasma volume changes in rodents (Eisner et al, 2012; Gillen et al, 1994). To date, the use of fluorescently labeled bovine serum albumin tracers and fluorescence spectroscopy to monitor intraperitoneal volume and osmotic water transport across the peritoneal membrane has not been tested.

In addition, experimental models of PD represent a useful tool to characterize potential regulators of AQP expression or function, and effects of alternative osmotic agents used in daily clinical practice, including glucose polymer icodextrin. Contrarily to glucose, icodextrin induces a progressive and sustained water flow across the peritoneal membrane, in the absence of any osmotic gradient, suggesting it may act as a colloid agent. However, this assumption has not been confirmed yet, and the pathways for water transport during crystalloid *versus* colloid osmosis have not been investigated.

AIMS OF THE THESIS

Over the last decades, major technical advances and a better understanding of the peritoneal physiology contributed to establish peritoneal dialysis (PD) as an effective form of renal replacement therapy for patients with end-stage renal disease. However, functional alterations in the dialysis capacity of the peritoneal membrane still represent a major obstacle to successful long-term therapy. As a result, poor peritoneal ultrafiltration and subsequent fluid overload - which affects up to 50% of the prevalent dialysis population (Van Biesen et al, 2011) - contribute to an increased risk of cardiovascular complications, technique failure and death (Churchill et al, 1998; Brown et al, 2003; Brimble et al, 2006; Johnson et al, 2010).

Investigating the mechanisms of water and solute transport is therefore critical to improve our knowledge of the basic principles of PD, and to develop novel strategies to enhance ultrafiltration and improve outcome in patients treated with PD. In addition, PD represents a unique model to investigate the mechanisms of osmosis across biological membranes, the role and regulation of aquaporins (AQPs), and – from a wider perspective - vascular biology and fibrosis.

In this work, we combined data from large cohorts of patients on PD (at clinical, functional, structural, molecular, and genetic levels), computer simulations and well-established mouse models to address some of the gaps in the current knowledge in the physiology of peritoneal transport in normal and diseased states.

The discovery of AQPs and the generation of transgenic animals have stressed the need for novel and accurate methods to unravel molecular mechanisms of water permeability *in vivo*. **In the first chapter of the thesis, we tested and validated fluorescently-labeled bovine serum albumin and fluorescence spectroscopy as a novel indicator of osmotic water transport**

across the mouse peritoneal membrane. After characterization of the intrinsic properties of the dilution tracer, its accuracy to monitor intraperitoneal volume over time during PD was validated against direct volumetry – the gold-standard method. The technique was then applied to quantify osmotic water transport across the mouse peritoneal membrane following changes in dialysate osmolality and invalidation of *Aqp1*.

The AQP1 channel facilitates the osmotic transport of water across the peritoneal microvasculature and is therefore critical for ultrafiltration during PD. The possibility to modulate AQP1-mediated water flow by using a pharmacologic agent, and the potential relevance for PD have not been investigated. **In the second chapter, we used a multi-disciplinary approach to characterize the effects of AqF026, identified as the first AQP1 agonist, on peritoneal water and solute transport.** These studies deciphered the mechanisms of action of AqF026, including potential interference with intracytoplasmic loop D – which has been involved in the gating of plant and mammal AQPs, and established its efficacy in mouse models of PD.

Encapsulating peritoneal sclerosis (EPS) is a rare but severe complication of PD characterized by an extensive fibrosis of the peritoneum leading to bowel encapsulation and obstruction. Changes in peritoneal water transport have been suggested to precede EPS, but the mechanisms and potential predictive value of that transport defect have not been investigated. **In the third chapter, we used serial testing of peritoneal transport in a large cohort of incident PD patients and systematic peritoneal biopsies to characterize the transport defects preceding EPS; to evaluate their ability to predict the risk of subsequent EPS; and to investigate the mechanisms of impaired water transport in this rare complication of PD**.

Osmosis represents the driving force for ultrafiltration and water balance in PD patients. While previous studies have demonstrated that endothelial AQP1 play a significant role in crystalloid osmosis induced by hypertonic glucose, their contribution in water removal induced by alternative osmotic agents such as icodextrin has not been established. **In the fourth chapter, we investigated pathways of water transport during colloid *versus***

crystalloid osmosis, and their fundamental mechanisms, using an experimental model of peritoneal transport combined to computer simulations and biophysical studies.

Peritoneal function testing at initiation of PD shows a large inter-individual variability in AQP-mediated water transport, but the determinants of such variability remain ill-defined. **In the fifth chapter, we analyzed the genetic, demographic and clinical parameters of a multicentric European cohort of incident PD patients to investigate the potential impact of common variants in the *AQP1* gene on peritoneal transport parameters and the risk of death and/or technique failure.**

CHAPTER I

QUANTIFICATION OF OSMOTIC WATER TRANSPORT *IN VIVO* USING FLUORESCENT ALBUMIN

Johann Morelle,[1] Amadou Sow,[1] Didier Vertommen,[2] François Jamar,[3] Bengt Rippe,[4] and Olivier Devuyst[1,5]

[1]Division and laboratory of Nephrology, Cliniques universitaires Saint-Luc, Université catholique de Louvain Medical School, Brussels, Belgium; [2]de Duve Institute, Université catholique de Louvain Medical School, Brussels, Belgium; [3]Department of Nuclear Medicine, Cliniques universitaires Saint-Luc, Université catholique de Louvain Medical School, Brussels, Belgium; [4]Department of Nephrology, University Hospital of Lund, Lund, Sweden; [5]Institute of Physiology, Zurich Center for Integrative Human Physiology, University of Zurich, Zurich, Switzerland

***Am J Physiol Renal Physiol*. 2014;307:F981-9**

SUMMARY

Osmotic water transport across the peritoneal membrane is applied during peritoneal dialysis to remove the excess water accumulated in patients with end-stage renal disease. The discovery of aquaporin water channels and the generation of transgenic animals have stressed the need for novel and accurate methods to unravel molecular mechanisms of water permeability *in vivo*.

Here, we describe the use of fluorescently labeled albumin as a reliable indicator of osmotic water transport across the peritoneal membrane in a well-established mouse model of peritoneal dialysis. After detailed evaluation of intraperitoneal tracer mass kinetics, the technique was validated against direct volumetry, considered as the gold standard. The pH-insensitive dye Alexa Fluor 555-albumin was applied to quantify osmotic water transport across the mouse peritoneal membrane resulting from modulating dialysate osmolality and genetic silencing of the water channel aquaporin-1 (AQP1). Quantification of osmotic water transport using Alexa Fluor 555-albumin closely correlated with direct volumetry and with estimations based on radioiodinated (^{125}I) serum albumin (RISA). The low intraperitoneal pressure probably accounts for the negligible disappearance of the tracer from the peritoneal cavity in this model.

Taken together, these data demonstrate the appropriateness of pH-insensitive Alexa Fluor 555-albumin as a practical and reliable intraperitoneal volume tracer to quantify osmotic water transport *in vivo*.

INTRODUCTION

Water transport across biological membranes is a process of paramount importance in all living organisms. For more than 150 years, fluid transport has been studied across artificial porous membranes and tissues of animal or vegetal origin. The discovery of the aquaporin (AQP) family of water channels (Agre, 2004) and the generation of transgenic mice lacking such water channels have stressed the need for novel strategies to accurately assess osmotic water transport *in vivo* (Verkman, 2000). The AQPs are strongly expressed in the kidney, central nervous system, eye, skin, and exocrine glands. Studies in knockout mice have demonstrated the critical role of these channels in processes ranging from epithelial fluid transport to brain swelling, cell migration, and neuroexcitation (Verkman, 2012).

Peritoneal dialysis (PD) is a life-sustaining therapy that applies the principle of osmosis across the peritoneal mem brane to remove water and solutes accumulated in patients with end-stage renal disease. The efficiency of osmosis during PD is crucial for technique and patient survival (Brown et al, 2003; Devuyst et al, 2010; Nishino et al, 2008). The high expression of AQP-1 (AQP1) in the endothelial cells lining peritoneal capillaries led to the early suggestion of a potential role for water channels in water transport generated during PD (Devuyst et al, 1998; Yang et al, 1999). The development of a mouse model of PD (Ni et al, 2005) and its application to *Aqp1* mice indeed demonstrated that AQP1 accounts for ~50% of osmotic water transport when hypertonic glucose is used as osmotic agent (Ni et al, 2006). Mouse models of PD have also contributed to the development and characterization of the first identified AQP1 agonist (Yool et al, 2013), opening perspectives for the treatment of conditions associated with defective water handling.

During the last decades, radioiodinated (^{125}I) serum albumin (RISA) has been the most widely used tracer for intraperitoneal volume (IPV) measurement in rodent models of PD (Rippe et al, 2007; Rippe, 2006). However, the use of RISA is limited by the emission of ionizing radiation, imposing stringent safety regulations for storage, use, and waste handling. Fluorescent probes have been developed to overcome the limitations of radioactive agents and are increasingly used to assess various processes *in vivo*, including plasma volume changes in rodents (Eisner et al, 2012; Gillen et al, 1994). In the present study, we developed and validated a highly sensitive method using fluorescently labeled BSA tracers and fluorescence spectroscopy to monitor IPV and osmotic water transport across the

peritoneal membrane. The relevance of this new technique to measure osmotic water transport and ultrafiltration (UF) was substantiated by using various osmotic solutions and mice lacking AQP1 and by comparing the accuracy of fluorescent tracers to direct volumetry and RISA.

RESULTS

Intraperitoneal kinetics of tracer albumin labeled with ^{125}I or fluorescent dyes

We first investigated the recovery of RISA and BSA labeled with fluorescent dyes (FITC, Alexa Fluor 488, Alexa Fluor 555, and Alexa Fluor 647) (Fig. 1A) at the end of 2-h dwells with 3.86% glucose-based dialysate (pH 7.4) in a mouse model of PD (Table 1). The recovery of the mass of RISA, as well as all types of fluorescent BSA, was almost complete (~99%), indicating negligible disappearance of the tracer from the peritoneal cavity in this model. This conclusion was supported by the minimal (~1%) appearance of the instilled mass of RISA in plasma, with only traces (~0.1%) of RISA retrieved in the visceral peritoneum of exposed mice (data not shown).

According to the mass-balance principle, since the mass transfer of tracer albumin outside the peritoneal cavity is insignificant, IPV at time t can be calculated using the following equation:

$$Vt = \frac{C_0 \times V_0}{C_t}$$

where V_0 is the instilled volume of dialysate, and C_0 and C_t, the concentrations of labeled albumin in the dialysate at time 0 and t, respectively. The IPV value derived from the tracer concentration at the end of the dwell was concordant with direct volumetric measurement of IPV, considered as the gold standard, for all tracers (Table 1).

Since the conventional dialysate solutions are acidic, we next evaluated the pH sensitivity of fluorescent albumin tracers in vitro. As expected, FITC-labeled BSA showed the most significant pH sensitivity whereas the fluorescence intensity of Alexa Fluor-labeled BSA is less (Alexa Fluor 488 and Alexa Fluor 647) or even not (Alexa Fluor 555) affected by acidic pH changes (ranging from 7.0 to 5.2) (Fig. 1B). Accordingly, the linear relationship between fluorescence intensity and dialysate concentration of

Alexa Fluor 555-BSA remained unaffected by changes in dialysate pH (Fig. 1C).

Table 1. Fluorescent emission properties and intraperitoneal kinetics of albumin tracers

Albumin label	Fluorescence properties			Intraperitoneal kinetics		
	Exc. (nm)	*Em. (nm)*	*Ext. Coeff.*[1]	*Recovery (%)*	*Volumetric IPV120*[2] *(µl)*	*Estimated IPV120*[2] *(µl)*
^{125}I	-	-	-	98.7±1.0	3690±51	3741±39
FITC	491	515	75,000	99.1±1.1	3511±29	3501±22
Alexa Fluor 488	491	515	73,000	99.7±0.7	3610±48	3721±75
Alexa Fluor 555	555	565	155,000	99.1±1.5	3504±55	3535±46
Alexa Fluor 647	650	668	270,000	99.8±1.0	3667±123	3663±67

1, Extinction coefficient of the reactive dye at emission maximum in $cm^{-1}M^{-1}$.
2, IPV_{120}, intraperitoneal volume at 120min of the dwell measured volumetrically or estimated from tracer dilution.
Exc., excitation; Em., emission; Ext. Coeff., extinction coefficient
All exchanges were performed with 3.86% glucose-based dialysate during 120min in SV129 mice. Results are given in mean ± SEM. For intraperitoneal kinetics studies, n=6 mice/group for radio-iodinated ^{125}I human serum albumin and AlexaFluor^{555}-labeled bovine serum albumin, and n=3 for FITC (fluorescein-isothiocyanate), AlexaFluor^{488} and AlexaFluor^{647}-labeled bovine serum albumins.

Alexa Fluor 555-BSA to assess osmotic water transport during peritoneal dialysis

The pH insensitivity of Alexa Fluor 555-BSA, associated with its long wavelength, preventing potential interference from autofluorescence, justified the further characterization of Alexa Fluor 555-BSA as a tracer to assess IPV in a mouse model of PD using conventional dialysis solutions. The standard dialysis procedure (2-h dwell with 3.86% glucose-based dialysate) by itself did not affect the fluorescence intensity of the dye, and no free fractions were detected at the end of the dwells (data not shown). The addition

of Alexa Fluor 555-BSA to the dialysate had no effect on transport [net ultrafiltration: 48.4±1.9 µl/g vs. 47.8±1.9 µl/g; glucose disappearance rate (D_{120}/D_0): 0.44±0.01 vs. 0.43±0.02 in mice exposed or not to Alexa Fluor 555-BSA, respectively; n = 6 in each group] and inflammation [nitrite/ nitrate (NOx): 19.0±2.2 vs. 22. 8±1.3 µM; albumin leakage (D_{120} albumin): 0.45±0.03 vs. 0.45±0.03 µg/µl in mice exposed or not to Alexa Fluor 555-BSA, respectively; n = 6 in each group] parameters during the exchange, further supporting its safe use in mouse models of PD.

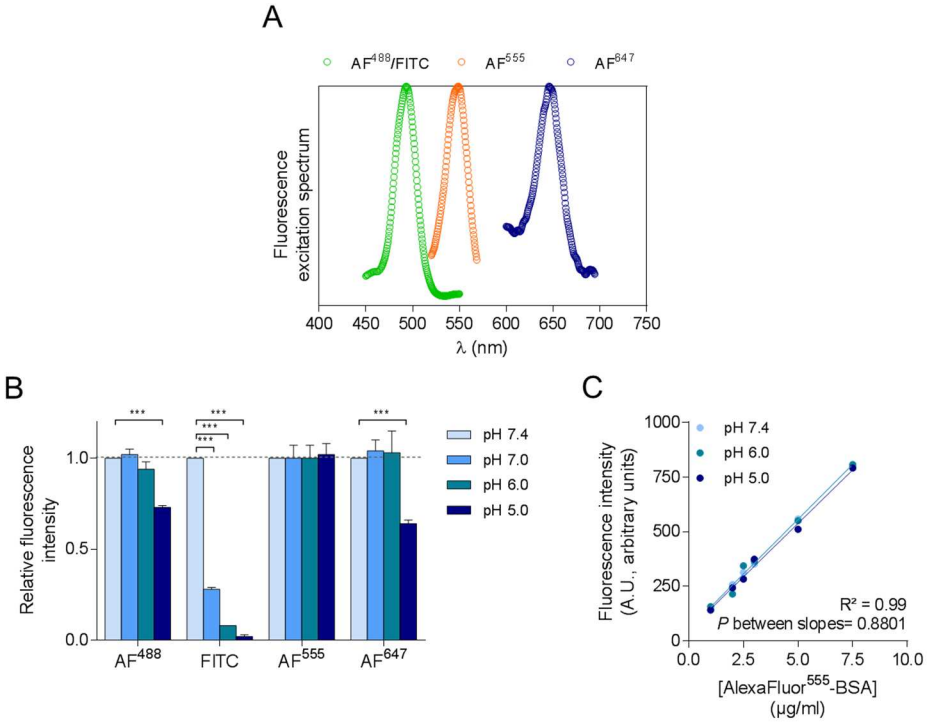

Fig. 1. Spectral characteristics and pH sensitivity of fluorescent dyes. A: fluorescence excitation spectrum of BSA labeled with FITC, Alexa Fluor (AF) 488, Alexa Fluor 555, or Alexa Fluor 647. B: effect of varying pH (from 7.4 to 5.2) of the dialysis solution in vitro on the relative fluorescence intensity of BSA labeled with FITC, Alexa Fluor 488, Alexa Fluor 555, or Alexa Fluor 647 (n = 4 measures/group). C: linear relationship between fluorescence intensity measured with a LS55 spectrometer (PerkinElmer) in arbitrary units (A.U.) and Alexa Fluor 555-BSA concentration in the dialysis solution. The relationship is unaffected by changes in pH in the studied range (pH 5.2–7.4).

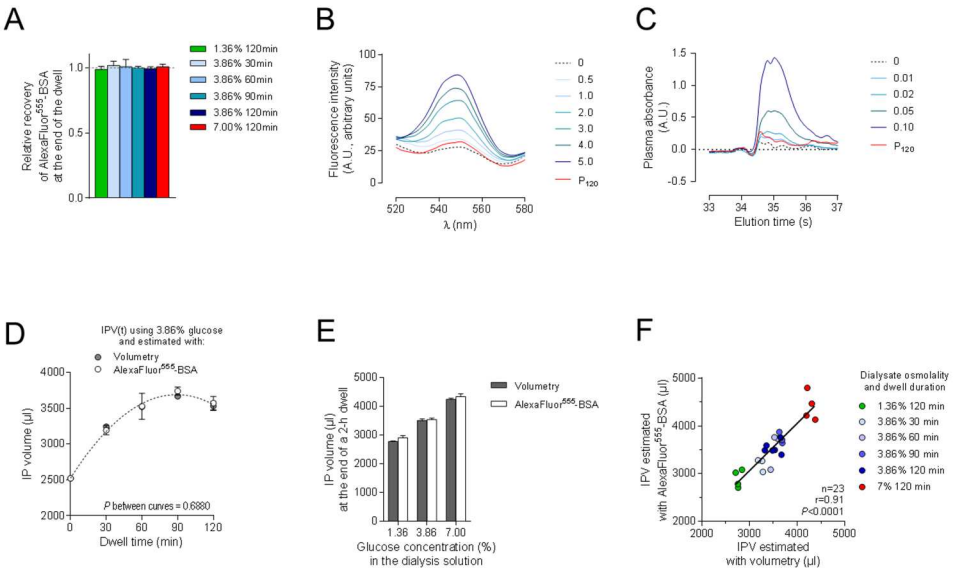

Fig. 2. Intraperitoneal kinetics of Alexa Fluor 555-BSA and comparison of intraperitoneal volume estimated from the dilution of Alexa Fluor 555-BSA or measured by volumetry. A: recovery of the injected mass of Alexa Fluor 555-BSA in the drained dialysate after 30-, 60-, 90-, and 120-min dwells with 3.86% glucose and after 120-min dwells with 1.36 and 7% glucose. The disappearance of the tracer from the peritoneal cavity is minimal at each time point, irrespective of the type of dialysate. B: fluorescence excitation spectrum of control plasma from SV129 mice spiked with various concentrations of Alexa Fluor 555-BSA (blue lines) and after intraperitoneal (IP) exposure to the fluorescent tracer during a 120-min dwell (P_{120}, red line). No significant amount of tracer is detected using fluorescence spectroscopy on the plasma of exposed mice, with a lower limit of detection of 1 µg/ml (1% of the injected tracer mass). C: HPLC and absorbance at 555 nm of control plasma from SV129 mice spiked with various concentrations of Alexa Fluor 555-BSA (blue lines) and after intraperitoneal exposure to the fluorescent tracer during a 120-min dwell (P_{120}, red line). The peak of absorbance at 555 nm after an elution time of 34.6 min corresponding to Alexa Fluor 555-BSA in standards is negligible in the plasma of exposed mice. D: intraperitoneal volume (IPV) estimated with Alexa Fluor 555-BSA is concordant with direct volumetry at each time point during PD with 3.86% glucose-based dialysate. E: estimated and volumetrically measured IPV are in good agreement at the end of 2-h dwells performed with 1.36, 3.86, and 7% glucose-based dialysates. F: IPV estimated using the dilution of Alexa Fluor 555-BSA closely correlate with the data obtained by volumetry (Pearson $r = 0.91$, $P<0.0001$). Values are means ± SE; n = 3 for 30-, 60-, and 90-min dwells with 3.86% glucose, n = 6 for 120-min dwells with 3.86% glucose, and n = 4 for 120-min dwells with 1.36 and 7% glucose.

We next confirmed that the instilled intraperitoneal mass of Alexa Fluor 555-BSA is completely recovered at the end of the procedure, independently of dwell duration and dialysate osmolality (Fig. 2A). We used fluorescence spectroscopy (Fig. 2B) and HPLC (Fig. 2C), two independent and highly sensitive techniques (lower limit of detection of <1% of the total injected mass), to confirm the virtual absence of Alexa Fluor 555-BSA in extracts from visceral peritoneum and plasma of exposed mice.

The validity of Alexa Fluor 555-BSA as an IPV tracer during PD was assessed by the direct comparison of the estimated values with volumetric IPV taken as the gold standard. The absolute values and kinetics of IPV estimated using Alexa Fluor 555-BSA were concordant to volumetric IPV (Fig. 2D), irrespective of dialysate osmolality (Fig. 2E). A close correlation between the estimated IPV and the volumetric IPV (Pearson coefficient, r = 0.91, P<0.001, n=23) was observed after dwells of different durations and using various concentrations of glucose (Fig. 2F).

Since transperitoneal macromolecule absorption depends on intraperitoneal pressure (IPP) (Zakaria et al, 1995), we hypothesized that the very low IPP (<2 mmHg up to 10 ml of instilled dialysate) (Suppl Fig. 2A) accounts for the lack of tracer disappearance from the peritoneal cavity in our mouse model of PD. We therefore evaluated the effect of modulating IPP (by external abdominal compression) on tracer kinetics. Increasing IPP from 0 to 10 mmHg resulted in a significant reduction of Alexa Fluor 555-BSA mass recovery in the dialysate at the end of 2-h dwells (from 1.00±0.02 to 0.85±0.02, respectively; P<0.001) (Suppl. Fig. 2B), and in a significant increase in the amount of Alexa Fluor 555-BSA detected in the plasma using fluorescence spectroscopy (Suppl. Fig. 2C). Similarly, mice exposed to elevated IPP had a higher Alexa Fluor 555-BSA content in their visceral peritoneum at the end of the dwell (data not shown). These observations support the hypothesis that low IPP accounts for the negligible disappearance of macromolecular tracers in our mouse model of PD.

Alexa Fluor 555-BSA to assess IPV kinetics: applications to mouse models of PD

Having established the validity and accuracy of Alexa Fluor 555-BSA to assess IPV kinetics, we next assessed the usefulness of the fluorescent indicator dilution technique to detect changes in osmotic water transport over time. Modulation of water transport across the mouse peritoneum was achieved in two independent models, first by varying the transperitoneal osmotic gradient, and second by genetic deletion of the water channel AQP1.

Increasing glucose concentration in the dialysate from 1.36 to 3.86 and further to 7% was reflected by a faster movement of water across the peritoneum and increased final IPV (Fig. 3A, Table 2). Both the osmotic water transport over 120 min, estimated by the area under the IPV curves (Fig. 3B) and the AQP1-mediated water transport, corresponding to the UF rate during the first 30 min of the dwell (Fig. 3C), showed a linear relationship with dialysate osmolality (Pearson coefficient, $r = 0.98$, $P<0.001$; and 0.94, $P< 0.001$, respectively; n = 14 for both measures).

Mice lacking AQP1 represent a useful model to assess the ultrasmall pore component of water transport during PD. Previous studies based on RISA have demonstrated that the lack of AQP1 is reflected by a significant decrease in the initial UF rate and a loss of ~50% of the UF capacity during a hypertonic dwell (Yang et al, 1999; Ni et al, 2006). We first showed that the tracer mass of Alexa Fluor 555-BSA was constant during the 120-min dwell in *Aqp1* mice (mean tracer recovery 99.0±2.0%, n = 12). There was a close correspondence between the IPV at the end of the dwell estimated from the tracer dilution vs. that obtained by volumetry (Table 2). Comparison of the osmotic water transport parameters assessed by using Alexa Fluor 555- BSA vs. those obtained with RISA in the seminal work in *Aqp1* mice (Ni et al, 2006) demonstrated that both techniques yield highly correlated values of IPV (Pearson coefficient, $r = 0.98$, $P<0.0001$) (Fig. 4A-B, Table 2). In agreement with the role of AQP1 in mediating water transport during PD, the use of Alexa Fluor 555-BSA as a tracer yielded the same reduction in net UF, area under the IPV curve, and initial UF rate than RISA in the *Aqp1*$^{-/-}$ mice compared with their wild-type littermates (Fig. 4C).

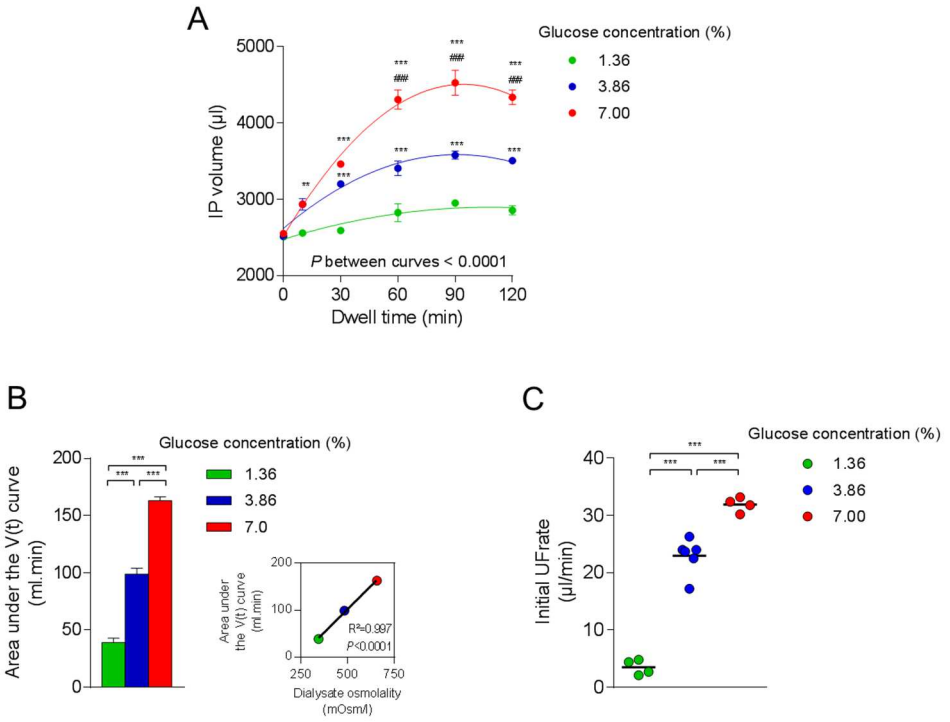

Fig. 3. Alexa Fluor 555-BSA to assess IPV kinetics: effect of the osmotic gradient. A: increasing glucose concentration from 1.36 to 3.86 and 7% in dialysate significantly enhances osmotic water transport during PD, as shown by IPV kinetics. *B*: enhanced osmotic water transport is reflected by the area under the net UF curves (39±3, 99±5, and 163±3 ml/min for 1.36, 3.86, and 7% glucose, respectively). Inset: linear relationship between osmotic water transport estimated using the area under the net UF curve and dialysate osmolality. C: increasing dialysate osmolality drives a faster UF rate during the first 30 min of the dwell (3.5±0.6, 23.1±1.1 and 31.9±0.5 µl/min for 1.36, 3.86, and 7% glucose, respectively), when the contribution of aquaporin-1 to transcapillary UF is maximal. All exchanges were performed using 2.5 ml of 1.36 (green), 3.86 (blue), or 7% (red) glucose-based dialysate. Values are means ± SE; n = 4 for 1.36 and 7%, and n = 6 for 3.86% glucose. ***P<0.001 vs. 1.36% glucose, and ###P<0.001 versus 3.86% glucose.

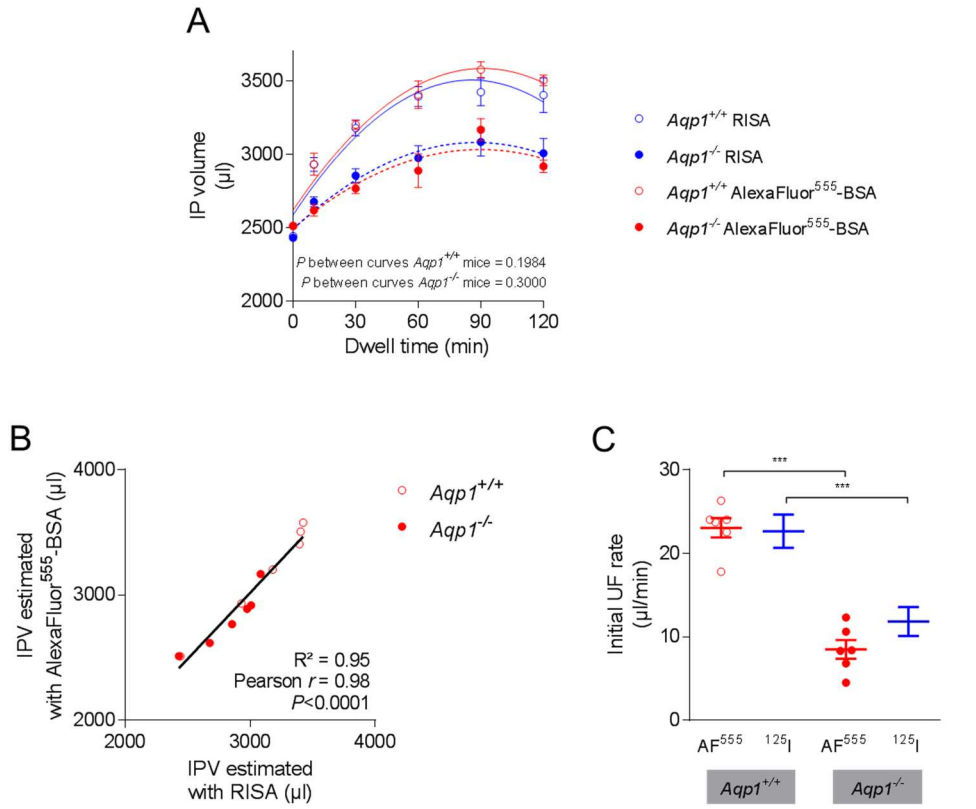

Fig. 4. Alexa Fluor 555-BSA to assess IPV kinetics: effect of deleting *Aqp1*. A: use of Alexa Fluor 555-BSA in *Aqp1* mice yields IPV over time curves that are similar to those obtained using radioiodinated serum albumin (RISA; P = 0.19 and 0.30 between curves using the 2 different techniques, in *Aqp1*$^{+/+}$ and *Aqp1*$^{-/-}$ mice, respectively). B: mean IPV at different time points in *Aqp1* mice using Alexa Fluor 555-BSA closely correlate with those obtained with RISA (Pearson r = 0.98, P<0.0001). C: use of RISA and Alexa Fluor 555-BSA provide similar UF rates during the first 30 min of the dwell in wild-type (22.7±1.8 and 23.1±1.1 µl/min, P = 0.87, using RISA and Alexa Fluor 555-BSA) and *Aqp1* knockout mice (11.8±1.5 and 8.5±1.0 µl/min, P = 0.15). All exchanges were performed using 2.5 ml of 3.86% glucose-based dialysate. Values are means ± SE; n = 6 *Aqp1*$^{+/+}$ (open red circles) and 6 *Aqp1*$^{-/-}$ (filled red circles) mice for experiments using Alexa Fluor 555-BSA, and n = 5 *Aqp1*$^{+/+}$ (open blue circles) and 5 *Aqp1*$^{-/-}$ (filled blue circles) mice using RISA. Results obtained with RISA in *Aqp1* mice are adapted from Ni et al, 2006. ***P<0.001 vs. wild-type mice.

Table 2. Parameters of osmotic water transport during PD in mice using Alexa Fluor 555-BSA as an indicator dilution technique.

Group	*n*	Dialysate glucose (%)	Net UF (µl/g BW)	Volumetric IPV_{120} (µl)	Estimated IPV_{120} (µl)	AUC net UF (ml.min)	UF rate 0-30min (µl/min)
Aqp1$^{+/+}$	6	3.86	38.7±3.2	3473±53	3505±36	99±5	23.1±1.1
	4	1.36	11.1±0.9***	2898±79***	2767±24***	39±3***	3.5±0.6***
	4	7	60.8±1.1***	4402±129***	4274±38***	163±3***	31.9±0.5***
Aqp1$^{-/-}$	6	3.86	18.2±2.8***	2881±42***	2918±41***	46±6***	8.5±1.0***

UF, ultrafiltration; BW, body weight; volIPV120, intraperitoneal volume at 120min of the dwell measured volumetrically or estimated from the tracer dilution technique; AUC, area under the curve. ***P<0.001 versus *Aqp1*$^{+/+}$ mice using 3.86% glucose.

DISCUSSION

Fluorescent dyes are increasingly used in biomedical research to avoid limitations and safety risks of radiolabeled tracers (Eisner et al, 2012; Gillen et al, 1994; Lin et al, 2011). In this study, we used well-established models of PD to demonstrate that Alexa Fluor 555-BSA is an easy-to-use, neutral, and accurate IPV tracer that allows the study of osmotic water transport *in vivo*.

Alexa Fluor dyes are a new family of bright, photostable, and water-soluble fluorophores obtained by sulfonation of rhodamine or coumarin molecules (Berlier et al, 2003; Panchuk-Voloshina et al, 1999). Sulfonation makes Alexa Fluor molecules negatively charged and hydrophilic, contributing to the stability of these dyes, and to their strong pH insensitivity, allowing their efficient use in a broad range of pH (21). Among Alexa Fluor dyes, Alexa Fluor 555 was shown to be the more pH insensitive in the studied range of pH (5.2–7.4), in agreement with previous observations in which red-orange fluorescent dyes have the lowest pK_a values, as low as 2.7 (Chudakov et al, 2010). During PD with conventional solutions, rapid changes in intraperitoneal pH occur, as a result of transperitoneal buffers and gas transport (Heimburger et al, 2003). Covalent conjugation of Alexa Fluor dyes to specific proteins such as BSA (Berlier et al, 2003) prevents the appearance

of free fractions, limiting the risk of free dye absorption. The addition of tracer concentrations of fluorescent albumin to the PD solution had no effect on parameters of transport and inflammation during PD.

The validity and accuracy of Alexa Fluor 555-BSA to assess osmotic water changes *in vivo* are demonstrated by the close correlation between IPV based on the dilution of the fluorescent tracer Alexa Fluor 555-BSA and IPV measured by volumetry, considered as the gold standard technique (Van Biesen et al, 2002). The use of Alexa Fluor 555-BSA as an indicator of osmotic water transport is further validated by the similar IPV values over time obtained with Alexa Fluor 555-BSA and RISA in *Aqp1* mice, which represent a critical tool to assess osmotic water transport in rodent models of PD. The serial assessment of IPV over time in the same animal yielded IPV curves exactly similar to those previously obtained using the RISA technique (Ni et al, 2006). Similar values of osmotic water transport and initial UF rates, two parameters that are directly linked to the nature of the dialysate and the availability of AQP1 water channels, respectively, were also obtained using either Alexa Fluor555-BSA or RISA (Ni et al, 2006; Yool et al, 2013).

Application of a macromolecular IPV tracer to assess osmotic water changes in mouse models of PD warrants a careful evaluation of the kinetics of the intraperitoneal mass of the tracer during the dwell. In the present model, the intraperitoneal mass of fluorescent albumins used as IPV tracers is constant throughout all experiments, independently of the fluorescent dye, dwell time, and dialysate osmolality. Minimal disappearance of Alexa Fluor 555-BSA from the peritoneal cavity is corroborated by the lack of significant tracer detection in plasma or visceral peritoneum of exposed mice based on fluorescence spectroscopy and HPLC, which are both highly sensitive (detection limit ~1 µg/ml) whereas HPLC allows to rule out any artifact due to fluorescence. The lack of disappearance of RISA from the peritoneal cavity in this mouse model confirms these results. The data presented here suggest that the very low IPP in basal conditions accounts for the lack of disappearance of fluorescent albumin tracers from the peritoneal cavity. Conversely, increasing IPP by external abdominal compression results in a significant reduction in tracer mass recovery in the dialysate, and a parallel increase in tracer appearance in the plasma and in the peritoneal membrane. In other rodent models of PD, disappearance of the macromolecular IPV tracer (RISA, dextrans, or autologous hemoglobin) from the peritoneal cavity (up to 10-30%) can occur as a result of an uptake into lymphatic vessels (mainly subdiaphragmatic) and interstitial tissues lining the peritoneal cavity

(Flessner, 1983; Zakaria et al, 1996). In those models, transperitoneal transport of macromolecules from dialysate to plasma indeed depends on the nature of the tracer (De Paepe et al, 1988; Nagy, 1992) and, more importantly, on IPP, which directly determines tracer disappearance (Flessner, 1991; Rippe, 2006; Zakaria et al, 1995; Zhu et al, 1998). When present, tracer disappearance requires correcting equations to avoid overestimation of IPV, and to accurately assess IPV over time (De Paepe et al, 1988; Mactier, 1989; Rippe et al, 2007). We speculate that differences in abdominal wall compliance among species, in the type of anesthesia and related effects on diaphragmatic contraction, and in the use or not of mechanical ventilation, influence IPP and account, at least partly, for the variability in macromolecular tracer disappearance in rodent models of PD (Lai-Fook et al, 2008; Rippe, 2009; Sarton et al, 2001; Shin et al, 2006). Careful evaluation of tracer mass kinetics is therefore a prerequisite for the application of indicator dilution techniques assessing IPV in animal models of PD.

Altogether, these data support the appropriateness of fluorescently labeled macromolecules, and more specifically Alexa Fluor 555-BSA, as alternative IPV tracers to RISA to accurately assess IPV in mouse models of PD, decipher the molecular mechanisms of water transport, and evaluate interventions modifying water transport in vivo. Further investigations are required to investigate the potential use of fluorescently labeled macromolecules to assess IPV over time in PD patients.

METHODS

Animals. Adult male SV129 mice (Charles River, Brussels, Belgium), aged 8 -14 wk, weighing 20 -30 g, were used to assess the kinetics of fluorescently labeled BSA and ^{125}I-human serum albumin and to evaluate the influence of the fluorescent tracer on transport and inflammation parameters in a mouse model of PD (Ni et al, 2005). Gender-matched *Aqp1* mouse littermates generated as previously described (Ma et al, 1998), aged 8 -12 wk, were used to assess the influence of the water channel AQP1. All animals had access to a standard diet and tap water *ad libitum*. The experiments were conducted in accordance with the National Research Council Guide for the Care and Use of Laboratory Animals and the Animal Ethics Committee of the Université catholique de Louvain Medical School.

Peritoneal transport studies and tissue sampling. Osmotic water transport across the peritoneum was investigated using a peritoneal equilibrium test, as previously described (Ni et al, 2005). Briefly, following anesthesia with ketamine (100 mg/kg sc, Merial) and xylazine (10 mg/kg sc, Bayer), mice were laid in a supine position and the fur over the abdominal wall was shaved after desinfection with 70% alcohol. A silicon catheter (Venflon 22 G, 0.9-mm diameter, Terumo) was inserted percutaneously into the right lower quadrant of the peritoneal cavity. This catheter was used for the infusion and sampling of PD solution. Mice were intraperitoneally injected with 2.5 ml of glucose-based dialysate containing 100 µg of albumin labeled with either a fluorescent dye (Alexa Fluor 488-, Alexa Fluor 555-, or Alexa Fluor647-BSA; Molecular Probes, Invitrogen), FITC-albumin (Sigma-Aldrich), or RISA (Seralb-125, IBA, Cis-BioInternational). The instilled volume of 2.5 ml is between that obtained when scaling to body weight (~0.7 ml) and to body surface area (~10 ml), when considering a standard infusion of 2,000 ml in a 70-kg adult. Previous observations have shown that using a 2.5-ml instilled volume in mouse models of PD induced very similar glucose disappearance rates and net ultrafiltration across species, including humans (Ni et al, 2005). The content of free ^{125}I in the spent dialysate was ~0.6% as checked by trichloroacetic acid (5% vol/vol) precipitation. A neutral pH dialysis solution (Physioneal 3.86%, pH ~7.4, Baxter Healthcare, Nivelles, Belgium) was used for tracer kinetics studies, while further experi- ments using Alexa Fluor 555-BSA were conducted with conventional dialysate [Dianeal 1.36 (344 mOsm/l) or 3.86% (483 mOsm/l), pH ~ 5.2, from Baxter Healthcare] or glucose 7% (657 mOsm/l). No intermediate sampling was performed during the assessment of the kinetics of the tracer mass to prevent the disappearance of the osmotic agent and tracer by multiple sampling (Van Biesen et al, 2002). Microsampling (10 µl) was used at intermediate time points in other experiments to assess fluorescence. Before each sampling, the abdomen was gently agitated to facilitate fluid mixing. Instilled and recovered dialysate volumes were weighed on a precision balance (AG35, Mettler Toledo; margin of error during experiments is 0.1 mg). Dialysate recovery was performed at the end of the dwell, using syringes and pre-weighed safe-lock tubes; the remaining dialysate in the peritoneal cavity was collected using gauze tissue and weighed using the same technique. The fluid taken from the gauze tissue accounted for 5% of total volume of the dialysate in both groups. Provided a 3.86% glucose dialysate density of 1.020±0.001 g/cm^3 in experimental conditions, the volume margin of error can be calculated as 0.1 µl. Values rounded off to 1 µl were used for both instilled and recovered volumes. These parameters were used to measure net UF by volumetry, as previously described (18). Mean arterial blood pressure was recorded using a pressure transducer (Harvard Apparatus, Holliston, MA) connected to the right common carotid artery in anesthetized mice at baseline and during 2-h dwells with 3.86% glucose.

The significant water removal and the resulting drop in blood pressure observed during PD had no effect on peritoneal water or solute transport in this mouse model (Suppl. Fig. 1). Samples from the visceral peritoneum were used for protein extraction, as previously described (Ni et al, 2005).

Intraperitoneal pressure and external abdominal compression. Direct assessment of intraperitoneal pressure (IPP) was performed in anesthetized mice using a catheter that was inserted in the peritoneal cavity and connected to a pressure transducer. This transducer was validated against a water column and showed a very close correlation with the gold standard technique (Pearson $r = 0.9991$, $P<0.0001$); the inter-assay coefficient of variability using the transducer was 2.4%. The circuit was filled and, after zeroing at the level of the heart, left at atmospheric pressure. IPP vs. IPV curves were obtained with the instillation of variable volumes of dialysate in the peritoneal cavity (via a cock in the circuit) and assessment of IPP on the transducer. In a subset of experiments, IPP was modulated by external abdominal compression to assess the effect of IPP on transperitoneal tracer kinetics. IPP was raised using a neonatal sphygmomanometer (Philips, Eindhoven, The Netherlands) that was applied around the abdomen of mice and inflated to produce and external abdominal compression, a method that has previously been applied to rats (Zakaria et al, 1995) and adapted to mice. IPP was continuously monitored, as previously described, raised to 10 mmHg, and maintained constant for the dwell duration.

Fluorescence and radioactivity assessment. Relative fluorescence intensity in the dialysate, plasma, and peritoneal membrane extracts was assessed on a LS55 fluorescence spectrometer (PerkinElmer) using appropriate standards to prevent quenching and nonspecific interference after tracer extraction, as described (Lin et al, 2011). Radioactivity in the dialysate, blood, and visceral peritoneum was assessed using a γ-counter (Cobra II, Canberra-Packard, Downers Grove, IL) with statistics ensuring <1% Poisson error (i.e., at least 10,000 counts/ positive sample).

Quantification of Alexa Fluor 555-BSA by HPLC. Proteins were separated by reverse-phase HPLC on a GRACE Vydac C4 column (214TP54, 4.6 mm x 25 cm) with an acetonitrile gradient in solvent A [2% (vol/vol) acetonitrile in 0.1% (vol/vol) trifluoroacetic acid]. Elution was performed with the following gradient program: 0 –90% solvent B [98% (vol/vol) acetonitrile in 0.085 trifluoroacetic acid] over 50 min at a flow rate of 500 µl/min generated by a model 1260 Agilent solvent delivery system. Absorbance was monitored simultaneously at three wavelengths, namely, 214, 280, and 555 nm. Quantification of protein was performed by integration of the area under the curve for each absorbance peak.

Free fractions of the fluorescent dye in the recovered dialysate. Ultramicrofiltration was performed on the recovered dialysate of mice to confirm the absence of free fraction of the fluorescent dye. Amicon columns with a nominal cutoff of 30,000 Da (Millipore, Bedford, MA) were loaded with 3.86% Dianeal containing Alexa Fluor 555- BSA sampled at the end of a 2-h dwell in SV129 mice, and centrifuged at 4,000 g for 10 min. Fluorescence was assessed on both the supernatant and the ultrafiltrate.

Nitrite/nitrate and albumin concentrations in the dialysate. The production of nitrite and nitrate in the dialysate was measured using a colorimetric assay (Cayman Chemical, Ann Arbor, MI). After 3-h incubation with nitrate reductase (670 mU/ml) and NADPH (160 mol/l) at room temperature, total nitrite concentration in the samples was measured by the Griess

reaction at 540 nm (Benchmark Plus Microplate Reader, Bio-Rad, Hercules, CA). Albumin concentration in the dialysate at the end of the dwell was assessed using the Bradford assay (Bio-Rad Protein Assay, Bio-Rad).

Statistical analysis. Data are presented as means ± SE. Comparisons between the means from different groups were performed using paired t-tests or one-way ANOVA, followed by Bonferroni's multiple comparison tests, as appropriate

CHAPTER II

AQF026 IS A PHARMACOLOGIC AGONIST OF THE WATER CHANNEL AQUAPORIN-1

Andrea J. Yool,* Johann Morelle,† Yvette Cnops,† Jean-Marc Verbavatz,‡ Ewan M. Campbell,* Elizabeth A.H. Beckett,* Grant W. Booker,§ Gary Flynn,| and Olivier Devuyst†¶

**School of Medical Sciences and the Adelaide Centre for Neuroscience Research and §School of Molecular & Biomedical Sciences, University of Adelaide, Adelaide, South Australia, Australia; †Division of Nephrology, Université catholique de Louvain Medical School, Brussels, Belgium; ‡Max Planck Institute of Molecular Cell Biology and Genetics, Dresden, Germany; |Spacefill Enterprises LLC, Tucson, Arizona; and ¶Institute of Physiology, Zurich Centre for Integrative Human Physiology, University of Zurich, Zurich, Switzerland*

***J Am Soc Nephrol*. 2013;24:1045-52**

SUMMARY

Aquaporin-1 (AQP1) facilitates the osmotic transport of water across the capillary endothelium, among other cell types, and thereby has a substantial role in ultrafiltration during peritoneal dialysis. At present, pharmacologic agents that enhance AQP1-mediated water transport, which would be expected to increase the efficiency of peritoneal dialysis, are not available.

Here, we describe AqF026, an aquaporin agonist that is a chemical derivative of the arylsulfonamide compound furosemide. In the *Xenopus laevis* oocyte system, extracellular AqF026 potentiated the channel activity of human AQP1 by >20% but had no effect on channel activity of AQP4. We found that the intracellular binding site for AQP1 I nvolves loop D, a region associated with channel gating. In a mouse model of peritoneal dialysis, AqF026 enhanced the osmotic transport of water across the peritoneal membrane but did not affect the osmotic gradient, the transport of small solutes, or the localization and expression of AQP1 on the plasma membrane. Furthermore, AqF026 did not potentiate water transport in *Aqp1*-null mice, suggesting that indirect mechanisms involving other channels or transporters were unlikely. Last, in a mouse gastric antrum preparation, AqF026 did not affect the Na-K-Cl cotransporter NKCC1.

In summary, AqF026 directly and specifically potentiates AQP1-mediated water transport, suggesting that it deserves additional investigation for applications such as peritoneal dialysis or clinical situations associated with defective water handling.

INTRODUCTION

Aquaporin-1 (AQP1) is the archetypal member of a family of membrane water channels that is conserved in mammals, microorganisms, and plants (Agre, 2004). Mammalian aquaporins (AQPs) are distributed in specific cell types in numerous tissues and organs, where they facilitate the osmotic transport of water and regulate body fluid homeostasis. Most AQPs are constitutively expressed in plasma membranes, where they exist as homo-tetramers. Each monomer has six membrane-spanning domains and two short hydrophobic loops containing conserved motifs and residues that are critical for the water selectivity of the pore (Fu et al, 2007). AQP1 is abundantly expressed in the endothelium-lining non-fenestrated capillaries located in the kidney, the airways, and the pleural and peritoneal membranes (Nielsen et al, 1993; Devuyst et al, 1998). In the kidney, AQP1 mediates the water transport across the vasa recta, which influences the medullary blood flow and urinary concentrating ability. A significant urinary-concentrating defect is observed in both *Aqp1*-null mice and humans deficient in AQP1 (Ma et al, 1998; King et al, 2001).

The development of pharmacologic agents able to modulate AQPs has been a highly anticipated goal, stimulated by insights in aquaporin structure and functional regulation (Verkman, 2012). As a proof of concept, induction of AQP1 transcription in endothelial cells by corticosteroids is associated with an increase in water trans-port *in vivo* (Stoenoiu et al, 2003). Antagonists for AQP1 and AQP4 have been developed, with a focus on arylsulfonamide compounds, including acetazolamide (Gao et al, 2006), antiepileptic agents (Huber et al, 2009), and derivatives of the loop diuretic bumetanide (Migliati et al, 2009). However, the effectiveness of acetazolamide and anti-epileptics as AQP blockers has been disputed (Yang et al, 2008). The bumetanide derivative AqB013 (Aq, aquaporin ligand; B, bumetanide scaffold) at 20 μM blocks AQP1 and AQP4 by a mechanism thought to involve physical occlusion of the intracellular water channel pore (Migliati et al, 2009). No direct pharmacologic agonist of AQPs has previously been described.

The functional relevance of AQP1 is particularly evident when osmotic water transport during peritoneal dialysis is considered (Devuyst et al, 2010). Peritoneal dialysis is based on diffusive and convective transport of solutes and water between peritoneal capillaries and a dialysis solution present in the peritoneal cavity. The capacity to remove water in excess across the peritoneal membrane (ultrafiltration) is a major predictor of outcome and mortality for patients treated by this modality (Brimble et al, 2006). Detailed

studies in *Aqp1*-null mice have demonstrated that AQP1 water channels correspond to water-specific pores located in peritoneal capillaries (Yang et al, 1999; Ni et al, 2006), which represent the major transport barrier of the membrane (Rippe et al, 1991). An agonist of AQP1 would be expected to enhance water transport and ultrafiltration, thereby increasing the efficiency of dialysis (Stoenoiu et al, 2003; Devuyst et al, 2010). Furthermore, because peritoneal dialysis allows the specific assessment of AQP1-mediated water transport, as opposed to effects on small solute transport and osmotic gradient, it is an advantageous model for assessing potential modulators of AQP1 *in vivo*.

RESULTS

In the present study, we tested the capacity of the novel agent AqF026 (Aq, aquaporin ligand; F, furosemide scaffold) to potentiate the water channel activity of AQP1 *in vitro* and *in vivo*. Rates of net water flux were measured in control and AQP1-expressing *Xenopus laevis* oocytes pre-incubated with and without externally applied AqF026 (Fig. 1). Increases in relative volume as a function of time in hypotonic saline (Fig. 1A) yielded slope values (relative swelling rates, Fig. 1B) that showed a maximal potentiation at 5 µM for AQP1, and loss of the agonist effect at AqF026 doses ≥100 µM. Dose-response curves (Fig. 1C) indicated an estimated half maximal effective concentration (EC_{50}) value of 3.3 µM for AQP1. AqF026 also potentiated the closely related AQP4, but with substantially reduced efficacy. AQP4-mediated water transport in-creased significantly only at ≥50 µM AqF026 (Fig. 1B-C). These results suggest a relatively high specificity for the potentiating effect, in that AqF026 distinguished between two aquaporins, AQP1 and AQP4, with >40% identity and 60% homology in amino acid sequence (based on GenBank Clustal analysis).

Using available crystal structure data, theoretical docking supported a direct interaction of AqF026 at a site located at the intracellular side of AQP1 (Fig. 2A). The chemically distinguishing feature of AqF026 compared with the parent compound furosemide is an aromatic ring linked to the sulfonamide moiety (Fig. 2B). *In silico* modeling suggested the binding of AqF026 involved residues in the loop D domain as well as other intracellular domain residues in the vicinity (Fig. 2C). Theoretical ligand docking suggested that the distinctive sulfhydryl-linked aromatic ring of AqF026 interacted with arginine 159 in human AQP1 (Arg 161 in bovine AQP1). Of note (Suppl.

Table 1), the equivalently positioned residue in AQP4 loop D is serine 180, the proposed site of water channel regulation by phos-phorylation (Zelenia et al, 2002). A second residue implicated in the putative AqF026-binding site in human AQP1 is threonine 157 (bovine Thr 159). The equivalent cysteine residue at position 178 in AQP4 loop D confers sensitivity to block by intracellularly applied mercurial compounds (Yukutake et al, 2008). The functional roles of AQP4 loop D residues support the proposal that the loop D region is an important regulatory do-main, and the observed differences be-tween AQP1 and AQP4 at key amino acid positions could contribute to the difference in efficacy of AqF026 (Fig. 1). Site-directed mutagenesis of intracellular residues in the AQP1 loop D domain that were modeled as being involved in ligand docking (Fig. 2D-E) showed that the agonist effect of AqF026 could be reversed by mutations of threonine 157 or arginine 159 and 160. Conversely, mutation of glycine 165, a loop D residue not implicated in the candidate binding site, did not prevent the agonist activity of AqF026. The magnitude of agonist potentiation with Gly165Pro was not significantly different from that seen with AqF026-treated wild type AQP1. A significant increase in osmotic water permeability over control levels demonstrated the functional expression of the AQP1 wild type and mutant constructs in the oocyte plasma membrane, a finding that was confirmed by immunocytochemical labeling and confocal imaging of whole oocytes (Fig. 2E). Taken together, these data demonstrate that AqF026 causes a dose-dependent potentiation of human AQP1 water channel activity and that the effect is likely to be mediated by ligand binding at an intracellular site involving specific amino acid residues in the loop D and possibly other adjacent intracellular domains.

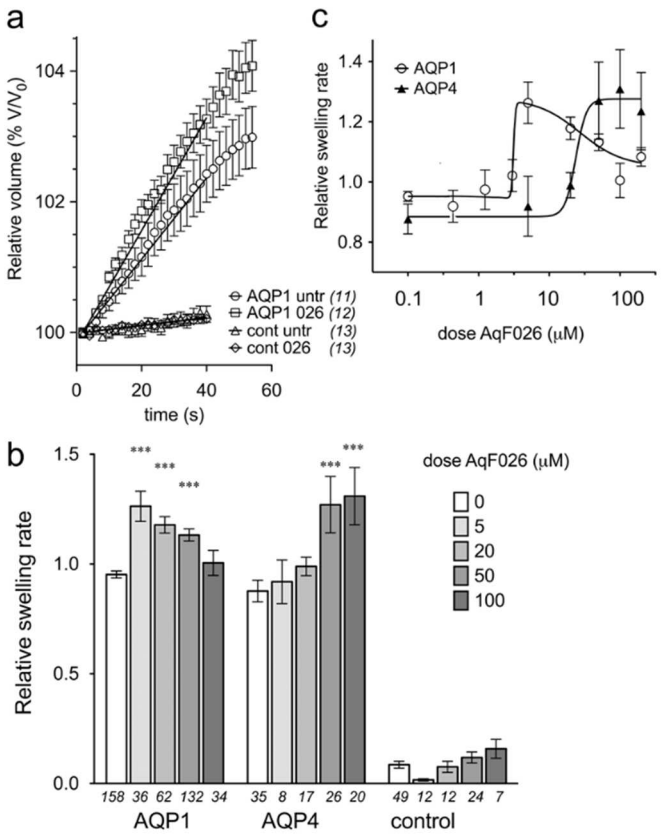

Figure 1. Potentiating effect of AqF026 on water channel activity of AQP1 and AQP4 expressed in *Xenopus laevis* oocytes. (A) Change in volume (V) due to osmotic swelling, standardized to the initial volume (V0) and plotted as a function of time in 50% hypotonic saline, for AQP1-expressing and -nonexpressing control (cont) oocytes. Oocytes were preincubated in 10 μM AqF026 or with DMSO alone (untr) as a vehicle control. Data are mean ± SEM for all oocytes tested in a single experimental day; n values are indicated in italics. (B) Histogram of compiled data showing maximal potentiation of AQP1 near 5 μM AqF026 and no potentiation of AQP4 at doses <50 μM. (C) Dose-response relationships for AqF026-mediated potentiation of AQP1 and AQP4 water channel activities, with an estimated EC_{50} value of 3.3 μM and a Hill coefficient of 1.8 for the stimulatory component for AQP1 (fit as the sum of two dose-response curves, one stimulatory and one inhibitory, using GraphPad Prism).

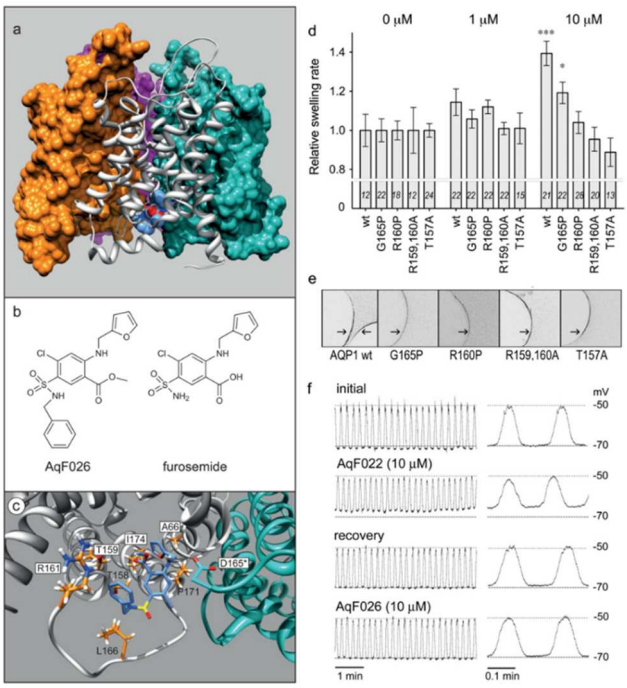

Figure 2. Ligand docking of AqF026 onAQP1: involvement of loop D domain residues and specificity of action using an NKCC1-sensitive bioassay. The identification of residues associated with the proposed intracellular binding pocket are based on the crystal structure of bovine AQP1. (A) Surface rendition of the tetramer with the docked pose of AqF026 in a ribbon structure of one AQP1 subunit. (B) Chemical structure of AqF026 and the parent compound furosemide. (C) A detailed view of the amino acid side chains relevant to the docked pose. The highlighted residue (D165*) indicates an amino acid contribution from a neighboring subunit. (D) Relative swelling rates were standardized to the untreated AQP1 wild-type or mutant channel responses within the same batches of oocytes, and data were compiled from at least three different batches for each group. Data are mean ± SEM; n values are shown in italics above the x axis. Asterisks indicate a significantly different effect for the comparison of 0 and 10 µM AqF026 for the same construct (*P<0.05; *** P<0.001). There was no significant difference between wild type and G165P at 10 µM (not indicated). (E) Confocal images of permeabilized immunolabeled oocytes expressing AQP1 wild-type or mutants, showing channel protein localization in plasma membranes (arrows). (F) Intracellular recording from a mouse gastric antrum preparation, continuously measured from a single circular smooth muscle cell. Traces show representative segments from the sequence: first confirming stable spontaneous slow-wave activity (initial); after treatment with a methylated furosemide compound (AqF022, 10 µM), which caused depolarization and a concomitant decline in slow-wave amplitude; after reversal of the effect by washout (recovery); and during the subsequent lack of effect of AqF026 (10 µM) over an extended period (30 minutes). Similar results were seen in three replicate cells.

To determine whether AqF026 retained any Na-K-Cl cotransporter (NKCC) blocking activity that is a hall-mark feature of the parent compound furosemide, we took advantage of a mouse gastrointestinal smooth muscle preparation as sensitive bioassay for NKCC activity (Fig. 2F). The mammalian gastrointestinal tract has pacemaker-driven slow-wave electrical activity, thought to be mediated by Ca^{2+}-activated chloride channels (Zhu et al, 2009). The maintenance of a negative baseline membrane potential is critically dependent on the function of NKCC1. Block of NKCC1 in mouse intestine with bumetanide (4 µM) produced a reversible 10-mV depolarization of the baseline membrane potential that was not seen in NKCC1 knockout mice (Wouters et al, 2006). Similar, reversible depolarizations were induced by bumetanide or by furosemide in the guinea pig gastric antrum (Tomita et al, 2000). We found that the classic slow-wave pattern in mouse gastric antrum similarly was altered within 10 minutes after application of a methylated furosemide agent (10 µM AqF022). The effect was reversed by washout, and AqF026 at the same dose had no discern-able effect on membrane potential or slow wave signaling over 30 minutes (Fig. 2F), indicating that the addition of the sulfonamide aryl group abolished any appreciable effect on NKCC1 while endowing AQP1 agonist activity. These results are consistent with structural modeling data indicating that the introduced aromatic ring appears to be key in the ligand interaction with loop D. Furthermore, the lack of effect of AqF026 on any properties of slow-wave signaling further supports the idea that this agent is unlikely to have indirect effects on general membrane properties or the broad array of channels and transporters also present in this preparation.

We used an established mouse model of peritoneal dialysis (Ni et al, 2005; Ni et al, 2006) to test the relevance of the agonist activity of AqF026 on water transport and ultrafiltration *in vivo* (Fig. 3). Treatment of wild-type mice with AqF026 resulted in an approximately 15% increase in fluid transport across the peritoneal membrane (Fig. 3A and Table 1), similar to the potentiation of AQP1 seen at 5-20 µM *in vitro*. The effect of AqF026 was dose dependent, with a maximal response observed for a concentration of 15 µM and an EC_{50} value of 4.2 µM (Fig. 3A). The effect of AqF026 on net ultrafiltration and initial ultrafiltration rate was maximal at about 120 minutes after injection (Fig. 3B), in agreement with *in vitro* studies. The ultrafiltration in *Aqp1*-null mice was 60% lower than in their wild-type littermates, and this measure was not affected by AqF026 administration (Fig. 3A). The agonist effect of AqF026 on osmotic water transport was further demonstrated by increased intraperitoneal volume curve over time (Fig. 3C) and an approximately 50%

increase in the initial ultrafiltration rate across the peritoneal membrane (Fig. 3D; 32.2±1.3 µl/min versus 21.9±0.8 µl/min, in AqF026 *versus* vehicle-treated *Aqp1*$^{+/+}$ mice, respectively; P<0.001). In contrast, treatment with AqF026 had no effect on the initial ultrafiltration rate in the *Aqp1*-null mice (Fig. 3D).

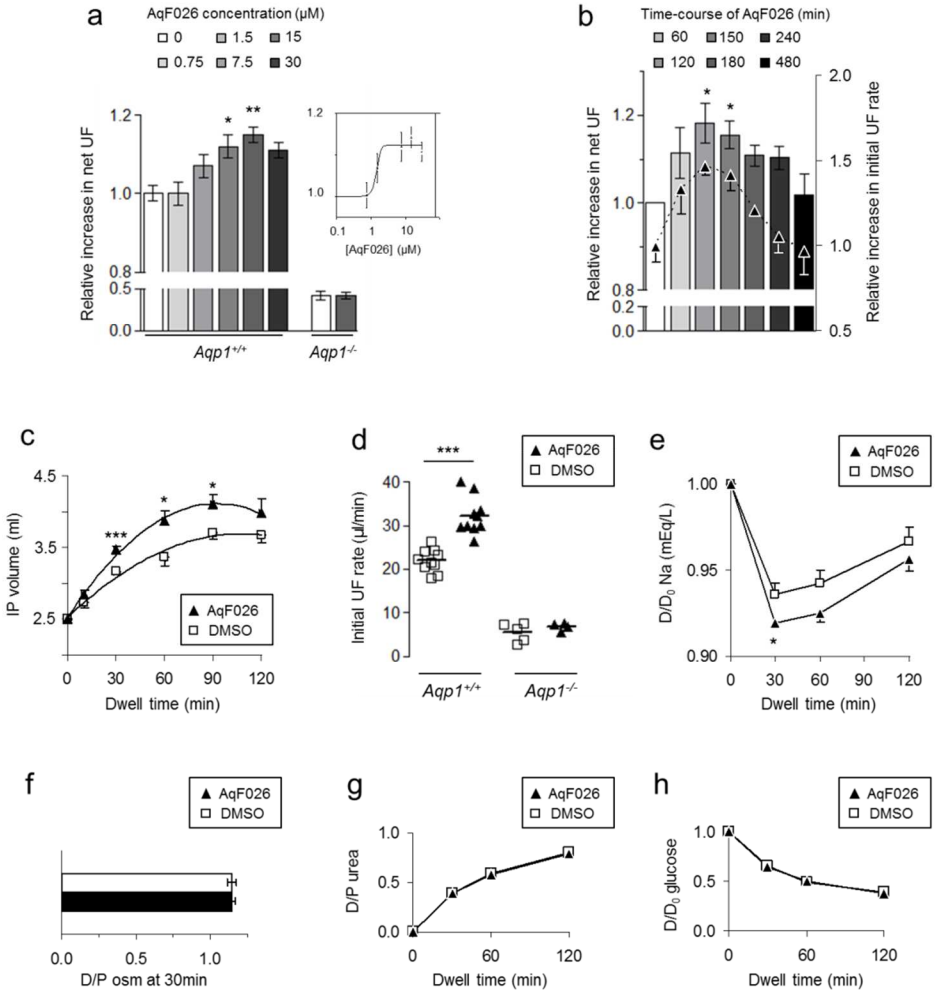

Figure 3. AqF026 specifically enhances AQP1-mediated osmotic water transport *in vivo*. (A) Wild-type *Aqp1*$^{+/+}$ mice treated with AqF026 have a significant, dose-dependent increase in net ultrafiltration (UF) across the peritoneal membrane. The maximal response is observed for a concentration of 15 µM, with an estimated EC_{50} value of 4.2 µM (inset). *Aqp1*$^{-/-}$ mice, characterized by a 60% reduction in ultrafiltration at baseline, show no potentiation of the ultrafiltration after treatment with 15 µM AqF026. Data are mean ± SEM; n=6 for each AqF026 concentration except for 0.75 µM (n=4). Net ultrafiltration rates were standardized to body weight and compared with rates in vehicle-treated mice (open bar). (B) Time course performed in wild-type mice shows that the effect of AqF026 (15 µM) on net ultrafiltration (bars) and initial ultrafiltration rate (triangles) is maximal 120-150 minutes after intravenous injection. Data are mean ± SEM; n=4 for each time point. Open bar corresponds to vehicle-treated mice. (C) Treatment of *Aqp1*$^{+/+}$ mice with 15 µM AqF026 results in increased intraperitoneal (IP) volume over time (P=0.02 between the AqF026 and vehicle curves), with significant differences at 30, 60, and 90 minutes in AqF026-treated (black triangles) compared with vehicle-treated (open squares) animals (P<0.01, P<0.05, and P<0.05 respectively; n=10 in each group). (D) Initial ultrafiltration rates, taken as an index of AQP1-mediated water transport during the first part of the dwell, are significantly increased in *Aqp1*$^{+/+}$ mice treated with 15 µM AqF026 *versus* vehicle (P<0.001, n=10 in each group). In contrast, AqF026 has no effect on the initial ultrafiltration rates in *Aqp1*$^{-/-}$ mice (AqF026, n=4 and vehicle-treated, n=5). (E) Treatment of wild-type mice with AqF026 (15 µM) induces a significant increase in sodium sieving (D/D_0 sodium at 30 min) compared with vehicle-treated animals (P<0.05; n=10 in each group). (F-H) The dialysate-to-plasma ratio of osmolality at 30 minutes (D/P_{osm}) (F), the dialysate-to-plasma ratio of urea (D/P_{urea}) (G), and the progressive removal of glucose from the dialysate (D/D_0 glucose) (H) were similar in mice treated with 15 µM AqF026 *versus* vehicle (n=12 pairs of *Aqp1*$^{+/+}$ mice).

Table1. Effect of AqF026 on water and small solute transport in vivo.

Group	Net UF (µl/g BW)	D/P_{osm} at 30min	MTAC urea (µl/min)
Aqp1$^{+/+}$ DMSO	37.2±1.3	1.14±0.03	35.0±2.3
Aqp1$^{+/+}$ AqF026	42.8±1.4[a]	1.15±0.03	34.2±1.7
Aqp1$^{-/-}$ DMSO	15.7±1.9[b]	1.28±0.02	35.5±3.6
Aqp1$^{-/-}$ AqF026	15.6±1.6[b]	1.27±0.03	36.4±7.0

Ultrafiltration and small solutes transport were measured in 16 pairs of *Aqp1*$^{+/+}$ mice and 6 pairs of *Aqp1*$^{-/-}$ mice. Osmolality was assessed in 12 pairs of *Aqp1*$^{+/+}$ mice and 6 pairs of *Aqp1*$^{-/-}$ mice. UF, ultrafiltration; BW, body weight; D/P_{osm}, dialysate-over-plasma osmolality; MTAC, mass transfer area coefficient (calculated from Waniewski equation, f=0.33). [a]P<0.05 AqF026 *versus* DMSO. [b]P<0.001 *versus Aqp1*$^{+/+}$.

The decrease in dialysate sodium concentration during the initial phase of a hypertonic dwell ('sodium sieving') is a reliable index of AQP1-mediated water transport in PD (Ni et al, 2006; Rippe et al, 1991). Administration of

AqF026 was also reflected by a significant increase in that variable (dip in sodium dialysate within the first 30 minutes of the dwell: 11.2±0.3 mEq/l *versus* 8.9±0.9 mEq/l in AqF026-treated *versus* vehicle-treated mice, n=10 pairs, *P*=0.03) (Fig. 3E). Administration of AqF026 had no detectable effects on the osmotic gradient (Fig. 3F and Table 1), small solute transport as measured for urea and glucose (Fig. 3G-H, and Table 1), and rate of albumin leakage in the dialysate (dialysis to plasma ratio albumin: 0.09±0.005 *versus* 0.10±0.003 in AqF026-treated *versus* vehicle-treated mice, n =6 pairs). No differences in urine output, hemolysis (lactate dehydrogenase), or liver toxicity (aspartate aminotransferase and alanine aminotransferase) variables were observed in mice exposed to AqF026 *versus* vehicle during the PD exchange (data not shown). Treatment with AqF026 did not appreciably change the levels of protein or mRNA expression of AQP1 in the peritoneum (Suppl. Fig. 1A-C). Immunogold electron microscopy showed that the distribution and abundance of AQP1 were not visibly different in wild-type mice treated with vehicle and AqF026 (density of AQP1-gold particles: 5.08±1.06 versus 5.78±0.63 particles/µm, respectively; n=7 pairs) (Suppl. Fig. 1D).

DISCUSSION

Results here are the first to define a pharmacologic ligand that potentiates AQP1 water channel activity, to show that it is effective *in vitro* and *in vivo*, and to identify a candidate molecular site of action. The data are consistent with direct binding of the novel arylsulfonamide compound AqF026 at a site involving the intracellular regulatory domain loop D in AQP1. The specificity of the drug on AQP1 is substantiated by several lines of evidence, obtained both *in vitro* and *in vivo*. First, AQP1 is much more sensitive to AqF026 than the closely related AQP4. Second, AqF026 has no effect on NKCC1 and no detectable diuretic effect during the peritoneal dialysis dwell. Third, AqF026 induces a strong increase in the initial ultrafiltration rate, reflecting the essential contribution of AQP1 to transcapillary ultrafiltration at this stage. The effect is abolished when AqF026 is administered to *Aqp1*-null mice. Fourth, the administration of AqF026 is reflected by an increase in the sodium sieving, which typically reflects the movement of free water through AQP1. Finally, the lack of effect of AqF026 on other compartments can be inferred by the unchanged transport of small solutes and the lack of structural changes in the membrane.

Modulators of AQP1 with translational potential have been slow to emerge. Blockers have only been described thus far, limited by toxicity, low efficacy, and lack of specificity (Yool et al, 2010). Arylsulfonamide compounds, including carbonic anhydrase inhibitors, appeared as potentially attractive candidates on the basis of efficacy and safety index (Gao et al, 2006; Huber et al; 2009). Of particular interest, a 4-aminopyridine carboxamide derivative of the loop diuretic bumetanide (AqB013) was shown to inhibit AQP1 *in vitro* (50% inhibitory concentration, approximately 20 μM, extracellularly) by acting at an intracellular side that occludes the water pore (Migliati et al, 2009).

In this study, we used another loop diuretic, furosemide, as a scaffold for the creation of the novel arylsulfonamide derivative, AqF026. Furosemide is relatively membrane impermeable, and it lacks a discernable effect on AQP1 or AQP4 water channel activity when applied extracellularly (Migliati et al, 2009). For the agonist AqF026, a furan-containing arylsulfonamide, the carboxylic acid of the furosemide scaffold was modified by conversion of its carboxylic acid group to a methyl ester and by addition of a benzyl group to the sulfonamide nitrogen. These modifications increased the calculated logP (logarithm of the oil:water partition coefficient, P) value to 2.97, a range that is consistent with drug-like properties (Leeson et al, 2007). An intracellular site of action of AqF026 on AQP1 channels was supported by the >1-hour latency for the agonist effect in the *Xenopus* system. Accumulating evidence suggests that AQPs are subject to complex mechanisms of regulation (Yool, 2007; Maurel et al, 2008). According to results of *in silico* modeling and mutagenesis, the added benzyl moiety appears to enable an interaction between the AqF026 ligand and residues in the proximal region of the loop D domain, within a zone that is increasingly investigated for AQP channel regulation (Yu et al, 2006; Törnroth-Horsefield et al, 2006; Campbell et al, 2012). In turn, such interaction could open the pore to increase unitary flux rates, remove a barrier or increase the probability of the open state.

The molecular mechanism for the biphasic action of AqF026 on AQP1 is not known. A testable hypothesis is that, at higher doses, the antagonistic effect might involve occlusion of the AQP1 water pore at the intracellular face at a site similar to that implicated for block by AqB013 (Migliati et al, 2009), whereas the agonist effect at lower doses appears to result from regulation of channel activity at a separate allosteric site involving loop D. Alternatively, AqF026 could have different effects at the same site depending on concentration.

Studies on *Aqp1* knockout mice have demonstrated that AQP1 facilitates the osmotic water transport across the peritoneal membrane (Yang et al, 1999). The fact that AqF026 increased water transport and ultrafiltration *in vivo* in this model, without detectable changes in small solute transport or modifications of the expression of AQP1, suggests this agent has translational potential for patients treated with peritoneal dialysis. As expected, the maximal potentiation of AQP1-mediated free-water transport occurs during the first part of the dwell, when the osmotic gradient is maximal. In agreement with previous studies addressing free-water transport in rat and mouse models (Stoenoiu et al, 2003; Ni et al, 2006) and simulations based on the three-pore model (B. Rippe, unpublished data), the effect of AqF026 on free-water transport was observed in the absence of any detectable change in small solute transport.

ESRD is a major global concern, and improved methods for delivering replacement therapy via peritoneal dialysis would be of substantial significance. The use of AQP1 agonists in patients undergoing peritoneal dialysis would be of prime interest in patients developing ultrafiltration failure, who may show water channel dysfunction alone or combined with enlarged vascular surface area and/or increased lymphatic absorption rate (Smit et al, 2004). By extension, a pharmacologic agonist of AQP1 might be useful in conditions associated with defective local water handling, including subretinal edema, neurodegenerative conditions and hydrocephaly, acute renal failure, and diabetes insipidus.

Because AqF026 is an agonist of AQP1 channels that are expressed in multiple organs, additional work on drug metabolism and potential toxicity will be important to evaluate potentially harmful effects. Loop diuretics are among the most widely used drugs worldwide, with a well-established safety index during acute or chronic administration (Musini et al, 2009). Our cumulative observations with arylsulfonamide compounds AqB013 and AqF026 in rodents suggest these derivatives are well tolerated and cause no appreciable overt tissue or organ toxicity under the specific conditions tested thus far.

The identification of the first pharmacologic agonist for AQP1 opens new avenues for analyses of AQP1-mediated water transport and has potential therapeutic value for clinical situations based on osmotic water transport, including peritoneal dialysis.

CONCISE METHODS

***In Vitro* Assays.** Expression of human AQP1 and rat AQP4 in *X. laevis* oocytes was done as described previously (Campbell et al, 2012). Site-directed mutations in AQP1 were generated by PCR using the QuikChange kit (Agilent Technologies, Australia). Non-AQP1-expressing control oocytes without cRNA injection were prepared from the same batches of oocytes. Responses were standardized to the mean swelling rate of the wild-type AQP1 untreated oocytes in the same batch of oocytes and compiled for multiple batches. All animal procedures were approved by the University of Adelaide Animal Ethics committee and performed in accord with the Australian Code of Practice for the Care and Use of Animals for Scientific Purposes.

***In Silico* Modeling.** The coordinates for the tetrameric model based on the crystal structure of bovine AQP1 were obtained from the Protein Data Bank (MMDB ID: 18789; PDB ID: 1J4N). The pdb file coordinates were prepared for docking by removing water molecules and adding charges using autodocktools-1.5.4. The co-ordinate files for the ligand molecules were obtained using Corina accessed via the National Cancer Institute's on-line SMILES translation tool and prepared for docking using autodocktools. The docking was performed using Autodock Vina (Trott et al, 2010) with a grid size of (80Å x 80 Å x 42Å) covering the entire cytoplasmic face of the tetramer. The highest ranked pose was used in the analysis.

AqF026 Synthesis and Application. AqF026 was prepared by following a two-step process, in which furosemide was first converted to its methyl ester derivative (AqF022); then, alkylation of the sulfonamide ester yielded AqF026 (Suppl. Fig. 2). Agents were purified by column chromatography. For *in vitro* assays of swelling, oocytes were incubated in isotonic Na^+ bath saline with AqF026 or DMSO vehicle before swelling assays. For *in vivo* studies, AqF026 or DMSO (vehicle control) diluted in sterile 0.9% NaCl was injected in the tail veins of mice at 30 minutes before the start of the experimental transport measurements.

Mouse Gastric Antrum Electrophysiology. By following published methods (Kim et al, 2002), adult Balb/C mice were anesthetized with isoflurane inhalation and euthanized by cervical dislocation. The stomach antral region (approximately 40 mm^2) with the mucosa removed was pinned into a recording chamber lined with Sylgard elastomer (Dow Corning), and maintained in 37°C Krebs solution (in mM: NaCl 118, KCl 4.75, $MgSO_4$ 1.2, $NaHCO_3$ 25, NaH_2PO_4 1, glucose 11 and $CaCl_2$ 2.5; pH 7.3) continuously bubbled with O_2 (95%) and CO_2 (5%). A Ca^{2+} channel antagonist nifedipine (dissolved at 10 mM in ethanol and used at a final concentration of 3 µM in control Krebs) minimized muscle contraction events. Circular smooth muscle cells were impaled with glass micro-electrodes filled with 3 M KCl (70–100 MOhm). The furosemide derivative AqF022 and the AQP agonist AqF026 were applied at final concentration (10 µM) with 0.01% DMSO in perfused Krebs; effects were re-versed by washout with control Krebs. Transmembrane potential was measured using a high impedance amplifier (Axoclamp-2B; Axon Instruments). Electrical signals were recorded with Axoscope 9.0 data acquisition software (Axon Instuments/Molecular Devices, Union City, CA).

***Aqp1* Mice.** Wild-type (*Aqp1*$^{+/+}$) and knockout (*Aqp1*$^{-/-}$) mice (Ma et al, 1998) were obtained from A.S. Verkman (University of California, San Francisco, CA). Studies were performed on sex-matched littermates aged 8-12 weeks. All animals had access to standard diet and tap water *ad libitum*. The experiments were conducted in accordance with the National Research

Council Guide for the Care and Use of Laboratory Animals and approved by the ethics committee of the Université catholique de Louvain.

Peritoneal Transport Studies and Tissue Sampling. Transport of water and solutes across the peritoneal membrane was investigated in a well-established mouse model of peritoneal dialysis (Ni et al, 2005; Ni et al, 2006). Changes in intraperitoneal volume over time and initial ultrafiltration rates were obtained using a fluorescent bovine serum albumin conjugate (Alexafluor555-BSA, Molecular Probe, Eugene, OR) as an indicator-dilution technique, as previously described (Ni et al, 2006; Lin et al, 2011). At the end of the dwell, mice were euthanized by exsanguination and samples were processed for mRNA and protein studies.

Real-time RT-PCR. Total RNA was extracted from peritoneum, treated with DNAse I and reverse-transcribed into cDNA with iScript TM cDNA Synthesis Kit (Bio-Rad Laboratories, Hercules, CA). Changes in target genes mRNA levels were determined by relative real-time quantitative PCR with a CFX96TM Real-Time PCR Detection System using iQ TM SYBR Green Supermix (Bio-Rad). Specific primers (Suppl. Table 2) were designed using Primer3 software. The normalization factor was based on the stability of four reference genes using the program geNorm version 3.4.

Immunoblotting. SDS-PAGE and immunoblotting were performed as described (Ni et al, 2006). The membranes were blocked, incubated overnight with polyclonal rabbit anti-AQP1 antibodies (Chemicon International, Temecula, CA), washed, incubated with secondary antibodies (Dako, Glostrup, Denmark), and visualized with enhanced chemiluminescence (Amersham, Little Chalfont, UK). Membranes were stripped and reprobed with a monoclonal antibody against ß-actin (Sigma, St. Louis, MO). Densitometry analyses were performed using NIH-Image V1-57 software.

Tissue Staining and Immunohistochemistry. Tissue samples were fixed in 4% paraformaldehyde and embedded in paraffin. Staining (hemalun-eosine and Sirius red) and immunostaining were performed as previously described (Ni et al, 2006). Oocytes were fixed on day 2 or 3 after cRNA injection in 4% paraformaldehyde, permeabilized for 1 hour with 0.1% Triton X-100, and incubated with rabbit polyclonal antibody against the carboxyl terminal domain of hAQP1 (kindly provided by WD Stamer, University of Arizona). Labeling was visualized with FITC-conjugated goat antirabbit antibody and imaged with a Leica TCS-4D laser scanning confocal microscope (Nussloch, Germany).

Transmission Electron Microscopy. Mouse peritoneum was processed for ultra-structural studies and immunogold labeling as previously reported (Ni et al, 2006). Sections were incubated with rabbit anti-AQP1 antibodies, followed by protein-A gold antirabbit antibody, and viewed using a Tecnai-12 microscope (FEI, Eindhoven). The number of particles per unit length of capillary was measured using the IMOD software.

Statistical Analyses. Data are given as mean ± SEM. Statistical significance was evaluated by one- or two-way ANOVA followed by *post hoc* Bonferroni tests, unless otherwise indicated.

CHAPTER III

INTERSTITIAL FIBROSIS RESTRICTS OSMOTIC WATER TRANSPORT IN ENCAPSULATING PERITONEAL SCLEROSIS

Johann Morelle[1], Amadou Sow,[1] Nicolas Hautem[1], Caroline Bouzin[2], Ralph Crott[3], Olivier Devuyst[1,4*], and Eric Goffin[1*]

[1]Division and laboratory of Nephrology, Cliniques universitaires Saint-Luc, Institute of experimental and clinical research, Université catholique de Louvain Medical School, Brussels, Belgium; [2] IREC Imaging Platform, Institute of experimental and clinical research, Université catholique de Louvain Medical School, Brussels, Belgium; [3]Public Health, Université catholique de Louvain Medical School, Brussels, Belgium; [4]Institute of Physiology, Zurich Center for Integrative Human Physiology, University of Zurich, Zurich, Switzerland

J Am Soc Nephrol. 2015;26:2521-33

SUMMARY

Encapsulating peritoneal sclerosis (EPS) is a rare but severe complication of peritoneal dialysis (PD) characterized by an extensive fibrosis of the peritoneum leading to bowel encapsulation and obstruction. Changes in peritoneal water transport have been suggested to precede EPS, but the mechanisms and potential predictive value of that transport defect have not been investigated.

Among 234 end-stage renal disease patients who initiated PD at our institution over a 20-year period, we evaluated changes in peritoneal transport over time on PD in 7 patients who subsequently developed EPS and in 28 matched controls, using 3.86% glucose peritoneal equilibration tests. As compared with long-term PD controls, patients with EPS showed an early loss of UF capacity and sodium sieving before the onset of overt EPS. Multivariate analysis revealed that loss of sodium sieving was the most powerful predictor of EPS in this cohort. We next assessed the molecular and structural mechanisms of impaired water transport in EPS using expression, structural and biochemical analyses of the peritoneal membrane. As compared with long-term PD controls and uremic patients, the EPS peritoneum showed a thicker submesothelial fibrosis, with increased collagen density and greater amount of thick collagen fibers. Reduced osmotic conductance strongly correlated with the degree of peritoneal fibrosis, but not with vasculopathy. Peritoneal fibrosis was paralleled by an excessive upregulation of vascular endothelial growth factor and endothelial nitric oxide synthase, while the expression of endothelial aquaporin-1 water channels was unaltered.

Our findings suggest that an early and disproportionate reduction in osmotic conductance during the course of PD is an independent predictor of EPS. This functional change is linked to specific alterations of the collagen matrix in the peritoneal membrane of patients with EPS, thereby validating the serial three pore membrane/fiber matrix and distributed models of peritoneal transport.

INTRODUCTION

Peritoneal dialysis (PD) is a technique of renal replacement therapy used by ~200.000 end-stage renal disease patients worldwide, a prevalence that is rapidly growing in many parts of the world (Jain et al, 2012; Mehrotra et al, 2011). Functional alterations of the peritoneal membrane constitute an obstacle to long-term PD, as they are associated with technical failure and increased morbidity and mortality (Davies et al, 2001; Devuyst et al, 2010; Devuyst et al, 2009). Prolonged exposure of the peritoneal membrane to non-physiologic dialysis solutions leads to vascular proliferation, vasculopathy and peritoneal fibrosis, with ensuing loss of ultrafiltration (UF) capacity resulting from enlarged vascular surface area, faster peritoneal solute transport rate and early dissipation of the osmotic gradient (Davies et al, 2001; Devuyst et al, 2010; Davies et al, 1998; Williams et al, 2002; Williams et al, 2003; Honda et al, 2008).

Encapsulating peritoneal sclerosis (EPS) is an exaggerated fibrogenic response of the peritoneal membrane, leading to encapsulation of the bowels and intestinal obstruction. This entity constitutes the most severe complication of PD (for review, Korte et al, 2011). Although EPS affects a minority (0.9-3.5%) of patients on long-term PD, it has a mortality rate reaching 50%, resulting from intestinal occlusion, malnutrition, and sepsis (Korte et al, 2011). EPS is probably a multifactorial disease, in which PD duration represents an important risk factor (Brown et al, 2009; Johnson et al, 2010; Korte et al, 2011). Other conditions that have been inconsistently associated with EPS include cumulative glucose exposure, younger age, peritonitis episodes, beta-blockers and kidney transplantation (Brown et al, 2009; Johnson et al, 2010; Korte et al, 2011). Surprisingly, symptoms of EPS occur after PD withdrawal in most cases (Brown et al, 2009; Johnson et al, 2010; Korte et al, 2011). There is currently no definitive criteria that enable the detection of early stages of EPS. Arguably, a better understanding of the early phase of the disease may help identifying patients at risk and developing prevention strategies. Preliminary studies suggested that a progressive loss of UF capacity often precedes EPS development (Lambie et al, 2010; Sampinon et al, 2011). However, these studies were limited by small numbers, the absence of appropriate matching with long-term PD controls and/or a lack of evaluation of free-water transport. In addition, the mechanisms of impaired water transport in EPS patients have not been investigated and remain unelucidated.

In this study, we took advantage of a large cohort of incident PD patients who underwent a systematic functional evaluation of the peritoneal membrane at baseline and during the course of PD, and of a unique collection of peritoneal biopsies to evaluate the specific changes in transport parameters and molecular components of the peritoneal membrane of patients with EPS vs. appropriate controls. For the first time, we provide evidence linking the development of a specific fibrotic reaction with an early loss of water transport in the peritoneal membrane of EPS patients.

RESULTS

Early loss in UF and sodium sieving predicts EPS

We first assessed the evolution of peritoneal transport parameters in PD patients who subsequently developed EPS, compared to PD controls without EPS, matched in a 1:4 ratio for PD duration and gender. Peritoneal function was assessed yearly, with a modified 3.86% glucose-based peritoneal equilibration test (PET). We identified 7 cases of EPS among the 234 end-stage renal disease patients who initiated PD at our

Table 1. Demographic and clinical characteristics of patients with EPS

Age at PD Onset (yr)	Sex	Renal Disease	PD Duration (mo)	RRT after PD	Time from PD Withdrawal to EPS (mo)	Recurrent Bowel Occlusion	Symptoms at Diagnosis	CT Diagnosis	Surgical Diagnosis	Outcome after EPS	Time from EPS Diagnosis to Death (mo)	Cause of Death
52	M	MPGN	102	TP	1.8	+	FNVP	+	+	Death	82	Bowel occlusion
57	M	Diabetic	60	HD (UFF)	25.0	+	FNVP, bloody ascites	+	NA	Death	6.6	Septic shock (peripheral arteritis)
39	M	Renal dysplasia	59	HD (UFF)	2.8	+	FNVP bloody ascites	+	+	Death	36.4	Septic shock (endocarditis)
62	M	Vascular	55	TP	2.5	+	FNVP	+	+	Alive, functioning transplant	NA	NA
34	F	Undetermined	39	HD (UFF and EPS)	0.0	+	NVP	+	+	Death	23.5	Bowel perforation
45	F	GN	34	HD (umbilical hernia)	49.6	+	NVP	+	+	Death	3.0	Undetermined
42	M	Undetermined	57	TP (UFF and EPS)	−2.8	+	NVP	+	NA	Alive, functioning transplant	NA	NA

M, male; F, female; MPGN, membranoproliferative GN; TP, transplantation; HD, hemodialysis; UFF, ultrafiltration failure; +, positive; F, fever; N, nausea; V, vomiting; P, pain; CT, computed tomography; −, negative; NA, not applicable.

institution between January 01, 1994 and December 31, 2013, representing an overall incidence of 3.0%. Demographic and clinical features of EPS patients are presented in Table 1; age at PD onset was 47.5 ± 3.6 years, sex ratio 5M/2F, and PD exposure 57.8 ± 7.6 months; EPS occurred after PD withdrawal in 5 out of 7 patients.

The comparison of baseline demographic and clinical data between cases and controls is shown in Table 2. The matching for PD duration and gender was effective. The net UF, sodium sieving and small solute transport parameters at baseline were similar in both groups. There were no significant differences in terms of PD modality, glucose exposure and peritonitis rates.

The longitudinal evolution of peritoneal transport parameters is shown in Figure 1. A total of 147 PETs were analysed, and the mean number of PETs per patient was 4.3 ± 0.5 and 4.0 ± 0.3 in EPS and control groups, respectively. Patients who subsequently developed EPS showed a progressive decline in water transport, with significantly lower net UF values during the last 2 years on PD, as compared with matched controls (Fig. 1A). This loss of UF capacity was associated with an increased solute transport (Fig. 1B). Importantly, increased solute transport did not fully account for the disproportionate loss of water transport, suggesting an uncoupling between water and solute transport in the EPS peritoneal membrane (Fig. 1C). In parallel, sodium sieving - a reliable indicator of free water transport and osmotic conductance -progressively decreased in the EPS group with time on PD, and this decline was faster in EPS than in controls (annual loss in sodium sieving -0.011 ± 0.001 versus -0.003 ± 0.001 in EPS versus control patients, respectively; P=0.0046) (Fig. 1D-E). The reduced osmotic conductance observed in EPS patients during the last 2 years on PD was associated with higher glucose exposure and a trend toward better preserved residual renal function in the same period, as compared with PD controls (Suppl. Fig. 1).

Table 2. Clinical, functional, and treatment characteristics of patients with EPS and long-term PD controls

Characteristic	Patients with EPS (*n*=7)	Controls (*n*=28)	*P* Value
Men	71	71	1.00
PD duration, mo	57.8±7.6	55.9±4.2	0.84
Age at PD start, yr	47.5±3.6	56.9±3.4	0.09
Underlying nephropathy			0.24
GN	43	32	
Vascular nephropathy	14	21	
Chronic pyelonephritis	0	21	
Genetic disease	14	21	
Other or undetermined	29	4	
Charlson comorbidity index	4.9±1.0	4.6±0.4	0.85
Diabetes, *n*	2	4	0.17
Residual diuresis, ml/d	1083±159	1021±130	0.78
Body mass index, kg/m^2	22.9±1.1	22.3±0.6	0.67
Medications			
ACE inhibitors and/or ARBs	57	63	0.78
Statins	43	29	0.10
β-blockers	29	14	0.58
Baseline adequacy			
Peritoneal Kt/V	1.51±0.22	1.46±0.07	0.84
Residual Kt/V	0.97±0.16	0.80±0.09	0.42
Total Kt/V	2.48±0.15	2.23±0.09	0.20
Baseline functional parameters			
Net UF, ml	743±124	648±57	0.54
D/P creatinine, 4 h	0.75±0.05	0.74±0.05	0.96
Sodium sieving	0.05±0.01	0.05±0.01	0.44
PD modality, % APD	100	68	0.11
Glucose and icodextrin exposure			
Mean annual glucose exposure, kg	122±9	110±7	0.20
Mean annual icodextrin exposure, kg	51±4	47±3	0.43
Peritonitis			
Patients with peritonitis	71	71	1.00
No. of peritonitis per patient	1.4±0.4	1.3±0.2	0.84
Peritonitis rate, patient^{-1}×year^{-1}	0.36±0.11	0.30±0.05	0.66
Patients with GNR peritonitis	14	43	0.12

Data are presented as the mean±SEM or percentage, unless otherwise indicated. ACE, angiotensin converting enzyme; ARB, angiotensin 2 receptor antagonist; D/P, dialysate-over-plasma; APD, automated peritoneal dialysis; GNR, Gram-negative rod.

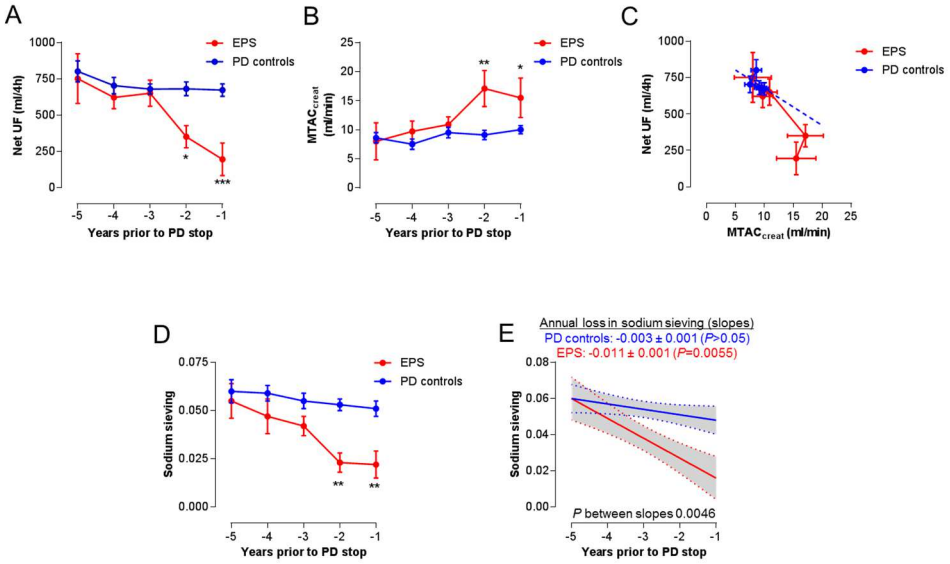

Figure 1. Early loss in UF capacity and sodium sieving in patients with EPS. (A) Patients who will develop EPS (red) have a premature loss in UF capacity, approximately 2 years before PD withdrawal, compared with PD controls (blue) matched in a 4:1 ratio for PD duration and sex. Control patients show a trend to lower UF with time on PD. (B) Small solute transport, evaluated by MTAC creatinine, tends to increase in PD controls but is significantly higher with time on PD in patients with EPS. (C) The loss of UF capacity is disproportionate to the increased MTAC creatinine in patients with EPS, suggestive of an uncoupling between peritoneal fluid and solute transport. The blue line corresponds to the projection of linear regression of net UF in control patients. (D) The sodium sieving significantly decreases with time on PD in patients with EPS, supporting the development of a low osmotic conductance to glucose. (E) The decline in sodium sieving over time on PD is more severe in patients with EPS compared with controls (slope -0.011±0.001 versus -0.003±0.001 in patients with EPS and controls, respectively; P=0.01). Longitudinal follow-up of membrane function was performed with annual modified 3.86% glucose-based dialysate. Data are presented as the mean ± SEM (A–D) or mean ± 95% confidence interval (E). n=7 patients with EPS versus n=28 PD duration-matched and sex-matched controls. *P<0.05; **P<0.01; ***P<0.001. MTAC, mass transfer area coefficient.

We next performed a multivariate analysis to test the predictive value of low sodium sieving values during the course of PD for subsequent development of EPS (Table 3). In this cohort, a first model (without considering sodium sieving values) identified younger age at dialysis onset, longer PD duration, lower residual kidney function, beta-blocker use and peritonitis rate as risk factors associated with EPS (Table 3). Among all potential risk factors integrated in this model, glucose exposure was the only variable that was not independently associated with the disease. Adding sodium sieving to the model showed that impaired free-water transport is a powerful and independent risk factor associated with EPS, outperforming other variables (Table 3). Logistic regression analysis showed a gradual increase in the risk of EPS with declining sodium sieving during the course of PD. In this cohort of long-term PD patients, the risk of EPS is negligible for patients with preserved UF capacity and sodium sieving during the whole course of PD, but increases above 25% for sodium sieving values ≤0.04, and to >50% for values ≤0.02. This risk is even greater for patients developing UF failure during the course of PD (Fig. 2).

Altogether, these analyses demonstrate that UF capacity is impaired in EPS patients before disease onset, resulting from an uncoupling with solute transport. Furthermore, there is a significant decline in sodium sieving in EPS cases, as compared with matched long-term PD controls. Multivariate analysis demonstrated that impairment in osmotic conductance to glucose during the course of PD is the most powerful indicator for the development of this rare complication and can help identifying patients at risk.

Table 3. Multivariate analysis performed using a logistic regression random-effects model and including potential risk factors for EPS, alone (model 1) or in association with the mean value of sodium sieving during the 2 last years of PD (model 2)

Characteristic	Model 1		Model 2	
	Coefficient (95% Confidence Interval)	*P* Value	Coefficient (95% Confidence Interval)	*P* Value
Sex	11.5 (−13.1 to 36.0)	0.36	2.4 (−1.8 to 6.7)	0.27
Age at PD start	−1.15 (−1.7 to −0.6)	<0.001	−0.1 (−0.2 to 0.05)	0.21
PD duration	0.6 (0.2 to 1.0)	0.003	7.10^{-4} (−0.07 to 0.08)	0.99
Residual Kt/V	33.6 (11.2 to 56.0)	0.003	−0.3 (−4.45 to 3.8)	0.87
β-blocker use	53.1 (27.7 to 78.5)	<0.001	4.2 (−1.1 to 9.5)	0.12
Peritonitis rate	20.8 (7.7 to 33.9)	0.002	0.4 (−2.8 to 3.6)	0.24
Annual glucose exposure	-9.4×10^{-5} (-3.1×10^{-4} to 1.2×10^{-4})	0.39	1.0×10^{-5} (-3.5×10^{-5} to 5.8×10^{-5})	0.46
Sodium sieving			−186.7 (−340.4 to −33.0)	0.02

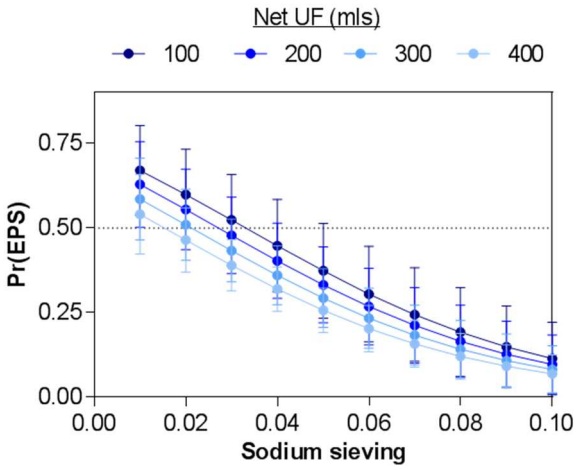

Figure 2. Low sodium sieving and net ultrafiltration during PD are predictive of the risk of EPS. The risk of EPS, estimated by logistic regression analysis, progressively increases with lower values of sodium sieving and impaired UF capacity. In this cohort of long-term PD patients, the combination of UF failure (<400 ml during the 4-hour 3.86% modified PET) with a sodium sieving <0.03 is associated with a risk of EPS .50%. All values of sodium sieving and net UF obtained during the course of PD are included in the logistic regression analysis. n=7 patients with EPS versus n=28 long-term PD controls. Pr(EPS), probability of developing EPS.

Expression of AQP1, eNOS and VEGF in the EPS peritoneum

Since AQP1 water channels mediate free-water transport and sodium sieving during PD (Ni et al, 2006), we evaluated their expression in the peritoneal membrane of EPS and long-term PD controls (Fig. 3). Clinical and functional characteristics of EPS and PD controls from whom peritoneal biopsies were analysed are provided in Suppl. table 1; the duration of PD exposure (62.4 ± 9.3 and 62.8 ± 9.2 months in control and EPS patients, respectively; *P*=0.98) and the number of peritonitis (1.5 ± 0.4 and 1.4 ± 0.4 in EPS and long-term PD, respectively; *P*=0.91) were similar in both groups. Parameters of peritoneal water and solute transport were comparable to those of the case-control study cohort.

Confocal immunofluorescence microscopy showed similar patterns of expression and density of AQP1 in the endothelium lining peritoneal capillaries in EPS and controls (mean fluorescence intensity in AQP1-positive areas: 79 ± 5 AU versus 82 ± 6 AU in EPS and PD controls,

respectively; *P*=0.71) (Fig. 3A-C). In contrast, the expression of the von Willebrand Factor (vWF), used as endothelial marker, was significantly upregulated in samples from EPS as compared with controls (mean fluorescence intensity in vWF-positive areas: 90 ± 5 AU versus 73 ± 3 AU in EPS and PD controls, respectively; *P*=0.01) (Fig. 3A-C). vWF-stained area was also significantly increased in the peritoneal membrane of EPS patients as compared with PD controls (*P*=0.01), together with a parallel increase in AQP1-positive area (Fig. 3D).

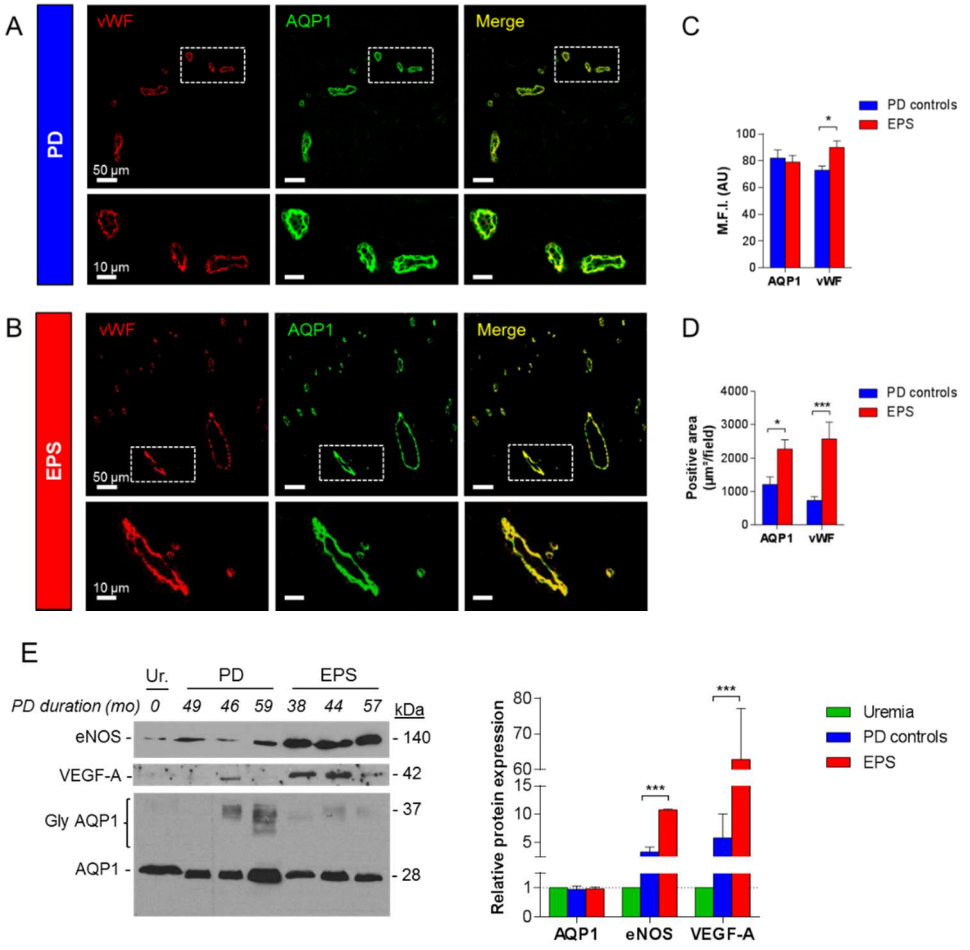

Figure 3. Expression of AQP1 in the peritoneum of patients with EPS. (A and B) Representative pictures of double immunostaining with anti-AQP1 (green channel) and anti-vWf (red channel) antibodies viewed under confocal fluorescence microscopy in peritoneal sections from a patient with EPS (A) and a long-term PD control (B). AQP1 is expressed in endothelial cells lining the capillaries and small vessels in the peritoneal membrane, both in the patient with EPS with impaired water transport (net UF=190 ml, and sodium sieving=0.02, during a 4-hour modified 3.86% glucose base PET) and in the long-term PD control (net UF 675 ml and sodium sieving 0.04). (C) MFI in AQP1-positive and vWf-positive areas in peritoneal sections of PD controls (blue) and patients with EPS (red). In contrast with the stable fluorescent intensity of AQP1, the endothelial marker vWf is significantly upregulated in peritoneal vessels from patients with EPS compared with PD controls. (D) Increase in both AQP1-positive and vWf-positive areas in the peritoneal membrane of patients with EPS compared with controls, suggesting vascular proliferation. n=7 long-term PD controls, and n=7 patients with EPS. (E) Representative immunoblot images and quantitative data showing levels of eNOS, VEGF-A, and AQP1 in the peritoneum of three patients with EPS, three PD duration-matched patients, and one uremic patient. PD controls and patients with EPS show a significant upregulation of eNOS (3- and 11-fold, respectively) and VEGF-A (6- and 63-fold, respectively) in their peritoneal membrane, whereas the expression of AQP1 remains unchanged. Twenty micrograms of proteins are loaded in each lane. Molecular mass (in kilodaltons) is indicated on the right side of the blot. PD duration (months) is indicated in italics. MFI, mean fluorescence intensity; A.U., arbitrary units; gly AQP1 and AQP1, glycosylated and unglycosylated isoforms of AQP1. **P*<0.05; ****P*<0.001. Bar, 50 mm in A and B (low magnification); 10 mm in A and B (detail). Original magnification, x20.

Immunoblotting (Fig. 3E) confirmed a virtually unchanged expression of AQP1 in the peritoneal membrane of patients with EPS, contrasting with the increased expression of the endothelial nitric oxide synthase (eNOS), as compared with PD-duration matched controls and uremic patients (relative AQP1 expression: 0.96 ± 0.06, 0.94 ± 0.12 and 1.00 [ref.], respectively; *P*=0.99; and relative eNOS expression: 10.8 ± 0.1, 3.3 ± 0.9 and 1.0 [ref], in the peritoneal membrane of EPS, PD and uremic patients, respectively; *P*<0.001) (Fig. 3E). The upregulation of eNOS in the peritoneum of EPS patients was paralleled by an increased expression of the vascular endothelial growth-factor (VEGF)-A (relative VEGF-A expression 62.8 ± 14.4, 5.8 ± 4.2 and 1.0 [ref] in EPS, PD and uremic peritoneum, respectively; *P*=0.003) (Fig. 3E).

Overall, these data demonstrate that the impaired UF capacity and free-water transport observed in EPS patients was not associated with an alteration in the expression of the AQP1 water channels, but with a significant upregulation of eNOS and VEGF.

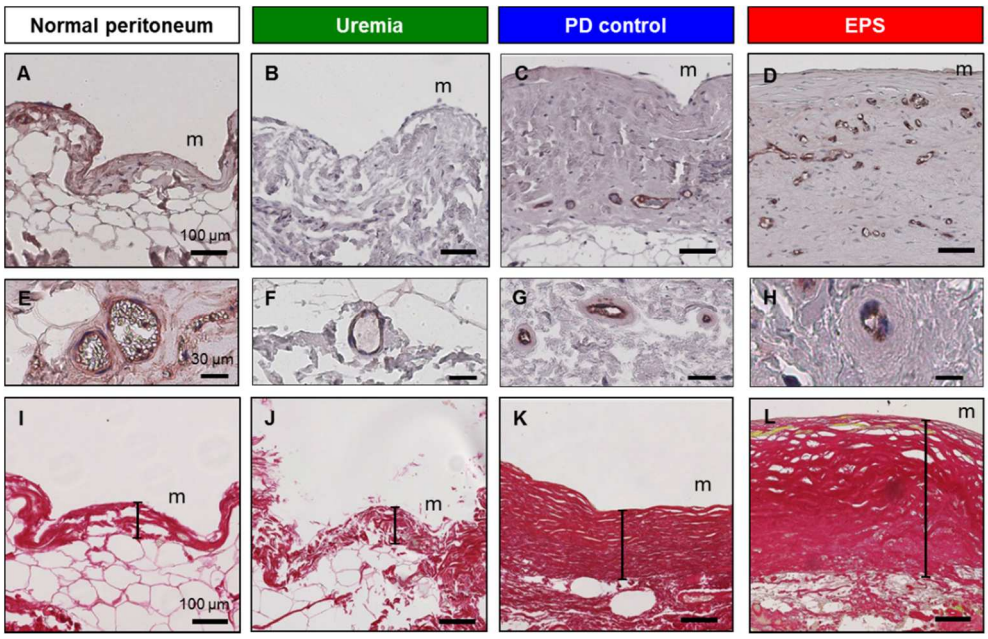
Normal peritoneum
Uremia
PD control
EPS
A
B
C
D
E
F
G
H
I
J
K
L
m
100 µm
30 µm

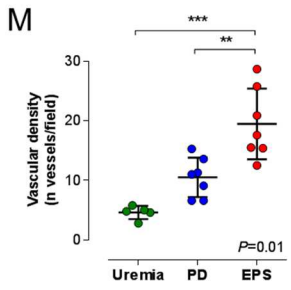
M
***
**
Vascular density (n vessels/field)
30
20
10
0
P=0.01
Uremia
PD
EPS

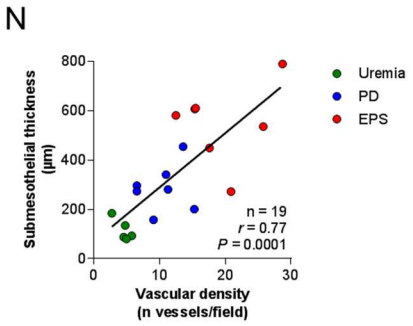
N
Submesothelial thickness (µm)
800
600
400
200
0
n = 19
r = 0.77
P = 0.0001
0
10
20
30
Vascular density (n vessels/field)
Uremia
PD
EPS

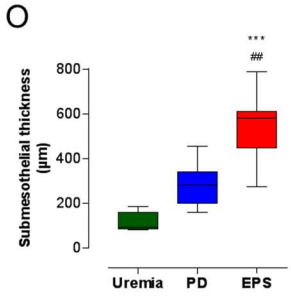
O
Submesothelial thickness (µm)
800
600
400
200
0
***
##
Uremia
PD
EPS

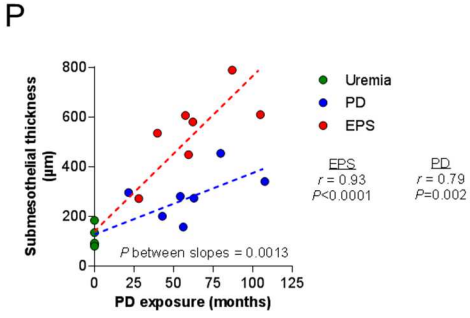
P
Submesothelial thickness (µm)
800
600
400
200
0
P between slopes = 0.0013
0
25
50
75
100
125
PD exposure (months)
Uremia
PD
EPS
EPS
r = 0.93
P<0.0001
PD
r = 0.79
P=0.002

Figure 4. The EPS peritoneum is characterized by an excessive vascular and fibrotic response to PD. (A–D) Immunostaining for vWf in normal (A), uremic (B), control PD (C), and EPS (D) peritoneum shows a progressive vascular proliferation from A to D. (E-H) Representative sections of peritoneum with evaluation of the degree of vasculopathy in the postcapillary venules stained for vWf in normal (E), uremic (F), control PD (G), and EPS (H) peritoneum. Long-term exposure to PD and EPS both associate with a thickening of the capillary wall in venules with a 25- to 50-µm diameter. (I-L) Representative sections of parietal peritoneum from normal (I), uremic (J), control PD (K), and EPS (L) peritoneum stained with picrosirius red. Submesothelial thickness, represented by the vertical bar drawn between the mesothelial surface and the upper limit of the adipose tissue, significantly increases from I to L. (M-O) Peritoneal vascular proliferation and fibrosis are more severe in patients with EPS compared with PD controls matched for the same PD duration. (P) Submesothelial fibrosis correlates with time on PD in both groups, but correlation is clearly steeper in patients with EPS compared with PD patients with no EPS. Peritoneal samples are from five uremic patients, seven long-term PD patients without EPS, and seven patients with EPS. Circles represent individuals (M, N, and P; green circles for uremic, blue for PD controls, and red for patients with EPS). Box and whiskers (minimum to maximum) are represented in C. $^{\#\#}P<0.01$ versus PD; $^{**}P<0.01$; $^{***}P<0.001$ versus uremia. m, mesothelium. Bar, 100 mm in A–D and I–L. Original magnification, x20 in A-D and I-L (top); x40 in A-D and I-L (bottom).

The peritoneal membrane of EPS patients undergoes severe angiogenesis and submesothelial fibrosis

Since both eNOS and VEGF promote angiogenesis and vascular permeability (Papapetropoulos et al, 1997), participating to fibrinogen leakage and stroma generation, we next evaluated the degree of angiogenesis and fibrosis in the peritoneal membrane of uremic, long-term PD and EPS patients (Fig. 4). Vascular density and submesothelial thickness were evaluated by light microscopy, in vWF- or picrosirius red -stained peritoneal sections, respectively, and quantified in each group. As compared to patients with uremia (Fig. 4; B, F and J), exposure to PD led to vascular proliferation and peritoneal fibrosis in the submesothelial area (Fig. 4; C, G and K), both processes progressing in parallel in the membrane (Fig. 4; M, N and O). For a same PD duration, patients with EPS had increased vascular densities and submesothelial thickness as compared with controls (vascular density: 19.5 ± 2.1 versus 10.5 ± 1.2 vessels/field, $P<0.01$; submesothelial thickness: 549 ± 56 versus 287 ± 34 µm in EPS versus PD controls, respectively; $P<0.001$), with slopes of fibrosis progression that were significantly higher in the former group (Fig. 4P; $P=0.001$). Signs of vasculopathy also increased with time on PD but to a same extent in EPS and non-EPS patients (lumen-to-vessel ratio

of post-capillary venules decreases from 0.72 ± 0.03 in uremic patients, to 0.51 ± 0.07 and 0.45 ± 0.06 in PD controls and EPS patients; *P*=0.57) (Fig. 4E-H, and Suppl. Fig. 2).

These data demonstrate that EPS patients are characterized by an excessive angiogenic and fibrotic response to PD exposure in the peritoneal membrane, causing severe peritoneal remodelling and scarring.

Specific changes in collagen density and quality in the peritoneum of EPS patients

To test whether EPS was also associated with qualitative changes in the peritoneal interstitium, we next assessed peritoneal collagen density and structure using picrosirius red polarization microscopy. This methodology allows the detection and structural analysis of collagen content based on its anisotropic molecular organization and birefringence under polarized light (Whittaker et al, 1989; Ducharme et al, 2000) (Fig. 5). These analyses revealed a 1.8 and 2.7-fold increase in the density of collagen fibers in the peritoneum of EPS, as compared with control PD and uremic patients, respectively (collagen volume fraction: 40.9 ± 2.9%, 22.3 ± 1.5%, and 14.9 ± 0.7% in EPS, PD, and uremic patients, respectively; *P*<0.001) (Fig. 5A-D). The increased density was paralleled by a change in the structure of collagen bundles in the submesothelial area, with an accumulation of thicker, red-orange, fibers in the EPS peritoneum, while the relative amount of thinner, green-yellow fibers remained unchanged (relative increase in red-positive area in the submesothelial area 2.2 ± 0.2; 1.5 ± 0.2 and 1.0 ± 0.1 [ref.], *P*=0.002; relative increase in green-positive area 0.8 ± 0.2, 1.0 ± 0.1 and 1.0 ± 0.05 [ref.], *P*=0.59, in the submesothelial area of EPS, PD and uremic patients, respectively) (Fig. 5E-K). These data demonstrate specific qualitative changes in the fibrotic interstitium of EPS patients, with increased collagen density and more abundant thick collagen fibers.

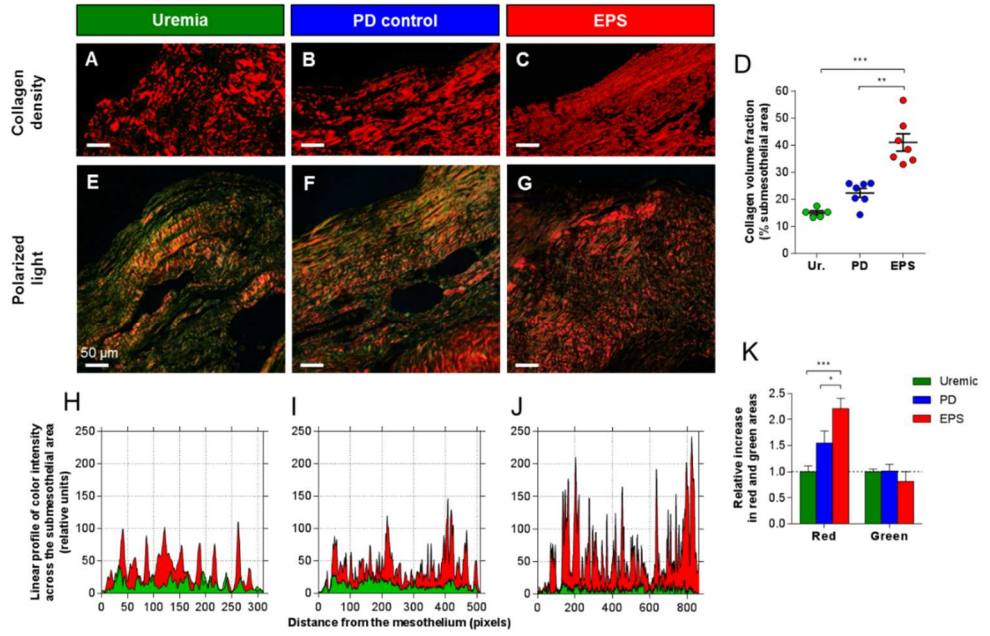

Figure 5. Changes in collagen density and quality in the peritoneal interstitium of patients with EPS. (A-C) Representative sections of the parietal peritoneum from uremic (A), PD (B), and EPS (C) patients stained with picrosirius red and visualized under circularly polarized light. Stained tissue (red mask) indicates collagen fibers in the submesothelial area. (D) Collagen volume fraction from picrosirius red-stained peritoneum as percentage of submesothelial area from uremic (green circles), PD (blue), and EPS (red) patients. (E-G) Representative sections of the peritoneum from uremic (E), PD (F), and EPS (G) patients stained with picrosirius red, visualized under circularly polarized light. Thick collagen fibers appear red-orange and thinner ones are green-yellow. (H-J) Profile of red and green intensities along a line perpendicular to the mesothelial surface, from the mesothelium to the adipose tissue in peritoneal biopsies from uremic (H), PD (I), and EPS (J) patients. The x axis represents the distance from the mesothelial surface, in pixels. (K) Relative increase in the red- and green-positive areas in the submesothelium of uremic (reference), PD, and EPS patients. The relative proportion of red, thicker, collagen fibers increases in the EPS submesothelial area compared with uremic and PD controls. Data are the mean±SEM. n=5, n=7, and n=7 in uremic, long-term PD, and EPS peritoneum, respectively. **P*<0.05; ***P*<0.01; ****P*<0.001. Bar, 50 mm. Original magnification, x20.

Fibrotic changes in the peritoneum of EPS patients associate with impaired water but not solute transport

Finally, we tested whether the morphological changes observed in the peritoneal membrane of EPS patients are involved in the early loss of osmotic conductance to glucose which characterizes these patients. Indeed, the three-pore model suggests that an expanded fibrotic interstitium constitutes an additional barrier to the transport of water and solute between peritoneal capillaries and the dialysate (Rippe et al, 2007). Accordingly, peritoneal remodelling could impair UF and free-water transport despite the fact that the capillary α_c (reflecting the relative capillary density of AQP1) is kept unchanged (Rippe et al, 2007). We therefore evaluated the correlation between water transport and structural changes in the peritoneal interstitium (Fig. 6). Both net UF and sodium sieving were inversely closely correlated with submesothelial thickness and with collagen volume fraction in the submesothelial area (Fig. 6A-B and Fig. 6D-E, and Table 4). In contrast, peritoneal fibrosis was not associated with impaired peritoneal solute transport, estimated by the dialysate-over-plasma creatinine ratio (Fig. 6C, Table 4) and by the glucose disappearance rate (data not shown). Taken together, these data give new insights into the mechanism of low osmotic glucose conductance and impaired UF capacity in EPS. They, support the hypothesis that a fibrotic interstitium restricts water transport, in line with the serial three-pore membrane/fiber matrix model (Fig. 6F).

Table 4. Relationship between parameters of peritoneal transport and structural changes in the peritoneum of uremic, long-term PD, and EPS patients

Parameter	Pearson Coefficient (*r*)	*P* Value
Submesothelial thickness versus		
Net UF	−0.68	0.003
Sodium sieving	−0.71	0.003
D/P creatinine 240 min	0.47	0.06
Collagen volume fraction in the submesothelial area versus		
Net UF	−0.56	0.03
Sodium sieving	−0.53	0.03
D/P creatinine 240 min	0.41	0.11

D/P, dialysate-over-plasma.

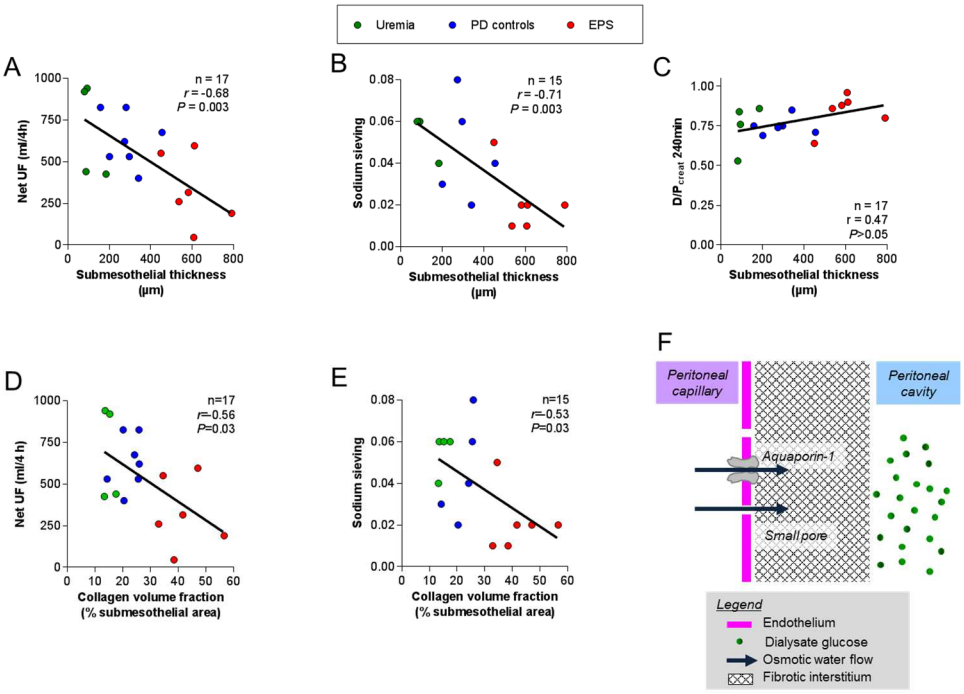

Figure 6. Fibrotic changes in the EPS peritoneum associate with impaired water but not solute transport. (A-C) Correlation between net UF (A), sodium sieving (B), and dialysate-over-plasma creatinine (D/P) ratio at 4 hours (C), and submesothelial thickness in PD patients. (D and E) Correlation between net UF (D) and sodium sieving (E), and collagen volume fraction in the submesothelial area. (A-E) Circles represent individuals; green circles for uremic patients, blue for PD patients, and red for EPS patients. The number of observations, *r* Pearson coefficients, and *P* values are shown in each panel. Peritoneal transport parameters are obtained using a modified 4-hour 3.86% glucose-based dialysate PET. (F) The serial three-pore membrane/fiber matrix model (adapted from Rippe et al, 2007). Interstitial fibrosis acts as a second resistance, in series with the capillary wall, and markedly reduces the UF coefficient of the membrane, contributing to the loss of sodium sieving and free-water transport, despite the fact that the capillary ac (i.e., AQP1 density) remains unchanged.

DISCUSSION

In this study, we combine clinical, molecular and modeling data to demonstrate that the reduction in osmotic conductance to glucose in PD patients is a predictive feature of EPS, and that reduced osmotic water transport is directly related to the degree of interstitial fibrosis and to changes in collagen content and structure in the EPS peritoneal membrane.

The availability of serial testing of peritoneal transport in a large cohort of incident PD patients allowed us to demonstrate that patients who will develop EPS show an early loss of UF capacity, due to a progressive impairment in osmotic conductance of the peritoneal membrane, as compared with PD duration- and gender-matched long-term PD patients. The loss of UF capacity in patients predisposed to EPS is disproportionate to the increase in small solute transport, revealing an uncoupling between peritoneal water and solute transport. This uncoupling suggests that increased small solute transport with earlier absorption of dialysate glucose – usually seen as the main cause of UF failure - is not sufficient to explain impaired UF capacity in EPS patients. These results are in line with those from an uncontrolled Dutch cohort showing that EPS patients had a progressive decline in UF capacity over 4 years and an inverse U-shaped trend in small solute transport (Sampinon et al, 2007). The use of time-matched controls in a UK cohort showed a clear difference in UF capacity between EPS and controls at least 2 years before PD withdrawal (Lambie et al, 2010). However, the latter study, based on 2.27% glucose PET, could not assess free-water transport. In contrast, we systematically used 3.86% glucose which provides a more accurate evaluation of UF capacity as well as sodium sieving, a surrogate for free-water transport (La Milia et al, 2006). Although most patients on long-term PD have a trend toward decreased sodium sieving during the course of PD (La Milia et al, 2006), we show here that the decline is significantly faster in EPS patients. The importance of this functional loss is substantiated by the multivariate analysis, which identifies for the first time the loss of sodium sieving as a powerful and independent predictor of EPS.

In addition to free-water transport across AQP1, sodium sieving also provides information on the maintenance of the osmotic gradient and properties of the membrane that affect osmotic conductance. In line with this, our data demonstrate that the early changes in water transport capacity reflect significant structural and molecular alterations in the peritoneal membrane of patients who subsequently developed EPS. Importantly, we show that the EPS peritoneum is characterized by an excessive fibrogenic response, with

specific changes in collagen density and structure. In agreement with previous observations (Mateijsen et al, 1999; Honda et al, 2003; Braun et al, 2012; Plum et al, 2001), we show a severe thickening of the submesothelial layer, as well as vascular proliferation in the EPS peritoneum. These changes are clearly excessive in EPS: after an average of 62 months of PD exposure, EPS patients had a 4.7- and a 1.9-fold increase in the thickness of the submesothelial area as compared with uremic and control PD patients, respectively. Using polarized light microscopy, we could then substantiate qualitative changes in the fibrotic interstitium of EPS patients, with an increased collagen density (+174% and +84% as compared with the uremic and control long-term PD peritoneum, respectively), and accumulation of thicker collagen fibers (2.2- and 1.4-fold increase as compared with uremic and control long-term PD, respectively). To our knowledge, this is the first time that such qualitative changes are evidenced in the peritoneum of EPS patients. Of note, similar changes in collagen content and optical properties have been evidenced as part of the scarring process after myocardial infarction (Whittaker et al, 1989; Ducharme et al, 2000; Whittaker et al, 1994).

The data presented here show that fibrotic changes in the peritoneum of patients on long-term PD closely correlate with impaired water transport across the membrane, thereby confirming the hypothesis that structural changes in the peritoneal interstitium account for the excessive reduction in osmotic conductance (Davies, 2004). The interstitium, which is mainly composed of collagen and glycosaminoglycans, constitutes a porous matrix across which interstitial fluid flows. Accumulation of collagen fibers leads to a decreased hydraulic conductance, depending on the volume occupied by collagen fibrils (Levick, 1987). The effect of interstitial collagen accumulation on water flow has been demonstrated *in vitro* both in normal interstitia from various organs (Levick, 1987) and in conditions of fibrosis (Ng et al, 2005). Reduced osmotic conductance by the fractional volume occupied by collagen fibrils results from three mechanisms: (*i*) exclusion of glycosaminoglycans from the intrafibrillar space, thereby increasing their extrafibrillar concentration; (*ii*) reduction of the mean hydraulic *radius* in the interstitium, leading to a reduced area for flow; and (*iii*) tortuosity, which increases the path length for flow (Levick, 1987). Our results show that increased collagen deposition and concentration in the peritoneal interstitium restricts water transport *in vivo*, leading to UF failure and loss of free-water transport in patients with EPS. These observations validate the serial three-pore membrane/fiber matrix model proposed by Rippe and colleagues (Rippe

et al, 2007). In this model, fibrotic alterations in the peritoneal interstitium have been suggested to constitute a second barrier outside the capillaries, restricting osmotic water transport without affecting small solute transport. Such an uncoupling between water and solute transport can be explained by the dependence of water filtration to the fourth power of the interstitial *radius* pores (r^4) according to Poiseuille's law, while solute diffusion is proportional to the surface of pores (r^2) (Rippe et al, 2007). As a result, a reduction of interstitial pore *radius* by increased collagen density and thicker collagen fibers will thus predominantly affect water transport, while its slight theoretical restriction on solute transport will be counterbalanced by vascular proliferation and larger effective vascular surface area. Simulations from the serial three-pore membrane/fiber matrix model showed that the sodium sieving is progressively reduced when interstitial fibrosis and the vascular surface area both progress in parallel, despite the fact that the relative capillary density of aquaporins is kept unchanged (Rippe et al, 2007). Alternatively, one could postulate that the thickening of the submesothelial area limits the penetration of glucose around peritoneal capillaries, thereby reducing the osmotic gradient across the capillary wall. Studies using ^{14}C-EDTA (molecular *radius*, 0.48 nm) have shown an inverse relationship between peritoneal tissue concentration of small substances (urea, creatinine and glucose) and the distance from the peritoneum, suggesting a distributed model for peritoneal transport (Flessner et al, 1984). In this model, severe peritoneal fibrosis is expected to alter of the dextrose concentration profile (Flessner, 1991), thereby reducing the osmotic gradient and AQP1-mediated water flow across the capillary wall.

We also observed a significant upregulation in VEGF, eNOS and vWF in the peritoneum of EPS patients and, to a lesser extent, in long-term PD patients with no EPS. In the latter group, the results were concordant with previous data indicating a 3-fold increase in eNOS as well as the induction of VEGF expression in peritoneal biopsies from long-term PD patients as compared with uremic patients (Combet et al, 2000). These molecular changes suggest a tight association between inflammation, angiogenesis, vascular permeability, and fibrosis in the peritoneal membrane of EPS patients (Combet et al, 2000; Wynn et al, 2012; Sekiguchi et al, 2012; Murohara et al, 1998; Ni et al, 2003; Carmeliet et al, 1996; Carmeliet et al, 2011; Fukumura et al, 2001; Lenting et al, 2012; Mojiri et al, 2013; Visher, 2006). In many organs, it has been established that perpetuation of tissue damage contributes to a chronic wound-healing response with continued tissue repair, regeneration and remodeling that ultimately leads to tissue

fibrosis (Wynn et al, 2012). In turn, fibrotic tissues - including the peritoneum (Sekiguchi et al, 2012) - become hypoxic when the expanding tissue remodeling outstrips its vascular supply. Hypoxia then potentiates and prolongs fibrogenesis and angiogenesis, through hypoxia-inducible factor 1α and VEGF (Sekiguchi et al, 2012). Endothelial NOS is a downstream effector of VEGF, and has been shown to promote angiogenesis in ischemic tissues (Murohara et al, 1998) and in the peritoneal membrane (Ni et al, 2003). Our data show that EPS is associated with VEGF and eNOS upregulation, either as residua of an early inflammatory phase or secondary to tissue hypoxia due to fibrosis.

The fact that impaired free-water transport is not associated with altered expression or location of AQP1 in EPS is surprising at first sight. AQP1 is the molecular counterpart of ultrasmall pore, accounting for half the UF and for the sodium sieving when hypertonic glucose is used as osmotic agent (Devuyst et al, 2014; Rippe et al, 1991). The loss of AQP1-mediated free-water transport has been suggested as a potential cause of UF failure in long-term PD patients (Goffin et al, 1999; Smit et al, 2004). Admittedly, the present study does not allow ruling out a dysfunction or biochemical modification of AQP1. However, free-water transport estimated by the sodium sieving can be affected not only by the availability of functional AQP1 water channels but also by any mechanism of membrane obstruction, such as severe peritoneal fibrosis (Rippe et al, 2001). The present study is in line with predictions of the three-pore membrane/fiber matrix and distributed models, by showing that the vascular density of water channels is kept unchanged in EPS patients, and by pointing toward excessive peritoneal fibrosis as the most important barrier to fluid flow in EPS patients.

In summary, reduced osmotic conductance during the course of PD was identified as a powerful and independent predictor of EPS. This functional change is linked to specific alterations of the collagen matrix in the peritoneal membrane of patients with EPS, rather than changes in the degree of vasculopathy or in the expression of water channels. Our multi-level data, based on transport, structural and expression studies, are thus clarifying the cause of the excessive reduction in osmotic conductance in patients with EPS.

CONCISE METHODS

EPS patients and peritoneal transport analysis. In agreement with EPS diagnosis criteria (Korte et al, 2011; Kawaguchi et al, 2000; Summers et al, 2011), EPS cases were defined as PD patients who presented with recurrent, partial or total, intestinal occlusion, with a definitive EPS diagnosis confirmed by CT-scan and/or laparotomy. Peritoneal function was assessed yearly, with a modified 3.86% glucose-based peritoneal equilibration test (PET) (La Milia et al, 2006; Clerbaux et al, 2006), which has the advantages over the conventional 2.27% glucose-based PET (Twardowski et al, 1987) to assess sodium sieving (La Milia et al, 2006) and allow the diagnosis of UF failure (net UF < 400ml at the end of the 4h dwell with 3.86% glucose, as defined by the International Society for Peritoneal Dialysis (Mujais et al, 2000)). All values of sodium sieving were corrected for the rate of sodium diffusion. The PET was part of the normal procedure of care for PD patients.

Peritoneal sampling and processing. Para-umbilical biopsy samples of human parietal peritoneum were obtained from uremic patients at the time of catheter insertion, and PD patients at the time of catheter removal because of renal transplantation or transfer to hemodialysis as part of a routine protocol in our center, and processed as previously described (Combet et al, 2000). The time between last PET and peritoneal biopsy was similar in EPS and control patients (9.1 ± 2.1 versus 7.5 ± 1.6 months in EPS and controls; P=0.61). Informed consent was obtained from patients. The use of human biopsy samples has been approved by the Ethical Review Board of the Cliniques universitaires Saint-Luc.

Immunoblot, immunohistochemistry and immunofluorescence. SDS-PAGE and immunoblotting, immunoperoxidase staining on human peritoneum sections and immunofluorescence were performed as previously described (Combet et al, 2000; Devuyst et al, 1998; de Arteaga et al, 2011). We used the following antibodies: mouse monoclonal anti-human eNOS (Transduction Laboratories, Lexington, KY); purified rabbit anti-von Willebrand factor (DAKO, Glostrup, Denmark), monoclonal anti-human VEGF (Santa Cruz Biotechnology, Santa Cruz, CA, USA); polyclonal rabbit anti-human AQP1 (Chemicon International, Temecula, CA).

Image analysis. Information on the criteria used for adequacy of each peritoneal specimen, the assessment of peritoneal fibrosis, vasculopathy, vascular proliferation, collagen volume fraction and collagen structure is available in Supplemental material. Image analysis was performed using ImageJ (1.47v).

Statistics. Data are presented as mean ± SEM. Comparisons between the means from different groups were performed using unpaired t-tests, Fisher's exact test, or one-way ANOVA, followed by Bonferroni's multiple comparison tests, as appropriated. Trends were assessed by linear ordinary least square regression. Multivariate analysis was performed using a logistic regression random-effects model and included potential risk factors for EPS (age at PD start, PD duration, peritonitis rate, beta blocker use, residual renal function, glucose exposure) in a first model; in a second model, the mean value of sodium sieving during the last 2 years of PD was added to these variables. Probabilities of EPS in function of sodium sieving and UF levels were estimated by multivariate logistic regression. All analyses were performed by GraphPad Prism (6.01 v) or Stata (12 v) software. Significance level is indicated in each figure (*p<0.05, **p<0.01, ***p<0.001).

REFERENCES

1. Agre P. Aquaporin water channels (Nobel Lecture). *Angew Chem Int Ed Engl* 2004;43:4278-4290.
2. Asgeirsson D, Axelsson J, Rippe C, Rippe B. Similarity of permeabilities for Ficoll, pullulan, charge-modified albumin and native albumin across the rat peritoneal membrane. *Acta Physiol (Oxf).* 2009;196:427-33.
3. Ateş K, Nergizoğlu G, Keven K, Sen A, Kutlay S, Ertürk S, Duman N, Karatan O, Ertuğ AE. Effect of fluid and sodium removal on mortality in peritoneal dialysis patients. *Kidney Int* 2001;60:767-776.
4. Berlier JE, Rothe A, Buller G, Bradford J, Gray DR, Filanoski BJ, Telford WG, Yue S, Liu J, Cheung CY, Chang W, Hirsch JD, Beechem JM, Haugland RP, Haugland RP. Quantitative comparison of long-wavelength Alexa Fluor dyes to Cy dyes: fluorescence of the dyes and their bioconjugates. *J Histochem Cytochem* 2003;51:1699-712.
5. Blake PG, Bargman JM, Brimble KS, Davison SN, Hirsch D, McCormick BB, Suri RS, Taylor P, Zalunardo N, Tonelli M; Canadian Society of Nephrology Work Group on Adequacy of Peritoneal Dialysis. Clinical Practice Guidelines and Recommendations on Peritoneal Dialysis Adequacy 2011. *Perit Dial Int* 2011;31:218-239.
6. Bragg-Gresham JL, Fissell RB, Mason NA, Bailie GR, Gillespie BW, Wizemann V, Cruz JM, Akiba T, Kurokawa K, Ramirez S, Young EW. Diuretic use, residual renal function, and mortality among hemodialysis patients in the Dialysis Outcomes and Practice Pattern Study (DOPPS). *Am J Kidney Dis* 2007;49:426-31.
7. Braun N, Fritz P, Ulmer C, Latus J, Kimmel M, Biegger D, Ott G, Reimold F, Thon KP, Dippon J, Segerer S, Alscher MD. Histological criteria for encapsulating peritoneal sclerosis - a standardized approach. *PLoS One* 2012;7:e48647.
8. Brimble KS, Walker M, Margetts PJ, et al. Meta-analysis: Peritoneal membrane transport, mortality, and technique failure in peritoneal dialysis. *J Am Soc Nephrol* 2006;17:2591-2598.
9. Brown EA, Davies SJ, Rutherford P, et al. Survival of functionally anuric patients on automated peritoneal dialysis: The European APD Outcome Study. *J Am Soc Nephrol* 2003;14:2948-2957.
10. Brown MC, Simpson K, Kerssens JJ, Mactier RA; Scottish Renal Registry: Encapsulating peritoneal sclerosis in the new millennium: a national cohort study. *Clin J Am Soc Nephrol* 2009;4:1222-1229.
11. Buis B, Koomen GC, Imholz AL, Struijk DG, Reddingius RE, Arisz L, Krediet RT. Effect of electric charge on the transperitoneal transport of plasma proteins during CAPD. *Nephrol Dial Transplant* 1996;11:1113-20.
12. Campbell EM, Birdsell DN, Yool AJ: The activity of human aquaporin 1 as a cGMP-gated cation channel is regulated by tyrosine phosphorylation in the carboxyl-terminal domain. *Mol Pharmacol* 2012;81:97–105.
13. Carlsson O, Nielsen S, el Zakaria R, Rippe B. In vivo inhibition of transcellular water channels (aquaporin-1) during acute peritoneal dialysis in rats. *Am J Physiol* 1996;271:H2254-2262.
14. Carmeliet P, Ferreira V, Breier G, Pollefeyt S, Kieckens L, Gertsenstein M,

Fahrig M, Vandenhoeck A, Harpal K, Eberhardt C, Declercq C, Pawling J, Moons L, Collen D, Risau W, Nagy A: Abnormal blood vessel development and lethality in embryos lacking a single VEGF allele. *Nature* 1996;380:435-439.

15. Carmeliet P, Jain RK. Molecular mechanisms and clinical applications of angiogenesis. *Nature* 2011;473:298-307.

16. Chaumont F, Tyerman SD. Aquaporins: highly regulated channels controlling plant water relations. *Plant Physiol* 2014;164:1600–18.

17. Chudakov DM, Matz MV, Lukyanov S, Lukyanov KA. Fluorescent proteins and their applications in imaging living cells and tissues. *Physiol Rev* 2010;90:1103-63.

18. Churchill DN, Thorpe KE, Nolph KD, et al. Increased peritoneal membrane transport is associated with decreased patient and technique survival for continuous peritoneal dialysis patients. The Canada-USA (CANUSA) Peritoneal Dialysis Study Group. *J Am Soc Nephrol* 1998;9:1285-1292.

19. Clerbaux G, Francart J, Wallemacq P, Robert A, Goffin E. Evaluation of peritoneal transport properties at onset of peritoneal dialysis and longitudinal follow-up. *Nephrol Dial Transplant* 2006;21:1032-1039.

20. Combet S, van Landschoot M, Moulin P, et al. Regulation of aquaporin-1 and nitric oxide synthase isoforms in a rat model of acute peritonitis. *J Am Soc Nephrol* 1999;10:2185-2196.

21. Combet S, Miyata T, Moulin P, Pouthier D, Goffin E, Devuyst O. Vascular proliferation and enhanced expression of endothelial nitric oxide synthase in human peritoneum exposed to long-term peritoneal dialysis. *J Am Soc Nephrol* 2000;11:717-728.

22. Crone C, Levitt DG. Capillary permeability to small solutes. In: Renkin EM, Michel CC (eds) *Handbook of Physiology*, Section 2, Vol 4. The Cardiovascular System. American Physiological Society: Washington DC, 1984;411.

23. Curry FE, Michel CC. A fiber matrix model of capillary permeability. *Microvasc Res* 1980;20:96-9.

24. Dallas F, Jenkins SB, Wilkie ME. Enhanced ultrafiltration using 7.5% icodextrin/1.36% glucose combination dialysate: a pilot study. *Perit Dial Int* 2004;24:542-546.

25. Davies SJ, Phillips L, Griffiths AM, Russell LH, Naish PF, Russell GI. What really happens to people on long-term peritoneal dialysis? *Kidney Int* 1998;54:2207-2217.

26. Davies SJ, Phillips L, Naish PF, Russell GI. Peritoneal glucose exposure and changes in membrane solute transport with time on peritoneal dialysis. *J Am Soc Nephrol* 2001;12:1046–1051.

27. Davies SJ, Woodrow G, Donovan K, Plum J, Williams P, Johansson AC, Bosselmann HP, Heimbürger O, Simonsen O, Davenport A, Tranaeus A, Divino Filho JC. Icodextrin improves the fluid status of peritoneal dialysis patients: results of a double-blind randomized controlled trial. *J Am Soc Nephrol* 2003;14:2338-2344.

28. Davies SJ. Longitudinal relationship between solute transport and ultrafiltration capacity in peritoneal dialysis patients. *Kidney Int* 2004;66:2437-45.

29. Davies SJ. Peritoneal solute transport and inflammation. *Am J Kidney Dis* 2014;64:978-86.

30. de Arteaga J, Ledesma F, Garay G, et al. High-dose steroid treatment increases free water transport in peritoneal dialysis patients. *Nephrol Dial Transplant* 2011;26:4142-4145.

31. De Paepe M, Belpaire F, Schelstraete K, Lameire N. Comparison of different volume markers in peritoneal dialysis. *J Lab Clin Med* 1988;111:421-9.

32. Devuyst O, Nielsen S, Cosyns JP, et al. Aquaporin-1 and endothelial nitric oxide synthase expression in capillary endothelia

of human peritoneum. *Am J Physiol* 1998;275:H234-242.
33. Devuyst O, van Westrhenen R, Topley N. Longterm peritoneal dialysis patients. In: Nolph and Gokal's Textbook of Peritoneal Dialysis, 3rd Ed., edited by Khanna R, Krediet RT, New York, Springer, 2009, pp 757-780.
34. Devuyst O, Margetts PJ, Topley N. The pathophysiology of the peritoneal membrane. *J Am Soc Nephrol* 2010;21:1077-1085.
35. Devuyst O, Rippe B. Water transport across the peritoneal membrane. *Kidney Int* 2014; 85:750-758.
36. de Waart DR, Zweers MM, Struijk DG, Krediet RT. Icodextrin degradation products in spent dialysate of CAPD patients and the rat, and its relation with dialysate osmolality. *Perit Dial Int* 2001;21:269-274.
37. Dodge JT, Mitchell C, Hanahan DJ. The preparation and chemical characteristics of hemoglobin-free ghosts of human erythrocytes. *Arch Biochem Biophys* 1963;100:119-30.
38. Dombros N, Dratwa M, Feriani M, Gokal R, Heimbürger O, Krediet R, Plum J, Rodrigues A, Selgas R, Struijk D, Verger C; EBPG Expert Group on Peritoneal Dialysis. European best practice guidelines for peritoneal dialysis. 7 Adequacy of peritoneal dialysis. *Nephrol Dial Transplant* 2005;20:ix24-ix27.
39. Ducharme A, Frantz S, Aikawa M, Rabkin E, Lindsey M, Rohde LE, Schoen FJ, Kelly RA, Werb Z, Libby P, Lee RT. Targeted deletion of matrix metalloproteinase-9 attenuates left ventricular enlargement and collagen accumulation after experimental myocardial infarction. *J Clin Invest* 2000;106: 55-62.
40. Eisner C, Ow H, Yang T, Jia Z, Dimitriadis E, Li L, Wang K, Briggs J, LevineM, Schnermann J, Espey MG. Measurement of plasma volume using fluorescent silica-based nanoparticles. *J Appl Physiol* 2012;112:681-7.
41. Faller B, Shockley T, Genestier S, Martis L. Polyglucose and amino acids: preliminary results. *Perit Dial Int* 1997;17:S63-S67.
42. Fine J, Gray R. A Proportional Hazards Model for the Subdistribution of a Competing Risk. *J Am Stat Assoc* 1999;94:496-509.
43. Flessner MF, Parker RJ, Sieber SM. Peritoneal lymphatic uptake of fibrinogen and erythrocytes in the rat. *Am J Physiol* 1983;244:H89-96.
44. Flessner MF, Dedrick RL, Schultz JS. A distributed model of peritoneal-plasma transport: theoretical considerations. *Am J Physiol* 1984;246:R597–607.
45. Flessner MF. Peritoneal transport physiology: insights from basic research. *J Am Soc Nephrol* 1991;2:122–35.
46. Flessner MF, Lofthouse J. Of mice and men: species and age differences in dialysis with icodextrin [Abstract]. *J Am Soc Nephrol* 1999;10:226A.
47. Frazer KA, Eskin E, Kang HM, Bogue MA, Hinds DA, Beilharz EJ, Gupta RV, Montgomery J, Morenzoni MM, Nilsen GB, Pethiyagoda CL, Stuve LL, Johnson FM, Daly MJ, Wade CM, Cox DR. A sequence-based variation map of 8.27 million SNPs in inbred mouse strains. *Nature* 2007;448:1050-3.
48. Freida P, Galach M, Divino Filho JC, Werynski A, Lindholm B. Combination of crystalloid (glucose) and colloid (icodextrin) osmotic agents markedly enhances peritoneal fluid and solute transport during the long PD dwell. *Perit Dial Int* 2007;27:267-276.
49. Freida P, Wilkie M, Jenkins S, Dallas F, Issad B. The contribution of combined crystalloid and colloid osmosis to fluid and sodium management in peritoneal dialysis. *Kidney Int* 2008;108:S102-S111.
50. Freida P, Issad B, Dratwa M, Lobbedez T, Wu L, Leypoldt JK, Divino-Filho JC. A combined crystalloid and colloid pd solution as a glucose-sparing strategy for volume control in high-transport apd patients: a

prospective multicenter study. *Perit Dial Int* 2009;29:433-442.
51. Fu D, Lu M: The structural basis of water permeation and proton exclusion in aquaporins. *Mol Membr Biol* 2007;24:366–374.
52. Fukumura D, Gohongi T, Kadambi A, Izumi Y, Ang J, Yun CO, Buerk DG, Huang PL, Jain RK. Predominant role of endothelial nitric oxide synthase in vascular endothelial growth factor-induced angiogenesis and vascular permeability. *Proc Natl Acad Sci U S A* 2001;98:2604-2609.
53. Gao J, Wang X, Chang Y, Zhang J, Song Q, Yu H, Li X: Acetazolamide inhibits osmotic water permeability by interaction with aquaporin-1. *Anal Biochem* 2006;350:165–170.
54. García-López E, Pawlaczyk K, Anderstam B, Qureshi AR, Kuzlan-Pawlaczyk M, Heimbürger O, Werynski A, Lindholm B. Icodextrin metabolism and alpha-amylase activity in nonuremic rats undergoing chronic peritoneal dialysis. *Perit Dial Int* 2007;27:415-423.
55. García-López E, Lindholm B. Icodextrin metabolites in peritoneal dialysis. *Perit Dial Int* 2009;29:370-376.
56. García-López E, Lindholm B, Davies S. An update on peritoneal dialysis solutions. *Nat Rev Nephrol* 2012;8:224-33.
57. Garred LJ, Canaud B, Farrell PC. A simple kinetic model for assessing peritoneal mass transfer in chronic ambulatory peritoneal dialysis. *ASAIO J* 1983;6:131–137.
58. Gillen CM, Takamata A, Mack GW, Nadel ER. Measurement of plasma volume in rats with use of fluorescent-labeled albumin molecules. *J Appl Physiol* 1994;76:485-9.
59. Goffin E, Combet S, Jamar F, Cosyns JP, Devuyst O. Expression of aquaporin-1 in a long-term peritoneal dialysis patient with impaired transcellular water transport. *Am J Kidney Dis* 1999;33:383–8.
60. Goodship TH, Lloyd S, McKenzie PW, Earnshaw M, Smeaton I, Bartlett K, Ward MK, Wilkinson R. Short-term studies on the use of amino acids as an osmotic agent in continuous ambulatory peritoneal dialysis. *Clin Sci (Lond)* 1987;73:471-478.
61. Graham T. Liquid Diffusion Applied to Analysis. *Philosophical Transactions of the Royal Society of London* 1861;151:183-224.
62. Guyton AC, Hall JE. The body fluid compartments: extracellular and intracellular fluids; interstitial fluid and edema. In: *Guyton and Hall Textbook of Medical Physiology*, edited by Saunders Elsevier, 11th edition, Philadelphia, 2005, pp 291-306.
63. Hansson JH, Watnick S. Update on Peritoneal Dialysis: Core Curriculum 2016. *Am J Kidney Dis* 2016;67:151-64.
64. Heimburger O, Mujais S. Buffer transport in peritoneal dialysis. *Kidney Int* 2003;88:S37-42.
65. Holmes CJ. Glucotoxicity in peritoneal dialysis -solutions for the solution! *Adv Chronic Kidney Dis* 2007;14:269-278.
66. Honda K, Nitta K, Horita S, Tsukada M, Itabashi M, Nihei H, Akiba T, Oda H. Histologic criteria for diagnosing encapsulating peritoneal sclerosis in continuous ambulatory peritoneal dialysis patients. *Adv Perit Dial* 2003;19:169-175.
67. Honda K, Hamada C, Nakayama M, Miyazaki M, Sherif AM, Harada T, Hirano H; Peritoneal Biopsy Study Group of the Japanese Society for Peritoneal Dialysis: Impact of uremia, diabetes, and peritoneal dialysis itself on the pathogenesis of peritoneal sclerosis: a quantitative study of peritoneal membrane morphology. *Clin J Am Soc Nephrol* 2008;3:720-728.
68. Ho-dac-Pannekeet MM, Schouten N, Langendijk MJ, Hiralall JK, de Waart DR, Struijk DG, Krediet RT. Peritoneal transport characteristics with glucose polymer based dialysate. *Kidney Int* 1996;50:979-86.
69. Huber VJ, Tsujita M, Kwee IL, Nakada T. Inhibition of aquaporin 4 by antiepileptic drugs. *Bioorg Med Chem* 2009;17:418–424.

70. Jain AK, Blake P, Cordy P, Garg AX. Global trends in rates of peritoneal dialysis. *J Am Soc Nephrol* 2012;23:533–544.
71. Jay AW, Rowlands S. The stages of osmotic haemolysis. *J Physiol* 1975;252:817-32.
72. Jenkins SB, Wilkie ME. An exploratory study of a novel peritoneal combination dialysate (1.36% glucose/7.5% icodextrin), demonstrating improved ultrafiltration compared to either component studied alone. *Perit Dial Int* 2003;23:475-480.
73. Jha V, Garcia-Garcia G, Iseki K, Li Z, Naicker S, Plattner B, Saran R, Wang AY, Yang CW. Chronic kidney disease: global dimension and perspectives. *Lancet* 2013;382:260-72.
74. Johnson DW, Arndt M, O'Shea A, Watt R, Hamilton J, Vincent K. Icodextrin as salvage therapy in peritoneal dialysis patients with refractory fluid overload. *BMC Nephrol* 2001;2:2.
75. Johnson DW, Hawley CM, McDonald SP, Brown FG, Rosman JB, Wiggins KJ, Bannister KM, Badve SV. Superior survival of high transporters treated with automated versus continuous ambulatory peritoneal dialysis. *Nephrol Dial Transplant* 2010;25:1973-9.
76. Johnson DW, Cho Y, Livingston BE, Hawley CM, McDonald SP, Brown FG, Rosman JB, Bannister KM, Wiggins KJ. Encapsulating peritoneal sclerosis: Incidence, predictors, and outcomes. *Kidney Int* 2010;77:904–912.
77. Jones MR, Gehr TW, Burkart JM, Hamburger RJ, Kraus AP Jr, Piraino BM, Hagen T, Ogrinc FG, Wolfson M. Replacement of amino acid and protein losses with 1.1% amino acid peritoneal dialysis solution. *Perit Dial Int* 1998;18:210-216.
78. Joos G, Freeman IM. *Theoretical Physics*, 2nd edition, London, edited by Blackie and Son, 1951, pp. 586-587.
79. Kawaguchi Y, Kawanishi H, Mujais S, Topley N, Oreopoulos DG. Encapsulating peritoneal sclerosis: definition, etiology, diagnosis, and treatment. International Society for Peritoneal Dialysis Ad Hoc Committee on Ultrafiltration Management in Peritoneal Dialysis. *Perit Dial Int* 2000;20:S43–55.
80. KDIGO CKD Work Group. KDIGO 2012 clinical practice guideline for the evaluation and management of chronic kidney disease. *Kidney Int Suppl* 2013;3: 1–150.
81. Keane TM, Goodstadt L, Danecek P, White MA, Wong K, Yalcin B, Heger A, Agam A, Slater G, Goodson M, Furlotte NA, Eskin E, Nellåker C, Whitley H, Cleak J, Janowitz D, Hernandez-Pliego P, Edwards A, Belgard TG, Oliver PL, McIntyre RE, Bhomra A, Nicod J, Gan X, Yuan W, van der Weyden L, Steward CA, Bala S, Stalker J, Mott R, Durbin R, Jackson IJ, Czechanski A, Guerra-Assunção JA, Donahue LR, Reinholdt LG, Payseur BA, Ponting CP, Birney E, Flint J, Adams DJ. Mouse genomic variation and its effect on phenotypes and gene regulation. *Nature* 2011;477:289-94.
82. Kiil F. Mechanism of osmosis. *Kidney Int* 1982;21:303-8.
83. Kim TW, Beckett EA, Hanna R, Koh SD, Ordög T, Ward SM, Sanders KM: Regulation of pacemaker frequency in the murine gastric antrum. *J Physiol* 2002;538:145–157.
84. King LS, Choi M, Fernandez PC, Cartron JP, Agre P: Defective urinary-concentrating ability due to a complete deficiency of aquaporin-1. *N Engl J Med* 2001;345:175–179.
85. Korte MR, Sampimon DE, Betjes MG, Krediet RT. Encapsulating peritoneal sclerosis: the state of affairs. *Nat Rev Nephrol* 2011;7:528–538.
86. Korte MR, Sampimon DE, Lingsma HF, Fieren MW, Looman CW, Zietse R, Weimar W, Betjes MG; Dutch Multicenter EPS Study. Risk factors associated with encapsulating peritoneal sclerosis in Dutch EPS study. *Perit Dial Int* 2011;31:269–278.

87. Kramer EM, Myers DR. Osmosis is not driven by water dilution. *Trends Plant Sci* 2013;18:195-7.
88. Krediet RT, Koomen GC, Koopman MG, Hoek FJ, Struijk DG, Boeschoten EW, Arisz L. The peritoneal transport of serum proteins and neutral dextran in CAPD patients. *Kidney Int* 1989;35:1064-72.
89. Krediet RT, Ho-dac-Pannekeet MM, Imholz AL, Struijk DG. Icodextrin's effects on peritoneal transport. *Perit Dial Int* 1997;17:335-341.
90. Krediet RT. The Physiology of Peritoneal Solute, Water, and Lymphatic Transport. In: *Nolph and Gokal's Textbook of Peritoneal Dialysis*, edited by Khanna R, Krediet RT, 3rd Ed., New York, Springer, 2009, pp 137-172.
91. Lai-Fook SJ, Houtz PK, Lai YL. End-expiratory and tidal volumes measured in conscious mice using single projection x-ray images. *J Appl Physiol* 2008;104:521-33.
92. Lambie ML, John B, Mushahar L, Huckvale C, Davies SJ. The peritoneal osmotic conductance is low well before the diagnosis of encapsulating peritoneal sclerosis is made. *Kidney Int* 2010;78:611–618.
93. Lambie M, Chess J, Donovan KL, Kim YL, Do JY, Lee HB, Noh H, Williams PF, Williams AJ, Davison S, Dorval M, Summers A, Williams JD, Bankart J, Davies SJ, Topley N; Global Fluid Study Investigators. Independent effects of systemic and peritoneal inflammation on peritoneal dialysis survival. *J Am Soc Nephrol* 2013;24:2071-80.
94. La Milia V, Di Filippo S, Crepaldi M, Del Vecchio L, Dell'Oro C, Andrulli S, Locatelli F. Mini-peritoneal equilibration test: A simple and fast method to assess free water and small solute transport across the peritoneal membrane. *Kidney Int* 2005;68:840-846.
95. La Milia V, Pozzoni P, Virga G, Crepaldi M, Del Vecchio L, Andrulli S, Locatelli F. Peritoneal transport assessment by peritoneal equilibration test with 3.86% glucose: a long-term prospective evaluation. *Kidney Int* 2006;69:927-933.
96. Leeson PD, Springthorpe B. The influence of drug-like concepts on decision-making in medicinal chemistry. *Nat Rev Drug Discov* 2007;6:881–890.
97. Lenting PJ, Casari C, Christophe OD, Denis CV. von Willebrand factor: the old, the new and the unknown. *J Thromb Haemost* 2012;10:2428-2437.
98. Levey AS, Coresh J. Chronic kidney disease. *Lancet* 2012;379:165-80.
99. Levick JR. Flow through interstitium and other fibrous matrices. *Q J Exp Physiol* 1987;72:409-437.
100. Levick JR, Michel CC. Microvascular fluid exchange and the revised Starling principle. *Cardiovasc Res*. 2010;87:198-210.
101. Lin X, Lin A, Ni Z, Yao Q, Zhang W, Yan Y, Fang W, Gu A, Axelsson J, Qian J. Daily peritoneal ultrafiltration predicts patient and technique survival in anuric peritoneal dialysis patients. *Nephrol Dial Transplant* 2010;25:2322-7.
102. Lin YC, Samardzic H, Adamson RH, Renkin EM, Clark JF, Reed RK, Curry FR. Phosphodiesterase 4 inhibition attenuates atrial natriuretic peptide-induced vascular hyperpermeability and loss of plasma volume. *J Physiol* 2011;589:341-53.
103. Liyanage T, Ninomiya T, Jha V, Neal B, Patrice HM, Okpechi I, Zhao MH, Lv J, Garg AX, Knight J, Rodgers A, Gallagher M, Kotwal S, Cass A, Perkovic V. Worldwide access to treatment for end-stage kidney disease: a systematic review. *Lancet* 2015;385:1975-82.
104. Ma T, Yang B, Gillespie A, Carlson EJ, Epstein CJ, Verkman AS. Severely impaired urinary concentrating ability in transgenic mice lacking aquaporin-1 water channels. *J Biol Chem* 1998;273:4296–9.
105. Mactier RA. Measurement of dialysate volumes in peritoneal dialysis. *Perit Dial Int* 1989;9: 155-7.
106. Magni F, Sarto C, Ticozzi D, Soldi M, Bosso N, Mocarelli P, *et al.* Proteomic

knowledge of human aquaporins. *Proteomics* 2006;6:5637–49.
107. Mateijsen MA, van der Wal AC, Hendriks PM, Zweers MM, Mulder J, Struijk DG, Krediet RT: Vascular and interstitial changes in the peritoneum of CAPD patients with peritoneal sclerosis. *Perit Dial Int* 1999;19:517-525.
108. Mathai JC, Mori S, Smith BL, Preston GM, Mohandas N, Collins M, van Zijl PC, Zeidel ML, Agre P. Functional analysis of aquaporin-1 deficient red cells. The Colton-null phenotype. *J Biol Chem* 1996;271:1309-13.
109. Maurel C, Verdoucq L, Luu DT, Santoni V: Plant aquaporins: Membrane channels with multiple integrated functions. *Annu Rev Plant Biol* 2008;59:595–624.
110. McGeachin RL, Gleason JR, Adams MR. Amylase distribution in extrapancreatic, extrasalivary tissues. *Arch Biochem Biophys* 1958;75:403-11.
111. Mehrotra R, Chiu YW, Kalantar-Zadeh K, Bargman J, Vonesh E. Similar outcomes with hemodialysis and peritoneal dialysis in patients with end-stage renal disease. *Arch Intern Med* 2011;171:110-118.
112. Mehrotra R, Devuyst O, Davies SJ, Johnson DW. The Current State of Peritoneal Dialysis. *J Am Soc Nephrol* 2016, *in press*.
113. Migliati E, Meurice N, DuBois P, Fang JS, Somasekharan S, Beckett E, Flynn G, Yool AJ: Inhibition of aquaporin-1 and aquaporin-4 water permeability by a derivative of the loop diuretic bumetanide acting at an internal pore-occluding binding site. *Mol Pharmacol* 2009;76:105–112.
114. Mistry CD, Mallick NP, Gokal R. Ultrafiltration with an isosmotic solution during long peritoneal dialysis exchanges. *Lancet* 1987;2:178-182.
115. Mistry CD, Gokal R, Peers E. A randomized multicenter clinical trial comparing isosmolar icodextrin with hyperosmolar glucose solutions in CAPD. MIDAS Study Group. Multicenter Investigation of Icodextrin in Ambulatory Peritoneal Dialysis. *Kidney Int* 1994;46:496-503.
116. Moberly JB, Mujais S, Gehr T, Hamburger R, Sprague S, Kucharski A, Reynolds R, Ogrinc F, Martis L, Wolfson M. Pharmacokinetics of icodextrin in peritoneal dialysis patients. *Kidney Int* 2002;S23-S33.
117. Mojiri A, Nakhaii-Nejad M, Phan WL, Kulak S, Radziwon-Balicka A, Jurasz P, Michelakis E, Jahroudi N: Hypoxia results in upregulation and de novo activation of von Willebrand factor expression in lung endothelial cells. *Arterioscler Thromb Vasc Biol* 2013;33:1329-1338.
118. Moon C, Preston GM, Griffin CA, et al. The human aquaporin-CHIP gene. Structure, organization, and chromosomal localization. *J Biol Chem* 1993;268:15772-8.
119. Morelle J, Sow A, Vertommen D, Jamar F, Rippe B, Devuyst O. Quantification of osmotic water transport in vivo using fluorescent albumin. *Am J Physiol Renal Physiol* 2014;307:F981–9.
120. Morelle J, Sow A, Hautem N, Bouzin C, Crott R, Devuyst O, *et al.* Interstitial fibrosis restricts osmotic water transport in encapsulating peritoneal sclerosis. *J Am Soc Nephrol* 2015;26:2521–33.
121. Morelle J, Devuyst O. Water and solute transport across the peritoneal membrane. *Curr Opin Nephrol Hypertens* 2015;24:434-43.
122. Murohara T, Asahara T, Silver M, Bauters C, Masuda H, Kalka C, Kearney M, Chen D, Symes JF, Fishman MC, Huang PL, Isner JM. Nitric oxide synthase modulates angiogenesis in response to tissue ischemia. *J Clin Invest* 1998;101:2567-2578.
123. Murata K, Mitsuoka K, Hirai T, et al. Structural determinants of water permeation through aquaporin-1. *Nature* 2000;407:599-605.
124. Mujais S, Nolph K, Gokal R, Blake P, Burkart J, Coles G, Kawaguchi Y, Kawanishi H, Korbet S, Krediet R, Lindholm B, Oreopoulos D, Rippe B, Selgas R. Evaluation and management of ultrafiltration problems in peritoneal

dialysis. International Society for Peritoneal Dialysis Ad Hoc Committee on Ultrafiltration Management in Peritoneal Dialysis. *Perit Dial Int* 2000;20:S5-S21.
125. Musini VM, Wright JM, Bassett K, Jauca CD: Blood pressure lowering efficacy of loop diuretics for primary hypertension. *Cochrane Database Syst Rev* 2009;4:CD003825.
126. Nagy JA. Lymphatic and nonlymphatic pathways of peritoneal absorption in mice: physiology versus pathology. *Blood Purif* 1992;10: 148-62.
127. Ng CP, Hinz B, Swartz MA: Interstitial fluid flow induces myofibroblast differentiation and collagen alignment in vitro. *J Cell Sci* 2005;118: 4731-4739.
128. Ni J, Moulin P, Gianello P, Feron O, Balligand JL, Devuyst O. Mice that lack endothelial nitric oxide synthase are protected against functional and structural modifications induced by acute peritonitis. *J Am Soc Nephrol* 2003;14: 3205-3216.
129. Ni J, Cnops Y, Debaix H, Boisdé I, Verbavatz JM, Devuyst O. Functional and molecular characterization of a peritoneal dialysis model in the C57BL/6J mouse. *Kidney Int* 2005; 2021-2031.
130. Ni J, Verbavatz JM, Rippe A, Boisdé I, Moulin P, Rippe B, Verkman AS, Devuyst O. Aquaporin-1 plays an essential role in water permeability and ultrafiltration during peritoneal dialysis. *Kidney Int* 2006; 69:1518-1525.
131. Nielsen S, Smith BL, Christensen EI, Agre P. Distribution of the aquaporin CHIP in secretory and resorptive epithelia and capillary endothelia. *Proc Natl Acad Sci U S A* 1993; 90:7275-7279.
132. Nishino T, Devuyst O. Clinical application of aquaporin research: aquaporin-1 in the peritoneal membrane. *Pflugers Arch* 2008;456 :721-7.
133. Noordzij M, Leffondré K, van Stralen KJ, Zoccali C, Dekker FW, Jager KJ. When do we need competing risks methods for survival analysis in nephrology? *Nephrol Dial Transplant* 2013;28:2670-7.
134. Ortiz A, Covic A, Fliser D, Fouque D, Goldsmith D, Kanbay M, Mallamaci F, Massy ZA, Rossignol P, Vanholder R, Wiecek A, Zoccali C, London GM. Epidemiology, contributors to, and clinical trials of mortality risk in chronic kidney failure. *Lancet* 2014;383:1831-43.
135. Oren A, Wu G, Anderson GH, Marliss E, Khanna R, Petitt J, Mupas L, Rodella H, Brandes L, Roncari DA, et al. Effective use of amino acid dialysate over four weeks in CAPD patients. *Trans Am Soc Artif Intern Organs* 1983;29:604-10.
136. Paganelli CV, Solomon AK. The rate of exchange of tritiated water across the human red cell membrane. J Gen Physiol. 1957;41:259-77.
137. Panchuk-Voloshina N, Haugland RP, Bishop-Stewart J, Bhalgat MK, Millard PJ, Mao F, Leung WY, Haugland RP. Alexa dyes, a series of new fluorescent dyes that yield exceptionally bright, photostable conjugates. *J Histochem Cytochem* 1999; 47:1179-88.
138. Papapetropoulos A, García-Cardeña G, Madri JA, Sessa WC: Nitric oxide production contributes to the angiogenic properties of vascular endothelial growth factor in human endothelial cells. *J Clin Invest* 1997;100:3131-3139.
139. Parikova A, Smit W, Struijk DG, Krediet RT. Analysis of fluid transport pathways and their determinants in peritoneal dialysis patients with ultrafiltration failure. *Kidney Int* 2006;70:1988-94.
140. Peers E. Icodextrin plus glucose combinations for use in CAPD. *Perit Dial Int* 1997;17:S68-S69.
141. Plum J, Hermann S, Fusshöller A, Schoenicke G, Donner A, Röhrborn A, Grabensee B. Peritoneal sclerosis in peritoneal dialysis patients related to dialysis settings and peritoneal transport properties. *Kidney Int* 2001;78:S42-S47.
142. Preston GM, Piaza Caroll T, Guggino WB, Agre P. Appearance of water channels in Xenopus oocytes expressing red cells

CHIP 28 protein. *Science* 1992;256:385-387.
143. Rippe B, Stelin G, Haraldsson B. Computer simulations of peritoneal fluid transport in CAPD. *Kidney Int* 1991; 40:315-325.
144. Rippe B, Levin L. Computer simulations of ultrafiltration profiles for an icodextrin-based peritoneal fluid in CAPD. *Kidney Int* 2000;57:2546-2456.
145. Rippe B, Rosengren BI, Venturoli D. The peritoneal microcirculation in peritoneal dialysis. *Microcirculation* 2001;8:303-20.
146. Rippe B, de Arteaga J, Venturoli D. Aquaporins are unlikely to be affected in marked ultrafiltration failure: results from a computer simulation. *Perit Dial Int* 2001; 21:S30–4.
147. Rippe B, Venturoli D, Simonsen O, de Arteaga J. Fluid and electrolyte transport across the peritoneal membrane during CAPD according to the three-pore model. *Perit Dial Int* 2004; 24:10-27.
148. Rippe B. Is intraperitoneal pressure important? *Perit Dial Int* 2006;26: 317-9.
149. Rippe A, Rippe C, Swärd K, Rippe B. Disproportionally low clearance of macromolecules from the plasma to the peritoneal cavity in a mouse model of peritoneal dialysis. *Nephrol Dial Transplant* 2007;22:88–95.
150. Rippe B, Venturoli D. Simulations of osmotic ultrafiltration failure in CAPD using a serial three-pore membrane/fiber matrix model. *Am J Physiol Renal Physiol* 2007;292:F1035-F1043.
151. Rippe B. Free water transport, small pore transport and the osmotic pressure gradient three-pore model of peritoneal transport. *Nephrol Dial Transplant* 2008;23:2147-53.
152. Rippe B. How to assess transport in animals? *Perit Dial Int* 2009;29:S32-5.
153. Rippe B, Davies S. Permeability of peritoneal and glomerular capillaries: what are the differences according to pore theory? *Perit Dial Int* 2011;31:249-58.
154. Roudier N, Verbavatz JM, Maurel C, Ripoche P, Tacnet F. Evidence for the presence of aquaporin-3 in human red blood cells. *J Biol Chem* 1998;273:8407-12.
155. Rumpsfeld M, McDonald SP, Johnson DW. Higher peritoneal transport status is associated with higher mortality and technique failure in the Australian and New Zealand peritoneal dialysis patient populations. *J Am Soc Nephrol* 2006;17:271-8.
156. Sampimon DE, Coester AM, Struijk DG, Krediet RT: Time course of peritoneal transport parameters in peritoneal dialysis patients who develop peritoneal sclerosis. *Adv Perit Dial* 2007;23:107-111.
157. Sampimon DE, Coester AM, Struijk DG, Krediet RT. The time course of peritoneal transport parameters in peritoneal dialysis patients who develop encapsulating peritoneal sclerosis. *Nephrol Dial Transplant* 2011;26:291-298.
158. Sarton E, Teppema LJ, Olievier C, Nieuwenhuijs D, Matthes HW, Kieffer BL, Dahan A. The involvement of the mu-opioid receptor in ketamine-induced respiratory depression and antinociception. *Anesth Analg* 2001;93: 1495-500.
159. Sekiguchi Y, Zhang J, Patterson S, Liu L, Hamada C, Tomino Y, Margetts PJ. Rapamycin inhibits transforming growth factor β-induced peritoneal angiogenesis by blocking the secondary hypoxic response. *J Cell Mol Med* 2012;16:1934-1945.
160. Shin SK, Kamerath CD, Gilson JF, Leypoldt JK. Effects of anaesthesia on fluid and solute transport in a C57BL6 mouse model of peritoneal dialysis. *Nephrol Dial Transplant* 2006;21:2874-80.
161. Siddique I, Brimble KS, Walkin L, Summers A, Brenchley P, Herrick S, Margetts PJ. Genetic Polymorphisms and Peritoneal Membrane Function. *Perit Dial Int* 2015;35:517-29.
162. Smit W, Schouten N, van den Berg N, Langedijk MJ, Struijk DG, Krediet RT; Netherlands Ultrafiltration Failure Study Group. Analysis of the prevalence and

causes of ultrafiltration failure during long-term peritoneal dialysis: A cross-sectional study. *Perit Dial Int* 2004;24:562–570.
163. Stoenoiu MS, Ni J, Verkaeren C, Debaix H, Jonas JC, Lameire N, Verbavatz JM, Devuyst O. Corticosteroids induce expression of aquaporin-1 and increase transcellular water transport in rat peritoneum. *J Am Soc Nephrol* 2003;14: 555–565.
164. Summers AM, Abrahams AC, Alscher MD, Betjes M, Boeschoten EW, Braun N, Brenchley PE, Davies S, Dunn L, Engelsman L, Fieren M, Garosi G, Goffin E, Heuveling L, Korte M, Lindholm B, Rutherford P, Struijk D, Verduijn M, Verger C, Westerhuis R: A collaborative approach to understanding EPS: the European perspective. *Perit Dial Int* 2011;31:245-248.
165. Taylor GS, Patel V, Spencer S, Fluck RJ, McIntyre CW. Long-term use of 1.1% amino acid dialysis solution in hypoalbuminemic continuous ambulatory peritoneal dialysis patients. *Clin Nephrol* 2002;58:445-450.
166. Tomita T, Hata T: Effects of removal of Na(+) and Cl(-) on spontaneous electrical activity, slow wave, in the circular muscle of the guinea-pig gastric antrum. *Jpn J Physiol* 2000;50:469–477.
167. Tonbul Z, Altintepe L, Sözlü C, Yeksan M, Yildiz A, Türk S. The association of peritoneal transport properties with 24-hour blood pressure levels in CAPD patients. *Perit Dial Int* 2003;23:46-52.
168. Törnroth-Horsefield S, Wang Y, Hedfalk K, Johanson U, Karlsson M, Tajkhorshid E, Neutze R, Kjellbom P. Structural mechanism of plant aquaporin gating. *Nature* 2006;439:688–694.
169. Tournaire-Roux C, Sutka M, Javot H, et al. Cytosolic pH regulates root water transport during anoxic stress through gating of aquaporins. *Nature* 2003; 425:393-397.
170. Trott O, Olson AJ. AutoDock Vina: Improving the speed and accuracy of docking with a new scoring function, efficient optimization, and multithreading. *J Comput Chem* 2010;31: 455–461.
171. Twardowski ZJ, Nolph KD, Khanna R, Prowant BF, Ryan LP, Moore HL, Nielsen MP: Peritoneal equilibration test. *Perit Dial Bull* 1987;7:138-147.
172. Van Biesen W, De Vriese AS, Carlsson O, Van Landschoot M, Dheuvaert T, Lameire NH. Comparison of the radioiodinated serum albumin (RISA) dilution technique with direct volumetric measurements in animal models of peritoneal dialysis. *Perit Dial Int* 2002;22:316-22.
173. Van Biesen W, Williams JD, Covic AC, Fan S, Claes K, Lichodziejewska-Niemierko M, Verger C, Steiger J, Schoder V, Wabel P, Gauly A, Himmele R; EuroBCM Study Group. Fluid status in peritoneal dialysis patients: the European Body Composition Monitoring (EuroBCM) study cohort. *PLoS One* 2011;6:e17148.
174. van Dijk PC, Jager KJ, de Charro F, Collart F, Cornet R, Dekker FW, Grönhagen-Riska C, Kramar R, Leivestad T, Simpson K, Briggs JD; ERA-EDTA registry. Renal replacement therapy in Europe: the results of a collaborative effort by the ERA-EDTA registry and six national or regional registries. *Nephrol Dial Transplant* 2001;16:1120-9.
175. Van't Hoff JH. Die Rolle des osmotischen druckes in der analogie zwischen lösungen and gasen. *Z Physik Chemie* 1887;1:481-508.
176. Verkman AS. Water permeability measurement in living cells and complex tissues. *J Membr Biol* 2000;173:73-87.
177. Verkman AS. Aquaporins in clinical medicine. *Annu Rev Med* 2012;63:303-16.
178. Verkman AS, Anderson MO, Papadopoulos MC. Aquaporins: important but elusive drug targets. *Nat Rev Drug Discov.* 2014;13:259-77.
179. Vischer UM. von Willebrand factor, endothelial dysfunction, and cardiovascular disease. *J Thromb Haemost* 2006;4:1186-1193.

180. Waniewski J, Werynski A, Heimbürger O, Lindholm B. Simple models for description of small solute transport in peritoneal dialysis. *Blood Purif* 1991;9:129–141.
181. Waniewski J, Heimbürger O, Werynski A, Lindholm B. Aqueous solute concentrations and evaluation of mass transport coefficients in peritoneal dialysis. *Nephrol Dial Transplant* 1992;7:50-56.
182. Whittaker P, Boughner DR, Kloner RA: Analysis of healing after myocardial infarction using polarized light microscopy. *Am J Pathol* 1989;134:879-893.
183. Whittaker P, Kloner RA, Boughner DR, Pickering JG. Quantitative assessment of myocardial collagen with picrosirius red staining and circularly polarized light. *Basic Res Cardiol* 1994;89:397-410.
184. Williams JD, Craig KJ, Topley N, Von Ruhland C, Fallon M, Newman GR, Mackenzie RK, Williams GT; Peritoneal Biopsy Study Group. Morphologic changes in the peritoneal membrane of patients with renal disease. *J Am Soc Nephrol* 2002;13:470–479.
185. Williams JD, Craig KJ, von Ruhland C, Topley N, Williams GT; Biopsy Registry Study Group. The natural course of peritoneal membrane biology during peritoneal dialysis. *Kidney Int Suppl* 2003;88:S43–S49.
186. Wouters M, De Laet A, Donck LV, Delpire E, van Bogaert PP, Timmermans JP, de Kerchove d'Exaerde A, Smans K, Vanderwinden JM. Subtractive hybridization unravels a role for the ion cotransporter NKCC1 in the murine intestinal pacemaker. Am J Physiol Gastro-intest Liver Physiol 2006;290:G1219–G1227.
187. Wynn TA, Ramalingam TR. Mechanisms of fibrosis: therapeutic translation for fibrotic disease. *Nat Med* 2012;18:1028-1040.
188. Yang B, Folkesson HG, Yang J, Matthay MA, Ma T, Verkman AS. Reduced osmotic water permeability of the peritoneal barrier in aquaporin-1 knockout mice. *Am J Physiol* 1999;276:C76-81.
189. Yang B, Zhang H, Verkman AS. Lack of aquaporin-4 water transport inhibition by antiepileptics and arylsulfonamides. *Bioorg Med Chem* 2008;16:7489–7493.
190. Yool AJ. Functional domains of aquaporin-1: keys to physiology, and targets for drug discovery. *Curr Pharm Des* 2007;13:3212–3221.
191. Yool AJ, Brown EA, Flynn GA. Roles for novel pharmacological blockers of aquaporins in the treatment of brain oedema and cancer. *Clin Exp Pharmacol Physiol* 2010;37:403–409.
192. Yool AJ, Morelle J, Cnops Y, Verbavatz JM, Campbell EM, Beckett EA, Booker GW, Flynn G, Devuyst O. AqF026 is a pharmacologic agonist of the water channel aquaporin-1. *J Am Soc Nephrol* 2013;24:1045-52.
193. Yu J, Yool AJ, Schulten K, Tajkhorshid E. Mechanism of gating and ion conductivity of a possible tetrameric pore in aquaporin-1. *Structure* 2006;14:1411–1423.
194. Yukutake Y, Tsuji S, Hirano Y, Adachi T, Takahashi T, Fujihara K, Agre P, Yasui M, Suematsu M. Mercury chloride decreases the water permeability of aquaporin-4-reconstituted proteoliposomes. *Biol Cell* 2008;100:355–363.
195. Zakaria ER, Rippe B. Intraperitoneal fluid volume changes during peritoneal dialysis in the rat: indicator dilution vs. volumetric measurements. *Blood Purif* 1995;13:255–270.
196. Zakaria ER, Rippe B. Peritoneal fluid and tracer albumin kinetics in the rat. Effects of increases in intraperitoneal hydrostatic pressure. *Perit Dial Int* 1995;15:118-28.
197. Zakaria ER, Simonsen O, Rippe A, Rippe B. Transport of tracer albumin from peritoneum to plasma: role of diaphragmatic, visceral, and parietal lymphatics. *Am J Physiol* 1996;270:H1549-56.
198. Zelenina M, Zelenin S, Bondar AA, Brismar H, Aperia A. Water permeability of

aquaporin-4 is decreased by protein kinase C and dopamine. *Am J Physiol Renal Physiol* 2002;283:F309– F318.
199. Zhang W, Freichel M, van der Hoeven F, Nawroth PP, Katus H, Kälble F, Zitron E, Schwenger V. Novel Endothelial Cell-Specific AQP1 Knockout Mice Confirm the Crucial Role of Endothelial AQP1 in Ultrafiltration during Peritoneal Dialysis. *PLoS One* 2016;11:e0145513.
200. Zhu Q, Carlsson O, Rippe B. Clearance of tracer albumin from peritoneal cavity to plasma at low intraperitoneal volumes and hydrostatic pressures. *Perit Dial Int* 1998;18:497-504.
201. Zhu MH, Kim TW, Ro S, Yan W, Ward SM, Koh SD, Sanders KM. A Ca(2+)-activated Cl(-) conductance in interstitial cells of Cajal linked to slow wave currents and pacemaker activity. *J Physiol* 2009;587:4905–4918.
202. Zweers MM, Douma CE, de Waart DR, et al. Amphotericin B, mercury chloride and peritoneal transport in rabbits. *Clin Nephrol* 2001;56:60-68.

SUPPLEMENTARY DATA

CHAPTER I

QUANTIFICATION OF OSMOTIC WATER TRANSPORT *IN VIVO* USING FLUORESCENT ALBUMIN

Suppl. Fig. 1. Effect of isotonic saline infusion on mean arterial blood pressure (MABP) and peritoneal water and solute transport during peritoneal dialysis (PD) in mice.

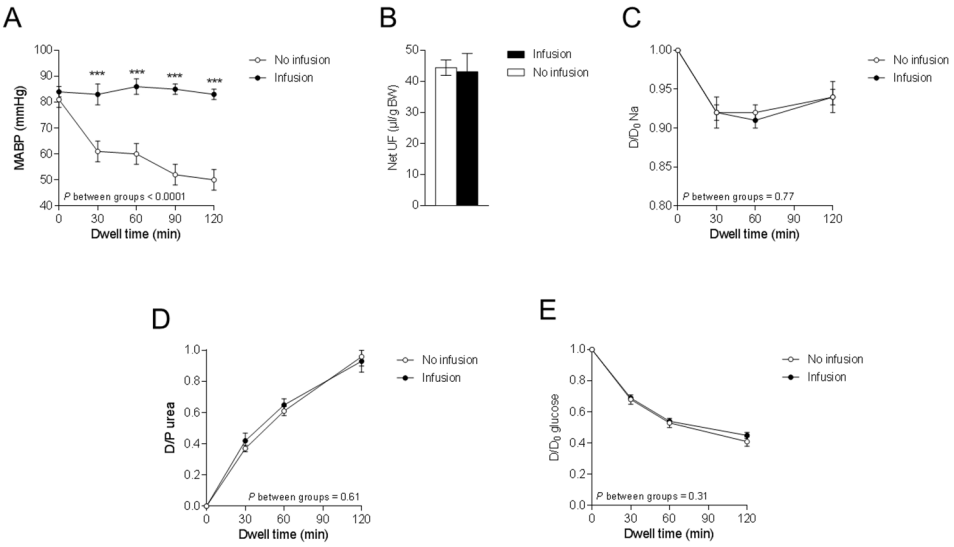

A: infusion of 0.5 ml/h [~total net ultrafiltration (UF)] of isotonic saline prevented the drop in MABP observed in control animals (final and baseline MABP 83±2 and 84±2 vs. 50±4 and 81±3 mmHg, in infusion and no infusion groups, respectively. $P<0.0001$). B-E: Compensating or not for net UF with isotonic saline had no significant effect on the parameters of peritoneal water (net UF: 43.1±5.9 vs. 44.4±2.5 µl/g in infusion and no infusion groups, respectively; $P = 0.87$; dip in dialysate sodium concentration during the first 30 min: 12.3±2.6 vs. 11.5±1.9 mEq/l in infusion and no infusion groups, respectively; $P = 0.66$) and solute transport [dialysate over plasma urea ratio (D/P) and glucose disappearance rate in the dialysate (D/D0)]. Values are means ± SE; n = 4 mice in each group. BW, body weight.

Suppl. Fig. 2. Influence of intraperitoneal pressure (IPP) on tracer kinetics in the mouse model of PD.

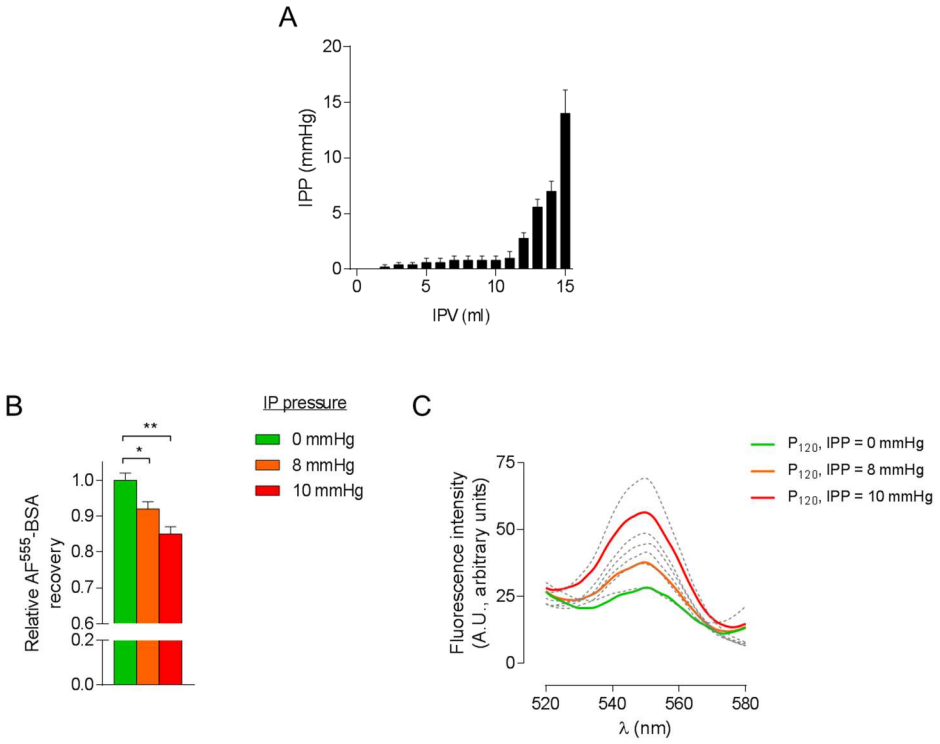

A: IPP vs. IPV curves in SV129 mice. IPP remains <2 mmHg for IPV <10 ml, then increases in an exponential way for larger IPV values; n = 5 adult male SV129 mice. Isotonic saline was progressively instilled into the peritoneal cavity to increase IPV from baseline to 15 ml. B: effect of external abdominal compression and elevated IPP on the recovery of Alexa Fluor 555-BSA in the drained dialysate. Increasing IPP from 0 to 8 and 10 mmHg significantly decreases tracer mass recovery at the end of the dwell in the peritoneal cavity of mice exposed to Alexa Fluor 555-BSA (from 100 to 92±2 and 85±2%, respectively; $P<0.001$). C: effect of external abdominal compression and elevated IPP on tracer appearance in the plasma. Fluorescence excitation spectrum of plasma from mice exposed to a 2-h PD with 100 µg of Alexa Fluor 555-BSA shows a progressive rise in the amount of Alexa Fluor 555-BSA detected in the plasma when IPP is increased from 0 to 8 and 10 mmHg (green, orange, and red lines, respectively). Results are compared with the fluorescence excitation spectrum of plasma from control mice spiked with different concentrations (0 –5 µg/ml, grey dotted lines) of Alexa Fluor 555-BSA. Dwells were performed with 3.86% glucose-based dialysate for 2 h; n = 4-5 in each group.

CHAPTER II

AQF026 IS A PHARMACOLOGIC AGONIST OF THE WATER CHANNEL AQUAPORIN-1

Suppl. Fig. 1. Effect of AqF026 on AQP1 expression in the peritoneal membrane.

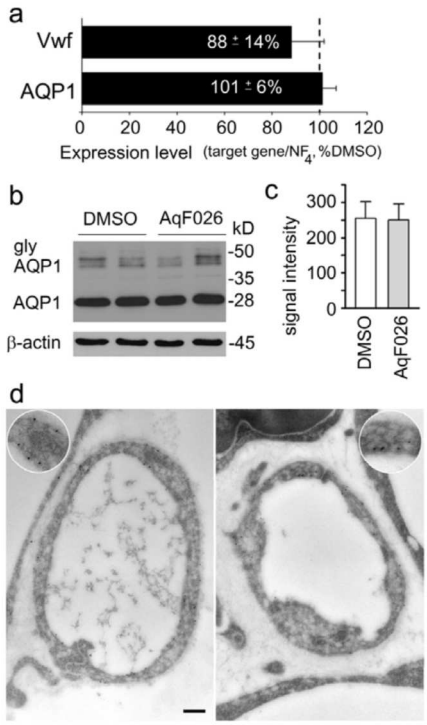

A. Real-time RT-PCR quantification for mRNA expression of aquaporin-1 (AQP1) and von Willebrand factor (Vwf) in the mouse peritoneum. Treatment with AqF026 did not induce significant changes in the expression of either endothelial marker. **B.** Representative immunoblots for AQP1 (1:20,000) in peritoneum extracts prepared from *Aqp1*$^{+/+}$ mice (20 µg protein/lane). The blots were stripped and reprobed with a monoclonal antibody against beta-actin (1:10,000) as a loading standard for accuracy. The core (28 kD) and glycosylated (35-50 kD) AQP1 isoforms were identified in the peritoneum, with no changes observed in the agonist- or DMSO vehicle-treated mice. **C.** Densitometric analysis of AQP1 signal on 4 pairs of peritoneal samples. **D.** Representative micrographs of immunogold labeling for AQP1 in control (left) and treated (right) samples. Gold particles decorated the endothelial cells of blood capillaries and exhibited no change in localization after treatment. Insets: x2 magnification. Bar = 250 nm.

Suppl. Fig. 2. Chemical synthesis of AqF026.

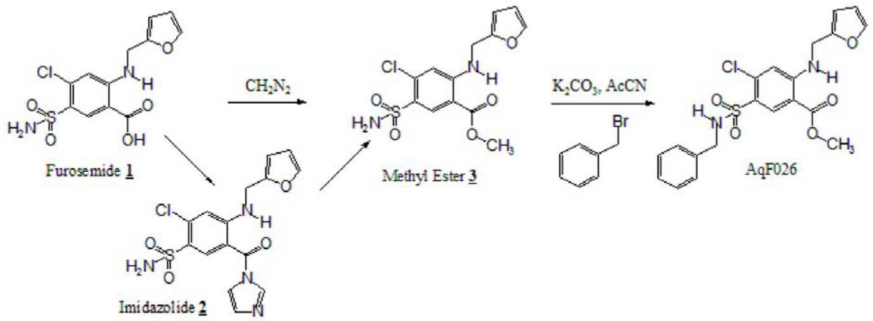

Furosemide (1) was converted to its methyl ester derivative (AqF022) (3) by monitoring the addition of diazolmethane until only a slight yellow tint remained. Prolonged treatment with excess diazomethane was found to result in varying degrees of sulphonamide methylation. Alternatively, furosemide was specifically converted by carbonyl diimidazole to its imidazolide derivative (2) which cleanly provided methyl ester (3) upon addition of methyl alcohol. Alkylation of sulphonamide ester (3) with benzyl bromide and potassium carbonate in acetonitrile afforded AqF026 after purification by column chromatography.

CHAPTER III

INTERSTITIAL FIBROSIS RESTRICTS OSMOTIC WATER TRANSPORT IN ENCAPSULATING PERITONEAL SCLEROSIS

Supplemental figure 1. Mean glucose exposure during the last two years on PD in EPS and PD controls.

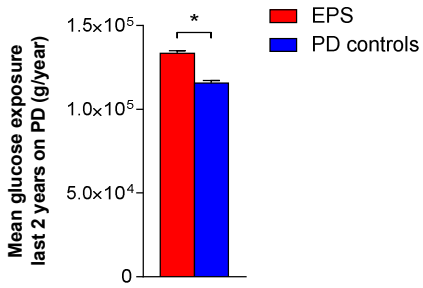

Glucose exposure was significantly higher during the last 2 years on PD in the EPS group as compared with PD controls (133,606±1332 versus 115,697±1586 g/year in EPS and PD controls, respectively; *P*=0.01).

Supplemental figure 2. Impaired water transport does not correlate with peritoneal vasculopathy.

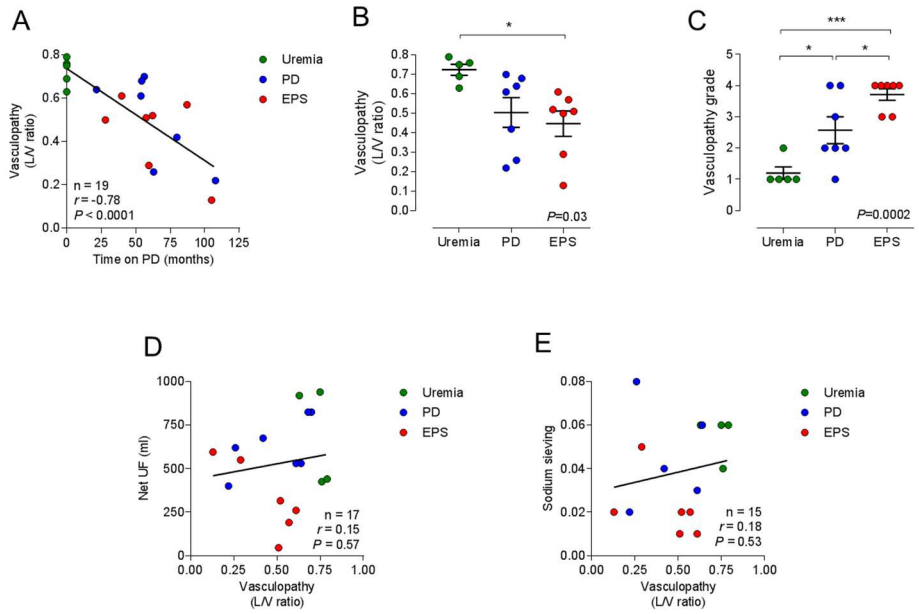

(A) The degree of vasculopathy (lumen-to-vessel ratio, L/V) is inversely correlated with time on PD (Pearson r=-0.78, P<0.0001). (B-C) EPS patients tend to have a higher degree of peritoneal vasculopathy (L/V ratio), and have a higher vasculopathy grade as compared with PD controls. (D-E) There is no correlation between net ultrafiltration or sodium sieving and the degree of vasculopathy in this cohort (Pearson r=0.15, P=0.57 and Pearson r=0.18, P=0.53, respectively). Peritoneal samples are from 5 uremic, 7 long-term PD without EPS, and 7 EPS patients. Circles represent individuals; green circles for uremic, blue for PD controls, and red for EPS patients.

Supplemental table 1. Clinical and functional characteristics of PD patients in which peritoneal biopsies were analyzed.

	Uremic	**Long-term PD**	**EPS**
	***n* = 5**	***n* = 7**	***n* = 7**
PD duration (months)	-	62.4 ± 9.3	62.8 ± 9.2
Charlson comorbidity index	4.8 ± 1.0	4.0 ± 0.8	4.9 ± 1.0
Diabetes, %	20%	29%	29%
Residual diuresis at PD start, ml/day	1252 ± 224	835 ± 143	1083 ± 159
Total number of peritonitis	-	1.5 ± 0.4	1.4 ± 0.4
Functional parameters at the time of biopsy			
Net UF (ml)	681 ± 124	629 ± 55	326 ± 79*
D/P creatinine 4h	0.75 ± 0.07	0.75 ± 0.02	0.84 ± 0.04
Sodium sieving	0.06 ± 0.00	0.05 ± 0.01	0.02 ± 0.01*
Time between last PET and biopsy (months)	-	7.5 ± 1.6	9.1 ± 2.1

EPS, encapsulating peritoneal sclerosis; PD, peritoneal dialysis; UF, ultrafiltration